

Laboratory and Field Testing of Automated Ultrasonic Testing (AUT) Systems for Steel Highway Bridges

PUBLICATION NO. FHWA-HRT-04-124

APRIL 2005



U.S. Department of Transportation
Federal Highway Administration

Research, Development, and Technology
Turner-Fairbank Highway Research Center
6300 Georgetown Pike
McLean, VA 22101-2296

FOREWORD

The need for quality control and quality assurance of welds in the fabrication of steel bridge structures has led to the development of a variety of nondestructive inspection techniques. For many years, radiographic testing (RT) has been the preferred nondestructive inspection method used to ensure the quality of butt welds in the fabrication of steel plates for bridge girders. The major advantage of RT has been the capability of producing a radiograph that serves as a permanent record of the inspection. However, the significant health hazards associated with the use of radiographic methods have long been a concern.

Recent advances in computers and ultrasonic technology have led to the development of automated ultrasonic testing (AUT) techniques that produce three-dimensional images of internal conditions in the weld. The AUT image can serve as a permanent record of the inspection and allows for subjective reviews of the inspection findings. Since AUT uses ultrasonic waves, there are minimal health concerns with this method.

This report presents the findings of a study initiated by the Federal Highway Administration's Nondestructive Evaluation Validation Center (NDEVC) to evaluate the effectiveness and viability of automated ultrasonic testing techniques as a replacement for radiographic testing methods for the inspection of butt welds during fabrication of steel plates for bridge girders.

T. Paul Teng, PE
Director, Office of Infrastructure
Research and Development

NOTICE

This document is disseminated under the sponsorship of the U.S. Department of Transportation in the interest of information exchange. The U.S. Government assumes no liability for its contents or use thereof. This report does not constitute a standard, specification, or regulation.

The U.S. Government does not endorse products or manufacturers. Trade and manufacturers' names appear in this report only because they are considered essential to the object of the document.

QUALITY ASSURANCE STATEMENT

The Federal Highway Administration (FHWA) provides high-quality information to serve Government, industry, and the public in a manner that promotes public understanding. Standards and policies are used to ensure and maximize the quality, objectivity, utility, and integrity of its information. FHWA periodically reviews quality issues and adjusts its programs and processes to ensure continuous quality improvement.

1. Report No. FHWA-HRT-04-124		2. Government Accession No.		3. Recipient's Catalog No.	
4. Title and Subtitle LABORATORY AND FIELD TESTING OF AUTOMATED ULTRASONIC TESTING (AUT) SYSTEMS FOR STEEL HIGHWAY BRIDGES				5. Report Date April 2005	
				6. Performing Organization Code	
7. Author(s) Ali Rezai, Ph.D., Mark Moore, P.E., Travis Green, P.E., and Glenn Washer, Ph.D., P.E.				8. Performing Organization Report No.	
9. Performing Organization Name and Address Wiss, Janney, Elstner Associates, Inc. 4165 Shackleford Road, Suite 100 Norcross, GA 30093				10. Work Unit No.	
				11. Contract or Grant No. DTFH61-02-C-00045	
12. Sponsoring Agency Name and Address Office of Infrastructure Research and Development Federal Highway Administration 6300 Georgetown Pike McLean, VA 22101				13. Type of Report and Period Covered Final Report August 2000-October 2004	
				14. Sponsoring Agency Code	
15. Supplementary Notes Contracting Officer's Technical Representative (COTR): Glenn Washer, Ph.D., PE, HRDI-10					
16. Abstract Fabrication inspection of welds is necessary to ensure the quality of workmanship during the fabrication process. The implementation of automated ultrasonic testing (AUT) methods for inspecting butt welds in steel bridge fabrication is the subject of this report. The primary goal is to evaluate the effectiveness of AUT as a replacement for radiographic testing (RT) for fabrication inspection of welds in steel highway bridges. The AUT results will be compared to RT results. The advantages of implementing AUT as compared to RT for inspecting butt welds in fabrication plants will be addressed. The study consists of laboratory testing to assess the viability of the AUT system under a controlled laboratory environment and field testing at fabrication plants, during the routine fabrication process, to assess the performance and practicality of the AUT technique and system for use in the fabrication shop environment. AUT, manual ultrasonic testing (UT), and RT systems are employed side by side for fabrication inspection of welds during field testing.					
17. Key Words NDE, ultrasonic, inspection, automated ultrasonic testing, AUT, auto UT, bridge fabrication inspection, butt weld, butt joint, steel bridge, and radiographic testing.			18. Distribution Statement No restrictions. This document is available to the public through the National Technical Information Service, Springfield, VA 22161.		
19. Security Classif. (of this report) Unclassified		20. Security Classif. (of this page) Unclassified		21. No. of Pages 139	22. Price

SI* (MODERN METRIC) CONVERSION FACTORS

APPROXIMATE CONVERSIONS TO SI UNITS

Symbol	When You Know	Multiply By	To Find	Symbol
LENGTH				
in	inches	25.4	millimeters	mm
ft	feet	0.305	meters	m
yd	yards	0.914	meters	m
mi	miles	1.61	kilometers	km
AREA				
in ²	square inches	645.2	square millimeters	mm ²
ft ²	square feet	0.093	square meters	m ²
yd ²	square yard	0.836	square meters	m ²
ac	acres	0.405	hectares	ha
mi ²	square miles	2.59	square kilometers	km ²
VOLUME				
fl oz	fluid ounces	29.57	milliliters	mL
gal	gallons	3.785	liters	L
ft ³	cubic feet	0.028	cubic meters	m ³
yd ³	cubic yards	0.765	cubic meters	m ³
NOTE: volumes greater than 1000 L shall be shown in m ³				
MASS				
oz	ounces	28.35	grams	g
lb	pounds	0.454	kilograms	kg
T	short tons (2000 lb)	0.907	megagrams (or "metric ton")	Mg (or "t")
TEMPERATURE (exact degrees)				
°F	Fahrenheit	5 (F-32)/9 or (F-32)/1.8	Celsius	°C
ILLUMINATION				
fc	foot-candles	10.76	lux	lx
fl	foot-Lamberts	3.426	candela/m ²	cd/m ²
FORCE and PRESSURE or STRESS				
lbf	poundforce	4.45	newtons	N
lbf/in ²	poundforce per square inch	6.89	kilopascals	kPa

APPROXIMATE CONVERSIONS FROM SI UNITS

Symbol	When You Know	Multiply By	To Find	Symbol
LENGTH				
mm	millimeters	0.039	inches	in
m	meters	3.28	feet	ft
m	meters	1.09	yards	yd
km	kilometers	0.621	miles	mi
AREA				
mm ²	square millimeters	0.0016	square inches	in ²
m ²	square meters	10.764	square feet	ft ²
m ²	square meters	1.195	square yards	yd ²
ha	hectares	2.47	acres	ac
km ²	square kilometers	0.386	square miles	mi ²
VOLUME				
mL	milliliters	0.034	fluid ounces	fl oz
L	liters	0.264	gallons	gal
m ³	cubic meters	35.314	cubic feet	ft ³
m ³	cubic meters	1.307	cubic yards	yd ³
MASS				
g	grams	0.035	ounces	oz
kg	kilograms	2.202	pounds	lb
Mg (or "t")	megagrams (or "metric ton")	1.103	short tons (2000 lb)	T
TEMPERATURE (exact degrees)				
°C	Celsius	1.8C+32	Fahrenheit	°F
ILLUMINATION				
lx	lux	0.0929	foot-candles	fc
cd/m ²	candela/m ²	0.2919	foot-Lamberts	fl
FORCE and PRESSURE or STRESS				
N	newtons	0.225	poundforce	lbf
kPa	kilopascals	0.145	poundforce per square inch	lbf/in ²

*SI is the symbol for the International System of Units. Appropriate rounding should be made to comply with Section 4 of ASTM E380.
(Revised March 2003)

TABLE OF CONTENTS

1. INTRODUCTION.....	1
PROJECT SCOPE AND OBJECTIVE.....	2
2. BACKGROUND	5
AWS D1.5 WELDING CODE	5
ACCEPTANCE-REJECTION CRITERIA FOR UT VERSUS RT.....	6
3. AUT EQUIPMENT DESCRIPTION.....	9
SYSTEM SELECTION.....	9
P-SCAN SYSTEM CHARACTERISTICS.....	10
System Components.....	10
System Setup.....	13
System Output.....	16
ANALOGY OF INDICATION RATING IN AUT VERSUS TRADITIONAL UT.....	23
UT Indication Rating Procedures.....	23
AUT Indication Rating Procedures.....	23
4. EQUIPMENT QUALIFICATION AND CALIBRATION	25
EQUIPMENT QUALIFICATION PROCEDURES	25
CALIBRATION PROCEDURES	29
5. TESTING AND EVALUATION PLAN	37
DESCRIPTION OF SPECIMENS.....	37
Laboratory Specimens.....	38
Field Specimens.....	41
LABORATORY TESTING	44
FIELD TESTING.....	44
6. RESULTS	47
LABORATORY RESULTS.....	47
BLIND FIELD-TESTING RESULTS	71
FIELD-TESTING RESULTS	78
ARTICULATION ANGLES.....	123
7. CONCLUSIONS	126
8. REFERENCES.....	128

LIST OF FIGURES

1.	Rating chart plotted from table 6.3 in the AASHTO/AWS D1.5M/D1.5: 2002 Bridge Welding Code, ⁽¹⁾ showing class A, B, C, and D decibel levels for 70-degree angle.....	7
2.	Photograph of the P-scan system showing the data acquisition system and the scanning arm holding the ultrasonic transducer.....	11
3.	Schematic diagram of the MWS-1 scanner, indicating three DOF: (1) scanner arm rotation angle α , (2) scanner arm extension L, and (3) transducer skew angle β	12
4.	Positioning/setup configuration of MWS-1 scanner on the plate: TSC configuration describes scanning the weld from the TSC side of the centerline	14
5.	Positioning/setup configuration of MWS-1 scanner on the plate: BSC configuration describes scanning the weld from the BSC side of the centerline	14
6.	Positioning/setup configuration of MWS-1 scanner on the plate: “Both” configuration describes scanning the weld from both sides of the centerline in a single setup	15
7.	Laboratory specimen S033: Schematic diagram showing two implanted cracks.....	17
8.	Laboratory specimen S033: Schematic diagram of toe crack.....	17
9.	Laboratory specimen S033: Schematic diagram of root crack.....	17
10.	Laboratory specimen S033: Radiographic image shows the two implanted cracks.....	17
11.	P-scan images of laboratory specimen S033: Displayed in logarithmic mode during scanning to ensure full coverage of the weld.....	18
12.	P-scan images of laboratory specimen S033: Displayed in linear mode after scanning (highlighting only the indications in the weld).....	18
13.	P-scan images on three projection planes	19
14.	Flaw-sizing scheme of the P-scan system for the root crack in laboratory specimen S033	22
15.	IIW reference block used for the P-scan calibration: Type I.....	27
16.	IIW reference block used for the P-scan calibration: Type RC	28
17.	IIW reference block used for the P-scan calibration: Type DSC.....	28
18.	Horizontal linearity check using a straight-beam transducer and IIW type I reference block.....	29
19.	Sound entry point check: Photograph shows the transducer position on the IIW reference block.....	30
20.	Sound entry point check: A-scan screen displays the echo reflected from the 100-mm (4-inch) radius circular reflector on the IIW type I reference block.....	30
21.	Sound-path angle check: Photograph shows that the selected angle transducer is positioned on the IIW type I reference block over the line indicative of the transducer angle.....	32
22.	Sound-path angle check: A-scan screen displays the echo reflected from the 50-mm (2-inch) diameter hollow-disk reflector in the reference block	32
23.	Resolution check: Photograph shows that the selected angle transducer is positioned on the IIW type RC reference block over the line indicative of the transducer angle.....	33
24.	Resolution check: A-scan screen displays the three distinguishable signals reflected from the three holes	33

LIST OF FIGURES (CONTINUED)

25.	Distance calibration check: Photograph shows that the angle transducer is positioned on the IIW type I reference block so that the transducer's sound entry point aligns with the radius line of the 100-mm (4-inch) reflector.....	34
26.	Distance calibration check: A-scan screen displays the signals reflected back and forth from the 100-mm (4-inch) radius circular reflector and 25.4-mm (1-inch) radius groove reflector.....	34
27.	Amplitude, sensitivity, or reference-level calibration: Photograph shows that the angle transducer is positioned on the IIW type I reference block.....	36
28.	Amplitude, sensitivity, or reference-level calibration: A-scan screen displays the signal reflected from the 1.5-mm (0.06-inch) sidewall hole that is maximized to attain a horizontal reference-line (i.e., green line) height indication.....	36
29.	Schematic diagram of specimen: Thickness transition at butt joint.....	38
30.	Schematic diagram of specimen: Width transition at butt joint.....	38
31.	AUT field testing: High Steel Structures, Inc.....	45
32.	AUT field testing: Stupp Bridge Company.....	45
33.	Laboratory specimen S034: Schematic diagram showing two implanted cracks.....	54
34.	Laboratory specimen S034: Schematic diagram of longitudinal/centerline crack.....	54
35.	Laboratory specimen S034: Schematic diagram of transverse crack.....	54
36.	Laboratory specimen S034: Radiographic image showing the two implanted cracks.....	54
37.	Laboratory specimen S034: Top view of joint.....	55
38.	P-scan images of laboratory specimen S034: Images of longitudinal/centerline indication in the weld.....	55
39.	Laboratory specimen S125: Top view of joint.....	56
40.	Laboratory specimen S125: Radiographic image showing discontinuities in the weld.....	56
41.	P-scan images of laboratory specimen S125: From TSC side of centerline.....	57
42.	P-scan images of laboratory specimen S125: From BSC side of centerline.....	57
43.	Laboratory specimen S126: Top view of joint.....	58
44.	Laboratory specimen S126: Radiographic image showing discontinuities in the weld.....	58
45.	P-scan images of laboratory specimen S126: From TSC side of centerline.....	59
46.	P-scan images of laboratory specimen S126: From BSC side of centerline.....	59
47.	Laboratory specimen S132: View of joint.....	60
48.	Laboratory specimen S132: Radiographic image showing discontinuities in the weld.....	60
49.	P-scan images of laboratory specimen S132: From TSC side of centerline between 0 and 177.8 mm (0 and 7 inches).....	61
50.	P-scan images of laboratory specimen S132: From BSC side of centerline between 0 and 177.8 mm (0 and 7 inches).....	61
51.	P-scan images of laboratory specimen S132: From TSC side of centerline between 177.8 and 304.8 mm (7 and 12 inches).....	62
52.	P-scan images of laboratory specimen S132: From BSC side of centerline between 177.8 and 304.8 mm (7 and 12 inches).....	62
53.	Laboratory specimen S133: Top view of joint.....	63
54.	Laboratory specimen S133: Radiographic image showing discontinuities in the weld.....	63
55.	P-scan images of laboratory specimen S133.....	64
56.	Laboratory specimen S135: Side view of joint.....	65

LIST OF FIGURES (CONTINUED)

57.	Laboratory specimen S135: Top view of joint	65
58.	Laboratory specimen S135: Radiographic image showing discontinuities in the weld between markers A and B	65
59.	Laboratory specimen S135: Radiographic image showing discontinuities in the weld between markers B and C	65
60.	P-scan images of laboratory specimen S135: From TSC side of centerline between 0 and 203.2 mm (0 and 8 inches).....	66
61.	P-scan images of laboratory specimen S135: From BSC side of centerline between 0 and 203.2 mm (0 and 8 inches).....	66
62.	P-scan images of laboratory specimen S135: From TSC side of centerline between 203.2 and 454 mm (8 and 17.875 inches).....	67
63.	P-scan images of laboratory specimen S135: From BSC side of centerline between 203.2 and 454 mm (8 and 17.875 inches).....	67
64.	Laboratory specimen S136: Side view of joint.....	68
65.	Laboratory specimen S136: Top view of joint	68
66.	Laboratory specimen S136: Radiographic image showing discontinuities in the weld between markers A and B	68
67.	Laboratory specimen S136: Radiographic image showing discontinuities in the weld between markers B and C	68
68.	P-scan images of laboratory specimen S136: From TSC side of centerline between 0 and 203.2 mm (0 and 8 inches).....	69
69.	P-scan images of laboratory specimen S136: From BSC side of centerline between 0 and 203.2 mm (0 and 8 inches).....	69
70.	P-scan images of laboratory specimen S136: From TSC side of centerline between 203.2 and 454 mm (8 and 17.875 inches).....	70
71.	P-scan images of laboratory specimen S136: From BSC side of centerline between 203.2 and 454 mm (8 and 17.875 inches).....	70
72.	Field specimen FG38K-TF2-TopF-FCM used in blind testing: Top view of joint	72
73.	Field specimen FG38K-TF2-TopF-FCM used in blind testing: Side view of joint	72
74.	P-scan images of field specimen FG38K-TF2-TopF-FCM using 45-degree probe: From TSC side of centerline between 0 and 279.4 mm (0 and 11 inches).....	73
75.	P-scan images of field specimen FG38K-TF2-TopF-FCM using 45-degree probe: From BSC side of centerline between 0 and 279.4 mm (0 and 11 inches).....	73
76.	P-scan images of field specimen FG38K-TF2-TopF-FCM using 45-degree probe: From TSC side of centerline between 279.4 and 558.8 mm (11 and 22 inches).....	74
77.	P-scan images of field specimen FG38K-TF2-TopF-FCM using 45-degree probe: From BSC side of centerline between 279.4 and 558.8 mm (11 and 22 inches).....	74
78.	P-scan images of field specimen FG38K-TF2-TopF-FCM using 45-degree probe: From TSC side of centerline between 558.8 and 857.25 mm (22 and 33.75 inches).....	75
79.	P-scan images of field specimen FG38K-TF2-TopF-FCM using 45-degree probe: From BSC side of centerline between 558.8 and 857.25 mm (22 and 33.75 inches).....	75
80.	Radiographic image of field specimen FG38K-TF2-TopF-FCM: Section A–B	76

LIST OF FIGURES (CONTINUED)

81.	Radiographic image of field specimen FG38K-TF2-TopF-FCM: Section B–C	76
82.	Radiographic image of field specimen FG38K-TF2-TopF-FCM: Section C–D	76
83.	Field specimen G5G-TF1-TopF: Top view of joint	86
84.	Field specimen G5G-TF1-TopF: Side view of joint.....	86
85.	Radiographic image of field specimen G5G-TF1-TopF: Section A–B	87
86.	Radiographic image of field specimen G5G-TF1-TopF: Section B–C	87
87.	P-scan images of field specimen G5G-TF1-TopF using 70-degree probe: From TSC side of centerline	88
88.	P-scan images of field specimen G5G-TF1-TopF using 70-degree probe: From BSC side of centerline.....	88
89.	Field specimen G2G-CF1-BottF-FCM: Top view of joint	89
90.	Field specimen G2G-CF1-BottF-FCM: Side view of joint	89
91.	Radiographic image of field specimen G2G-CF1-BottF-FCM: Section A–B.....	90
92.	Radiographic image of field specimen G2G-CF1-BottF-FCM: Section B–C.....	90
93.	Radiographic image of field specimen G2G-CF1-BottF-FCM: Section C–D.....	90
94.	Radiographic image of field specimen G2G-CF1-BottF-FCM: Section D–E.....	90
95.	P-scan images of field specimen G2G-CF1-BottF-FCM using 45-degree probe: From TSC side of centerline	91
96.	P-scan images of field specimen G2G-CF1-BottF-FCM using 45-degree probe: From BSC side of centerline.....	91
97.	Field specimen FG26G-TF2-BottF-FCM: Top view of joint	93
98.	Field specimen FG26G-TF2-BottF-FCM: Side view of joint	93
99.	Radiographic image of field specimen FG26G-TF2-BottF-FCM	94
100.	P-scan images of field specimen FG26G-TF2-BottF-FCM using 70-degree probe: From TSC side of centerline	95
101.	P-scan image of field specimen FG26G-TF2-BottF-FCM using 70-degree probe: From BSC side of centerline.....	95
102.	Field specimen FG16D-TF1-BottF-FCM: Top view of joint	96
103.	Field specimen FG16D-TF1-BottF-FCM: Side view of joint	96
104.	Radiographic image of field specimen FG16D-TF1-BottF-FCM	97
105.	P-scan images of field specimen FG16D-TF1-BottF-FCM: From TSC side of centerline using 60-degree probe	98
106.	P-scan images of field specimen FG16D-TF1-BottF-FCM: From BSC side of centerline using 60-degree probe	98
107.	P-scan images of field specimen FG16D-TF1-BottF-FCM: From BSC side of centerline using 70-degree probe	98
108.	Field specimen FG36K-TF2-TopF-FCM: Top view of joint	99
109.	Field specimen FG36K-TF2-TopF-FCM: Side view of joint.....	99
110.	Radiographic image of field specimen FG36K-TF2-TopF-FCM: Section C–D	100
111.	P-scan images of field specimen FG36K-TF2-TopF-FCM using 45-degree probe: From TSC side of centerline	101

LIST OF FIGURES (CONTINUED)

112.	P-scan images of field specimen FG36K-TF2-TopF-FCM using 45-degree probe: From BSC side of centerline.....	101
113.	Field specimen FG37K-TF3-BottF-FCM: Top view of joint.....	102
114.	Field specimen FG37K-TF3-BottF-FCM: Side view of joint.....	102
115.	Radiographic image of field specimen FG37K-TF3-BottF-FCM: Section C–D.....	103
116.	P-scan images of field specimen FG37K-TF3-BottF-FCM: Scan using 45-degree probe.....	104
117.	P-scan images of field specimen FG37K-TF3-BottF-FCM: Scan using 70-degree probe.....	104
118.	HSS procedural test plate TP2: Top view of joint.....	105
119.	HSS procedural test plate TP2: P-scan images from BSC side of centerline.....	105
120.	Field specimen FG40M-TF1-Curved-FCM: Top view of joint.....	107
121.	Field specimen FG40M-TF1-Curved-FCM: Side view of joint.....	107
122.	Radiographic image of field specimen FG40M-TF1-Curved-FCM: Section B–C.....	108
123.	P-scan images of field specimen FG40M-TF1-Curved-FCM: From TSC side of centerline between 0 and 228.6 mm (0 and 9 inches).....	109
124.	P-scan images of field specimen FG40M-TF1-Curved-FCM: From BSC side of centerline between 0 and 228.6 mm (0 and 9 inches).....	109
125.	P-scan images of field specimen FG40M-TF1-Curved-FCM: From TSC side of centerline between 228.6 and 457.2 mm (9 and 18 inches).....	110
126.	P-scan images of field specimen FG40M-TF1-Curved-FCM: From BSC side of centerline between 228.6 and 457.2 mm (9 and 18 inches).....	110
127.	P-scan images of field specimen FG40M-TF1-Curved-FCM: From TSC side of centerline between 457.2 and 685.8 mm (18 and 27 inches).....	111
128.	P-scan images of field specimen FG40M-TF1-Curved-FCM: From BSC side of centerline between 457.2 and 685.8 mm (18 and 27 inches).....	111
129.	P-scan images of field specimen FG40M-TF1-Curved-FCM: From TSC side of centerline between 685.8 and 993.8 mm (27 and 39.125 inches).....	112
130.	P-scan images of field specimen FG40M-TF1-Curved-FCM: From BSC side of centerline between 685.8 and 993.8 mm (27 and 39.125 inches).....	112
131.	Field specimen FG1A-TF2-BottF-FCM: Top view of joint.....	113
132.	Field specimen FG1A-TF2-BottF-FCM: Side view of joint.....	113
133.	P-scan images of field specimen FG1A-TF2-BottF-FCM: From TSC side of centerline using 60-degree probe.....	114
134.	P-scan images of field specimen FG1A-TF2-BottF-FCM: From TSC side of centerline using 70-degree probe.....	114
135.	P-scan images of field specimen FG1A-TF2-BottF-FCM: From BSC side of centerline using 70-degree probe.....	114
136.	Field specimen G3VHW-CF1-BottF: Top view of joint.....	115
137.	Field specimen G3VHW-CF1-BottF: Radiographic image of section A–B.....	115
138.	Field specimen G3VHW-CF1-BottF: P-scan images from TSC side of centerline using 70-degree probe.....	115
139.	Field specimen G5VHW-CF1-BottF: Top view of joint.....	116
140.	Field specimen G5VHW-CF1-BottF: Side view of joint.....	116

LIST OF FIGURES (CONTINUED)

141.	Field specimen G5VHW-CF1-BottF: Radiographic image of section B–C.....	116
142.	P-scan images of field specimen G5VHW-CF1-BottF: From TSC side of centerline using 45-degree probe	117
143.	P-scan images of field specimen G5VHW-CF1-BottF: From BSC side of centerline using 45-degree probe	117
144.	P-scan images of field specimen G5VHW-CF1-BottF: From BSC side of centerline using 70-degree probe	117
145.	Transducer articulation testing: Test setup	124
146.	Transducer articulation testing: Various articulation angle wedges	124
147.	Influence of transducer articulation angle on the maximum amplitude of the reflected signal	125

LIST OF TABLES

1.	Description of laboratory specimens	39
2.	Description of manufactured defects in the category 1 laboratory specimens	40
3.	Description of defects found by manual UT in the category 2 laboratory specimens	41
4.	Description of field specimens tested at HSS	42
5.	Description of field specimens tested at Stupp	43
6.	Inspection results of laboratory specimens	48
7.	Inspection results of blind field testing	77
8.	Inspection results of the first field testing at HSS	79
9.	Inspection results of the second field testing at HSS	79
10.	Inspection results of the third field testing at HSS	80
11.	Inspection results of the fourth field testing at HSS	83
12.	Inspection results of field testing at Stupp	85
13.	Consolidating the results of laboratory testing using laboratory specimens with rejectable defects	119
14.	Consolidating the results of field testing using field specimens with rejectable defects	120
15.	Assessing the detectability and rejectability of three inspection methods in the laboratory	122
16.	Assessing the detectability and rejectability of three inspection methods in the field	122

1. INTRODUCTION

This report documents efforts to evaluate the effectiveness of automated ultrasonic testing (AUT) as a replacement for radiographic testing (RT) for fabrication inspection of welds in steel bridges. An AUT system was tested in parallel with both RT and manual ultrasonic testing (UT) to determine the differences in the inspection results, to identify operational challenges that may be faced while implementing AUT in a fabrication shop environment, and to develop the appropriate procedures for implementing AUT as a replacement for RT.

Fabrication inspection of welds is intended to ensure the quality of workmanship during the fabrication process. Welding processes have the potential for introducing internal defects or discontinuities that are not observable by visual inspection. These discontinuities generally can be described as either volumetric defects that are three-dimensional (e.g., slag inclusions and porosity) or planar defects that are essentially two-dimensional (e.g., cracks or lack of fusion). Internal discontinuities can reduce the strength of the weld and provide stress risers that act as fatigue crack initiation sites. An inspection is intended to identify internal discontinuities and determine their severity so that significant discontinuities can be repaired during the fabrication process. Two nondestructive evaluation (NDE) methods are available in the American Association of State Highway and Transportation Officials (AASHTO)/American Welding Society (AWS) D1.5M/D1.5: 2002 Bridge Welding Code⁽¹⁾ to detect internal defects in welds, UT and RT.

The most commonly used inspection method is RT, which provides a radiographic image of the weld being inspected. This method is required by code for complete joint penetration (CJP) welds (e.g., groove welds) that are subject to tensile stresses or stress reversal. RT is preferred by bridge owners because the radiograph can be retained for future reference, and it provides quantitative confirmation of the inspection process through the visibility of image quality indicators (IQIs) in the radiograph. Also, the extent of the area inspected is observable on the radiograph, providing evidence that a given weld has been fully inspected. Furthermore, volumetric and planar defects can be observed on the radiograph, providing information on the spatial location and the extent of the discontinuity.

In general, RT is less likely to detect planar defects than volumetric defects. (See references 2, 3, 4, 5, and 6.) For example, if the crack is parallel to the x-ray photon path or is tightly closed, the crack may not be detected. Also, no information on the through-thickness depth of the crack is available on the radiograph.^(2,3)

A significant disadvantage of RT is the health risks associated with the use of radioactive materials within the fabrication shop. As a result of the health risks, RT inspections frequently are conducted in isolated locations within the shop or behind protective shielding. Inspections are sometimes conducted during overnight shifts when a shop is less populated. The relocation of the welded assemblies to conduct RT is common. The procedures required to protect workers from the health hazards of RT increase the time required and the costs associated with bridge fabrication.

UT reports provide substantially less information than radiographs relative to the nature of any internal discontinuities and the inspection process. UT reports typically consist of tabulated data indicating the amplitude of the ultrasonic response and the corresponding spatial data as recorded by the technician. The ultrasonic signals are not retained as part of the inspection report. The UT technician is relied on to ensure that a given weld has been inspected fully and effectively. The UT method has an inherent reliance on the capabilities of the inspector. The variability between UT inspectors is well known.^(2,3) Additionally, UT provides no information on the characteristics of a given discontinuity and, as such, all are analyzed as if they were cracks. As a result of these factors, bridge owners traditionally have preferred RT. However, UT has the advantage of minimal health hazards associated with the inspection process and can be conducted at any appropriate location within a fabrication shop. UT is also more sensitive to planar defects than RT. The effect of planar defects can be more severe than volumetric defects because of the high stress concentrations associated with their crack-like shape.

AUT provides significantly more information to the bridge owner than does UT. Images created by AUT systems can provide evidence that a given weld has been fully inspected, the ultrasonic signals can be retained for future reference, and the spatial location and extent of the defects can be displayed in images created by the system. In addition, the depth of a defect can be determined and used, making for efficient repairs. The differences in the detection of volumetric and planar defects that exist between RT and UT also exist between RT and AUT. The effects of these differences are explored in this research. AUT typically requires more sophisticated instrumentation, additional training for technicians, and may require additional time to complete scanning relative to UT or RT. These implications and the ability of AUT to perform in a shop environment are also explored as part of this project.

PROJECT SCOPE AND OBJECTIVE

The objective of this research is to determine if AUT can be used as a replacement for RT for fabrication inspection of steel bridges. There are many issues that need to be addressed to determine if such a replacement is possible and beneficial. These issues include the following:

- Does AUT provide equivalent or improved inspection results relative to RT?
- Is it possible to apply the manual UT procedures described in the code to an AUT system?
- Is it feasible to use AUT in and around a shop environment?
- Does AUT provide an effective quality control tool that would satisfy the needs of bridge owners?
- Is the cost or training requirements of AUT systems prohibitive?

To achieve the project objectives, an AUT system was identified and procured. Later, the AUT test results were compared to manual UT and RT test results. The tasks to be conducted were:

- Literature search to identify previous efforts to compare the three commonly used nondestructive weld inspection techniques (manual UT, AUT, and RT) in industries other than bridge fabrication.
- Market survey of the available sources for AUT systems.
- Laboratory proof-of-concept study comparing AUT and RT inspection of butt welds containing common defects.
- Field-testing studies to assess the feasibility, accuracy, reliability, and defect sensitivity of AUT relative to RT in a bridge fabrication shop during the fabrication process.

The identified tasks were executed between August 2000 and February 2003. Updates were provided to the National Steel Bridge Alliance (NSBA), a unified industry organization of businesses and agencies dedicated to the development of cost-effective steel bridges. This organization provides a forum for communicating research progress with both bridge owners and steel bridge fabricators.

2. BACKGROUND

The fundamental role of NDE for the quality control of welding practices is to detect internal defects, determine the severity of any defects, and identify the appropriate defect disposition (i.e., accept or reject). The requirements governing the inspection process are preeminent, and these are provided by the AASHTO/AWS D1.5M/D1.5: 2002 Bridge Welding Code.⁽¹⁾ The following sections provide background on the development of weld inspection and code requirements that influence the detection, evaluation, and disposition of defective welds.

AWS D1.5 WELDING CODE

AWS is a professional association concerned with the fabrication and welding industries. AWS produces and supports a wide range of technical resources regarding welding technology, including a series of consensus specifications regarding welding practices. AWS produced its first welding code in 1928 for fusion welding and gas cutting in building construction. A committee was formed in 1934 to prepare specifications for welding practices for highway and railway bridges. The first bridge specification was published in 1936 and was adopted for use by AASHTO in 1941. Two separate AWS committees, responsible for building and bridge specifications, respectively, were joined in 1963 to form the Structural Welding Committee.⁽¹⁾ In 1969, the first ultrasonic inspection procedures were issued by AWS as an appendix in both the Code for Welding in Building Construction (D1.0–69) and the Specification for Welded Highway and Railway Bridges (D2.0–69).⁽⁷⁾ The appendixes were identical in each code, with the exception of the minimum acceptance levels for weld discontinuities, with the bridge code being slightly more restrictive than the building code.⁽⁷⁾

Between 1962 and 1974, a series of Federal Highway Administration (FHWA) circular memorandums required alterations or additions to the existing AWS codes to meet specific needs related to highway bridges. This resulted in AASHTO publishing another welding code in 1974, separate from the AWS code, entitled Standard Specification for Welding of Structural Steel Highway Bridges. Finally, in 1982, a joint committee was formed from AWS and AASHTO representatives to develop a single document to meet the needs of the bridge community. The Bridge Welding Code D1.5⁽¹⁾ is the result of an agreement between AWS and AASHTO to produce a joint document that addresses AASHTO's needs and makes the AASHTO revisions mandatory. This code is similar to the present AWS D1.1: Structural Welding Code—Steel,⁽⁸⁾ but has several significant differences. Among these differences are the addition of a fracture control plan for highway bridges and the elimination of sections on statically loaded and tubular structures.

Chapter 6 of the D1.5 code,⁽¹⁾ “Inspection,” addresses the requirements for quality control of welding practices for bridges. This chapter is supplemented by requirements in chapter 12, “AASHTO/AWS Fracture Control Plan (FCP) for Nonredundant Members.” Commentaries on the requirements of chapter 6 are included in the code. Additional sections of the code that are relevant to chapter 6 include annex VII, which addresses alternate calibration procedures and various inspection forms.

Chapter 6 of the D1.5 code⁽¹⁾ includes provisions for magnetic particle testing (MT), RT, and UT. Section 6.7.1 of the code requires the use of RT for all CJP welds subject to calculated tension or stress reversal. CJP welds in corner joints require UT testing, while either RT or UT is allowed for CJP welds subject to compression or shear. Section 6.7.2 of the code requires MT for fillet welds and partial joint penetration (PJP) welds.

ACCEPTANCE-REJECTION CRITERIA FOR UT VERSUS RT

The AASHTO/AWS D1.5M/D1.5: 2002 Bridge Welding Code⁽¹⁾ includes defect acceptance criteria for both UT and RT. These criteria are an essential part of the effectiveness of the code in ensuring the quality of workmanship. This section will describe the defect acceptance criteria and issues surrounding classifying defects according to the code. For the application of RT, defects appearing on a radiographic film are typically termed *discontinuities*. For the application of UT, signals resulting from internal reflectors are termed *indications*. This terminology allows the internal features of welds to be identified without being considered acceptable or rejectable.

For RT, the defect acceptance criterion consists of two parts: First, for a weld to be acceptable, no cracks may be evident on the radiograph. Second, a combination of length, weld size, and spacing is used to determine if volumetric discontinuities are acceptable, and can remain in the weld, or are rejectable, thereby requiring the weld to be repaired.

The acceptance criteria for UT are based on two factors: (1) the amplitude of the ultrasound reflected from the surface of the indication, and (2) the indication length. The amplitude of the waveform is determined in decibels (dB) relative to a standard 1.5-millimeter (mm) (0.06-inch) side-drilled hole in a reference/calibration block. An indication is rated based on the amplitude of the reflected ultrasound and the indication length, and is placed in one of four classes: A, B, C, or D. Figure 1 illustrates the threshold acceptance levels for tension welds as defined in table 6.3 in the AASHTO/AWS D1.5M/D1.5: 2002 Bridge Welding Code.⁽¹⁾ From figure 1, assuming a 25.4-mm- (1-inch-) thick steel plate, a class A indication would have a rating of +8 dB or less. Class A indications are rejectable under all conditions. Class B indications having a rating of +9 dB in the same plate would be rejectable only if the length was greater than 20 millimeters (mm) (0.75 inch). Class C indications having a rating of +10 dB in this plate would be rejectable only if the indication length was greater than 50 mm (2 inches) and the indication was located in the middle half of the weld or the indication length was greater than 20 mm (0.75 inch) and located in the top or bottom quarter of the weld thickness. An indication of +11 dB or greater would be classified as class D and would be acceptable. There are two important issues to be recognized in this figure: First, the scale is such that the smaller the indication rating, the larger the reflection amplitude. Second, the difference between an indication that is acceptable and one that is unacceptable is very small. For example, the difference between an acceptable class D and rejectable class C indication may be as small as 1 dB.

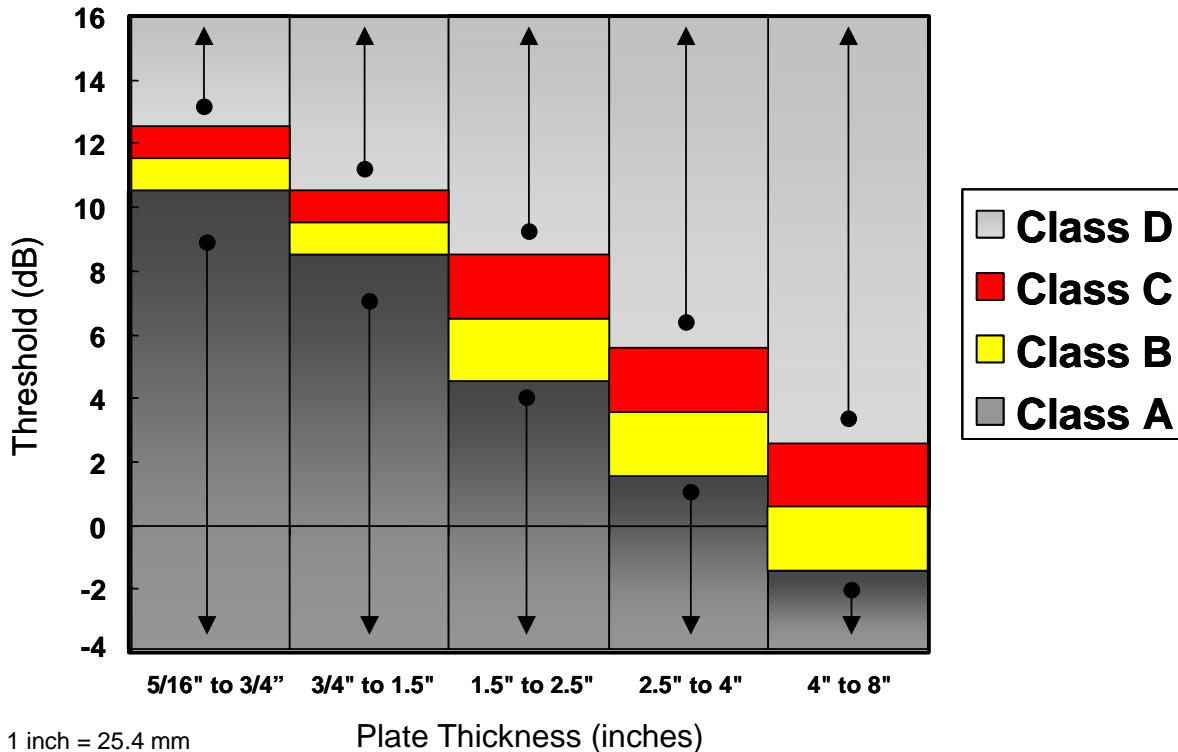


Figure 1. Rating chart plotted from table 6.3 in the AASHTO/AWS D1.5M/D1.5: 2002 Bridge Welding Code,⁽¹⁾ showing class A, B, C, and D decibel levels for 70-degree angle.

The differences between RT and UT are important to this study. In RT, a crack has a different appearance than a volumetric defect. However, the through-thickness extent of a crack cannot be known from the radiograph alone. The physics behind RT dictate a reduced sensitivity to cracks that lie parallel to the direction of photon travel. As a result, RT has reduced sensitivity to vertical cracks that may be critical defects from a fracture perspective. Based on RT's reduced sensitivity to vertical cracks, UT can produce significant safety advantages.⁽³⁾

There are several limitations in the ability of UT to determine the size and shape of defects. These limitations stem from theoretically invalid assumptions made in defining the threshold criteria used to rate defects. The first assumption is that the amplitude of a reflection is directly related to the through-wall extent, or height, of the indication. While the response amplitude is an important factor to be considered, it is affected by many test parameters (e.g., defect type, orientation, surface texture, reflectivity, and size).^(2,5) The second assumption is that reflection amplitude alone defines the severity of the defect. In this regard, the code assumes that all indications are cracks (the most severe type of defect from a fracture perspective). The code does not consider that defects may be slag inclusions or porosity, which can be less susceptible to fracture. The third assumption is that a unique relationship exists between the angle of incidence of the ultrasonic beam and the reflection amplitude from a given indication. The code assumes an angle of incidence equal of 90 degrees for reference. Furthermore, the code assumes that as the incidence angle decreases, the reflection amplitude decreases. Therefore, for a 70-degree incidence angle, the reflection amplitude would decrease by 6 decibels (dB) relative to the

reference reflection. Similarly, 60-degree and 45-degree incidence angles result in 9-dB and 11-dB reductions, respectively. This results in threshold values for defect categorization that vary according to the incidence angle of the transducer. For example, table 6.3 in the AASHTO/AWS D1.5M/D1.5: 2002 Bridge Welding Code⁽¹⁾ indicates that for plates greater than 38 mm (1.5 inches) through 60 mm (2.5 inches), a class A defect amplitude is +4 dB for a 70-degree angle, +7 dB for a 60-degree angle, and +9 dB for a 45-degree angle. However, the interaction of response amplitude, incidence angle, and defect size is complex. The amplitude of response for a given incidence angle will vary significantly based on the size of the defect, with smaller defects being less sensitive to the incident angle than larger defects.⁽⁹⁾

The scanning pattern prescribed in the code requires articulation of the transducer ± 10 degrees from normal to the weld length. This requirement recognizes the sensitivity of the reflection amplitude to the orientation of the defect in a horizontal plane. The articulation motion is intended to address defects that are misaligned (i.e., not parallel to the weld axis, and/or having a maximum response at incidence angles other than perpendicular to the weld axis). Articulation allows the inspector to achieve an improved alignment with a given defect, which can result in significantly larger ultrasonic responses. Research conducted by Serabian⁽⁹⁾ indicates that the reduction in amplitude for certain discontinuities skewed as little as 5 degrees can be greater than 40 dB. Recent research conducted by Thavasimuthu, et al.,⁽¹⁰⁾ indicates that for the 2.25-megahertz (MHz) transducer typically used for code inspections, a skew angle of 5 degrees can result in an amplitude reduction greater than 5 dB, while a skew angle of 10 degrees can result in an amplitude reduction greater than 10 dB. Given the relatively small difference between rating an indication as acceptable or rejectable (see figure 1), this effect could have a significant impact on the inspection results. The code provides for an optimum incidence angle to be obtained provided that a given defect is not skewed more than 10 degrees on a horizontal plane; however, it does not generally allow for variations in the inclination of a defect. The exception to this is the evaluation of fusion-type defects, for which the code requires transducer incidence angles be adjusted to maximize reflection amplitude. The available transducer incidence angles are limited to 45 degrees, 60 degrees, and 70 degrees.

Because of response amplitude variability, it is difficult to determine the size of the defect relative to the code. The threshold criteria set out in the code is modeled, to some extent, on the threshold criteria for RT.⁽²⁾ Generally, the amplitude thresholds are intended to mimic the capabilities of RT by setting threshold values at an assumed percentage of the plate thickness. For example, RT may provide a sensitivity of 2 percent of the material thickness, allowing for larger indications in thicker material. For UT, the code mimics this RT requirement by allowing larger amplitude reflections to be acceptable as the material thickness increases (see figure 1).

Despite some shortcomings in the present code, it has been used with relative success since it was introduced in 1969. A study by Jonas and Scharosch⁽³⁾ indicated significant variability in the results obtained by applying the code requirements to weld inspection using different operators. The research concluded that volumetric defects were more likely to be detected than planar defects; that vertical cracks as large as 40 percent of the plate thickness could be accepted in nearly 33 percent of the inspections; and that when using three operators, disagreement existed in the acceptance or rejection of 35 percent of the discontinuities examined. Therefore, operator variability was identified as a significant factor in poor UT results. The reduction of operator variability is an important advantage of AUT.

3. AUT EQUIPMENT DESCRIPTION

AUT systems have been introduced for many different applications—from the production of engineering materials to the inspection of rails, tubes, and piping.⁽¹¹⁾ The use of AUT systems in the nuclear field has been widespread for many years,⁽¹²⁾ and many different types of AUT systems have been developed for specific applications. One particular application involves the inspection of pipeline girth welds. The American Society for Testing and Materials (ASTM) standard test method, Standard Practice for Mechanized Ultrasonic Examination of Girth Welds Using Zonal Discrimination With Focused Search Units,⁽¹³⁾ is one of the first general standards to specifically allow the use of AUT systems for weld inspection. The procedures described in this standard are more complex than typically are applied to welds in highway bridges. AUT systems have also been developed for civil engineering applications (e.g., pin inspection).⁽¹⁴⁾ Recently, both manual and more automated scanning systems have been used to examine bridge components such as hanger pins.^(15,16) These systems typically generate C-scans to characterize any observed indications.

AUT systems typically consist of ultrasonic pulse-echo instrumentation and a computerized data acquisition (DAQ) system, coupled with a spatial control system that tracks the position of the ultrasonic transducer during testing. The spatial control system may be active (where a robotic scanner moves the transducer across a specified scanning pattern) or passive (where the position of the transducer is recorded as the transducer is controlled manually). The position of the transducer and the associated ultrasonic waveforms are recorded by the DAQ system and can be presented in a variety of formats for interpretation by qualified personnel. Typical formats for data presentation include A-scans, B-scans, and C-scans. A-scan displays are commonly used in UT and consist of a two-dimensional image of the ultrasonic waveform with time along the abscissa (x-axis) and signal amplitude along the ordinate (y-axis). A B-scan display consists of time plotted along the ordinate and scan position along the abscissa. The amplitude of the ultrasonic waveform is color-coded and displayed along with its associated time data. A C-scan display is a planar image with three dimensions (the x- and y-positions of an indication plotted along the abscissa and the ordinate, respectively, and the third dimension being a particular characteristic of the A-scan data plotted by color). The amplitude of the ultrasonic signal is the most commonly plotted characteristic; however, a time or frequency characteristic may also be displayed.

SYSTEM SELECTION

To select an appropriate AUT system for application to highway bridges, a series of commercially available systems were considered. These systems were compared with the existing code requirements to determine if the systems were capable of conducting an inspection that substantially conformed to the existing requirements. There are several reasons to use the existing code as a guideline to AUT system selection: First, the code is widely accepted as being effective by bridge owners and, as such, an AUT system meeting the current requirements could be adopted easily for use. The code currently allows the use of UT for compression members, all tee and corner CJP welds, and uses UT to enhance RT for the inspection of fracture-critical tension welds (see section 12.16).⁽¹⁾ Second, revisions to portions of the code that define

rejectable and acceptable defect criteria may need to be adjusted for AUT systems that cannot perform the scanning described in the code. Specifically, AUT systems that are not capable of articulating a transducer ± 10 degrees during scanning will be unable to maximize the reflected signal. As a result, the rating for a particular indication may be different when an AUT system without articulation is employed. Adjustments to the decibel rating scale would be required to provide a level of sensitivity equal to manual UT. Modifications to this particular portion of the code would be difficult and, at a minimum, would require significant additional research. Third, inspectors are knowledgeable in the existing code, so changing from UT to AUT would require minimal retraining.

P-SCAN SYSTEM CHARACTERISTICS

The projection image scanning (P-scan) system in figure 2 was selected for this project. The P-scan system is an integrated computer-based, digital ultrasonic testing and analysis system.

System Components

The P-scan system has three main components: (1) the processor unit, (2) the scanner module, and (3) the laptop personal computer (PC) platform. The data acquisition, digitizing, and digital signal processing functions are all carried out in the P-scan processor unit. The scanner module is a position encoding device designed to record the position and rotation of the ultrasonic transducer during scanning. The laptop PC is used for post-processing and graphical presentation of data.

The scanner module, known as the manual weld scanner (MWS-1), includes a magnetic base that is attached to the steel plate adjacent to the weld being inspected. A 300-mm- (12-inch-) long scanner arm is attached to the magnetic base and has three degrees of freedom (DOF) as indicated in figure 3. The arm can rotate about the magnetic base and extend along a linear bearing attached to the base. The rotation (α) and extension (L) of the scanner arm are recorded by encoders in the magnetic base so that the position of a transducer is defined in polar coordinates. A third DOF is provided at the end of the scanner arm where the transducer is mounted. The rotation of the transducer or skew angle (β) is also recorded by an encoder. The operating range of α is limited to 180 degrees, while L is limited to 300 mm (12 inches) and β is limited to 300 degrees. Even though the transducer can freely rotate 360 degrees, the rotation output of β is only valid within the specified range of 300 degrees (as shown in figure 3). The positional data (α , L, and β) are combined with the time-of-flight information contained in the A-scan to determine the reflection location. The length of the scanner arm (300 mm (12 inches)) is user-selectable. Longer scanner arms are available from the manufacturer.

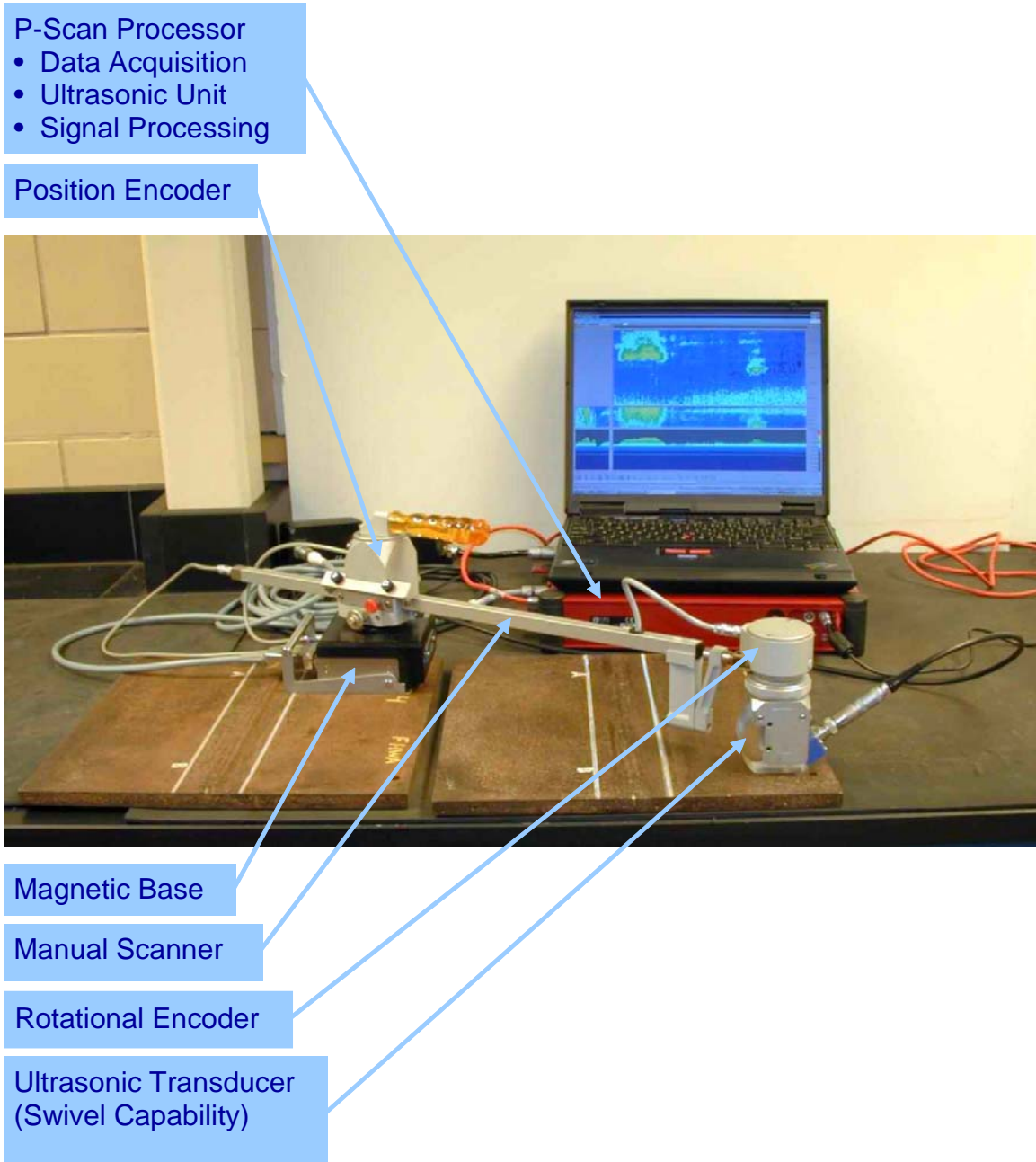
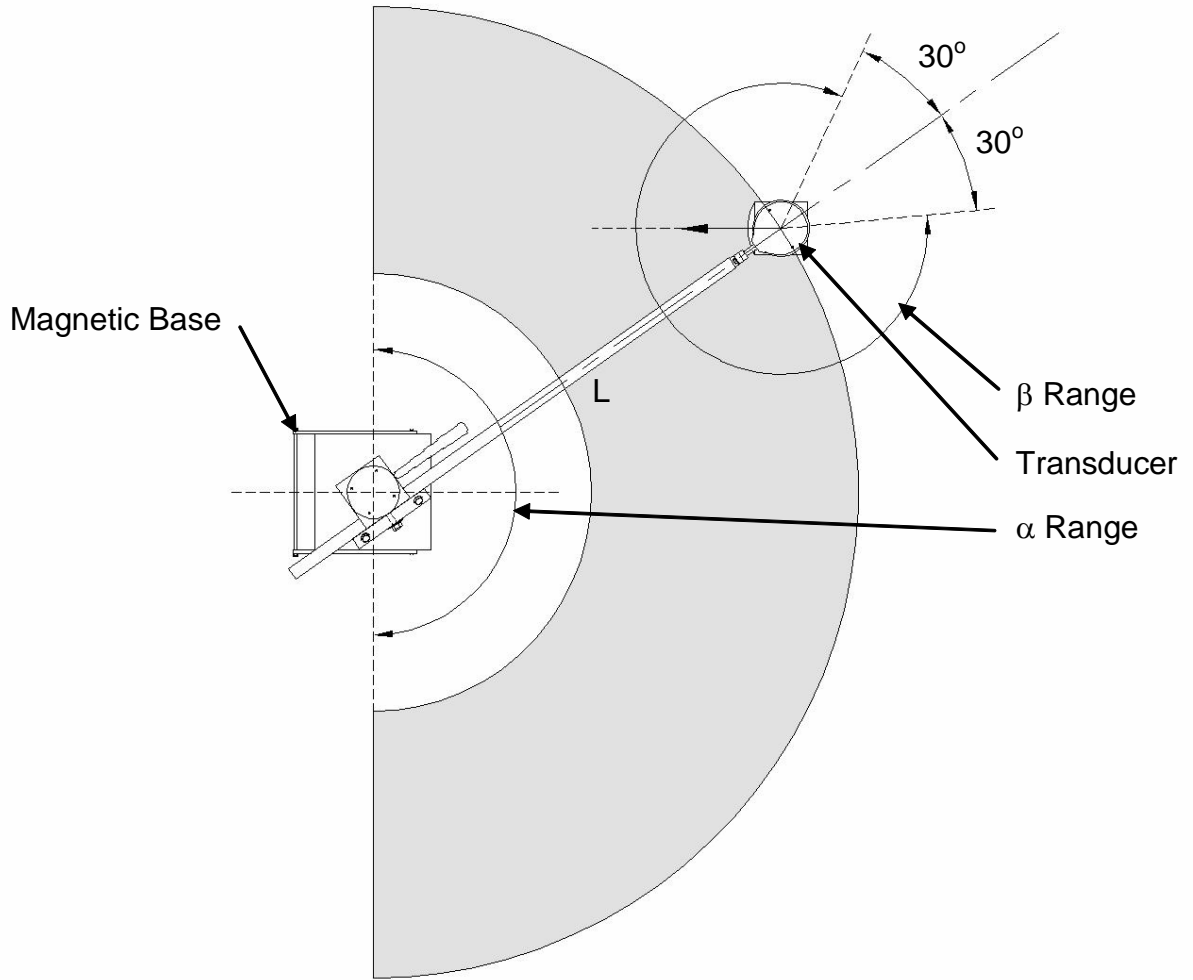



Figure 2. Photograph of the P-scan system showing the data acquisition system and the scanning arm holding the ultrasonic transducer.



 Free movement area of the probe

α Range: 180°

L Range: 300 mm (12 inches)

β Range: 300°

1 inch = 25.4 mm

Figure 3. Schematic diagram of the MWS-1 scanner, indicating three DOF: (1) scanner arm rotation angle α , (2) scanner arm extension L, and (3) transducer skew angle β .

System Setup

MWS-1 can be positioned on the plate in three different scanning configurations. Figures 4 through 6 show schematic diagrams of the scanner positioning configurations. Depending on the plate width, plate thickness, and the availability of a convenient location adjacent to the weld to place the magnetic base, a suitable configuration can be selected for the inspection. For example, consider the plate shown in figures 4 and 5. The coordinate origin (or datum) is placed at the far left edge of the plate on the centerline so that the positive y-axis coincides with the weld centerline. The x-axis lies along the left edge of the plate with the positive x-axis directed upward and the positive z-axis directed into the plate. For convenience, the section of the plate that falls in the positive x-axis is designated as the top section of the centerline (TSC), and the section of the plate that falls in the negative x-axis is designated as the bottom section of the centerline (BSC). The TSC configuration shown in figure 4 has the scanner's magnetic base placed on the BSC side, with the transducer scanning the weld from the TSC side. Conversely, the BSC configuration shown in figure 5 has the scanner's magnetic base placed on the TSC side, with the transducer scanning the weld from the BSC side. Using the TSC and BSC configurations together, the weld can be inspected from both sides of the weld centerline; however, separate setups and data files should be created for each configuration. By placing the magnetic base at the positions shown in figures 4 and 5, the BSC and TSC configurations allow plates up to 609.6 mm (24 inches) wide and 31.75 mm (1.25 inches) thick to be inspected even though the scanner arm's extension length is only 300 mm (12 inches). For plates greater than 609.6 mm (24 inches) wide and 31.75 mm (1.25 inches) thick, the scanner arm cannot reach the entire weld using the BSC and TSC configurations. Thus, the width of the plate must be segmented and each segment must be scanned separately. The third configuration is designated as the *Both* configuration (figure 6) and permits the inspection of the weld from both sides of the centerline with a single setup and data file. With the Both configuration, the setup time is reduced by approximately 66 percent, leading to a faster inspection. Plates up to 304.8 mm (12 inches) wide and 12.7 mm (0.5 inch) thick can be inspected using the Both configuration. For plates greater than 304.8 mm (12 inches) wide and 12.7 mm (0.5 inch) thick, the scanner arm does not extend sufficiently to scan the entire weld from both sides. Thus, the width of the plate must be segmented and each segment must be scanned separately. Carefully examining and comparing figures 4 and 5 with figure 6 reveals the reason behind the differences in the width and thickness limitations of each configuration. In the TSC or BSC configuration (figure 4 or 5, respectively), the scanner base is placed on one side of the weld in the middle of the plate. This allows the scanner arm to essentially rotate along the length of the weld. Meanwhile, in the Both configuration (figure 6), the scanner base is positioned in line with the weld but to the side of the plate. This forces the scanner arm to essentially rotate transverse to the weld axis. Thus, the thickness and area of the plate that can be scanned using the TSC or BSC configuration is approximately twice as large as the thickness and area that can be scanned using the Both configuration.

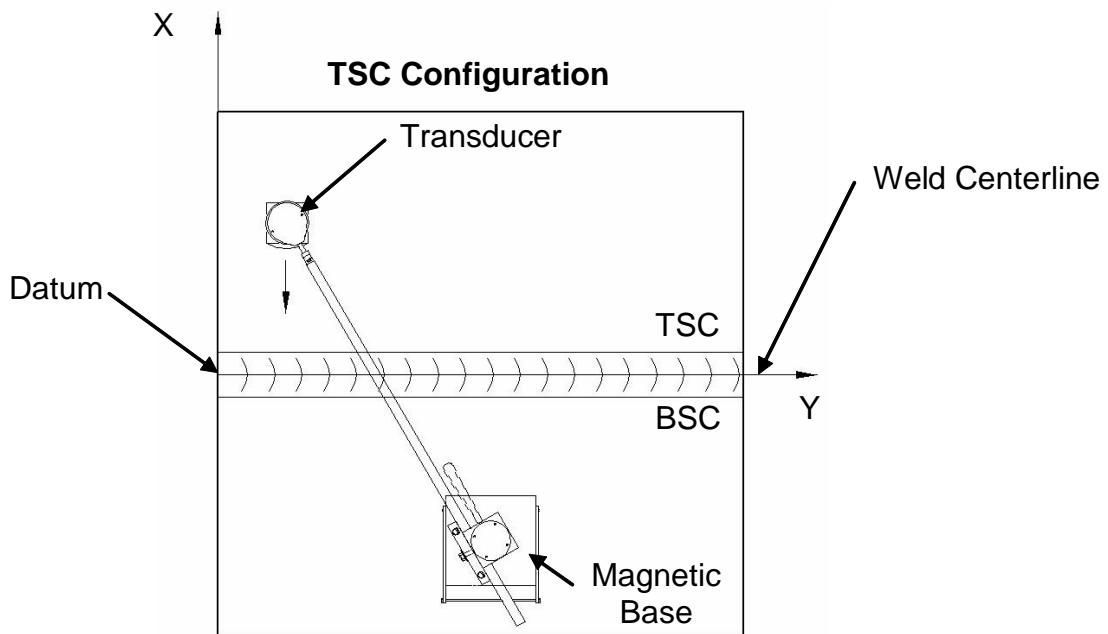


**Figure 4. Positioning/setup configuration of MWS-1 scanner on the plate:
TSC configuration describes scanning the weld from the TSC side
of the centerline.**

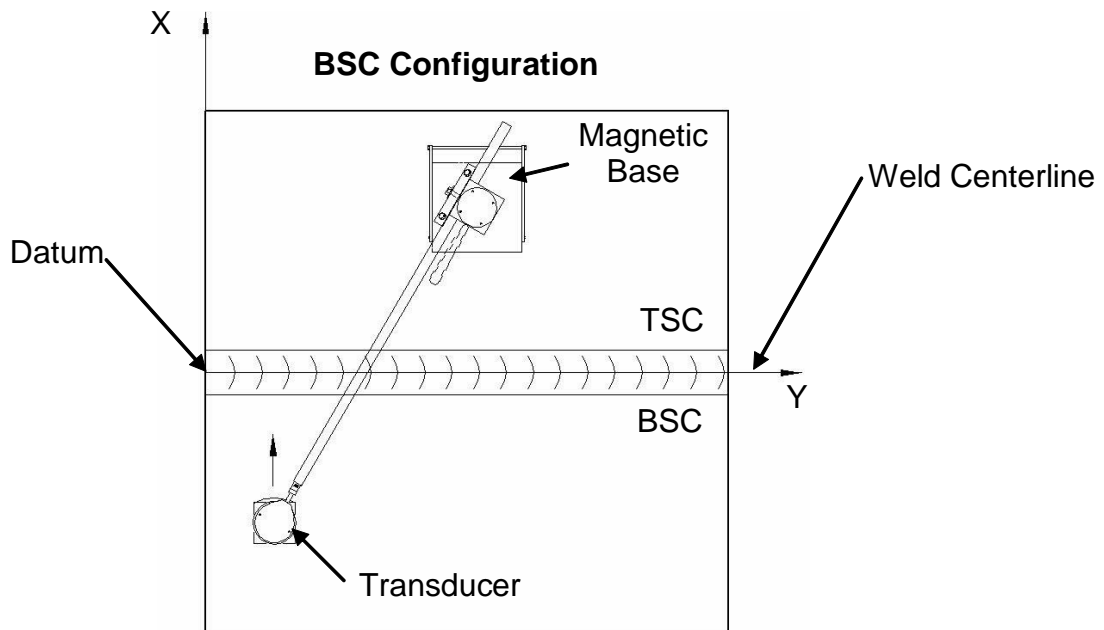


**Figure 5. Positioning/setup configuration of MWS-1 scanner on the plate:
BSC configuration describes scanning the weld from the BSC side
of the centerline.**

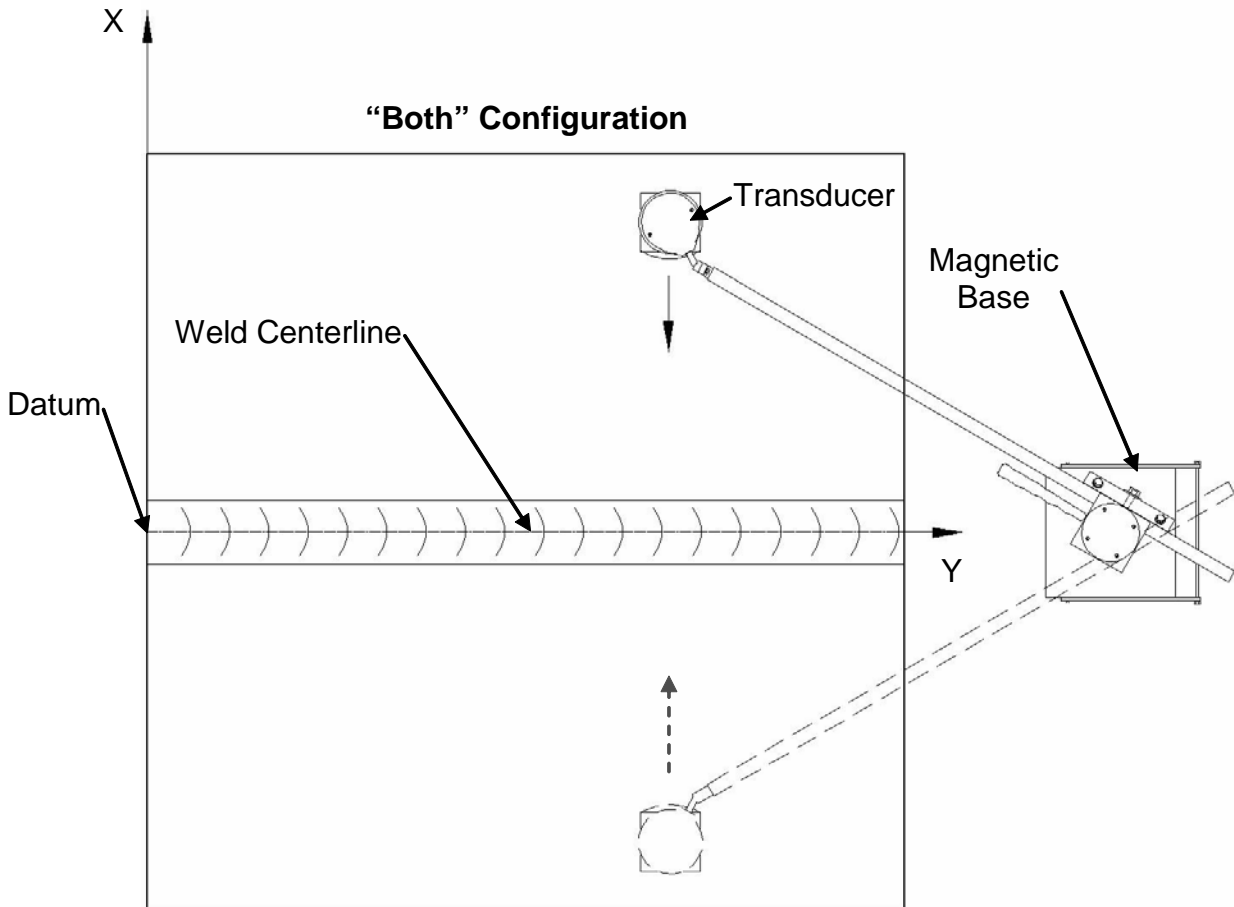
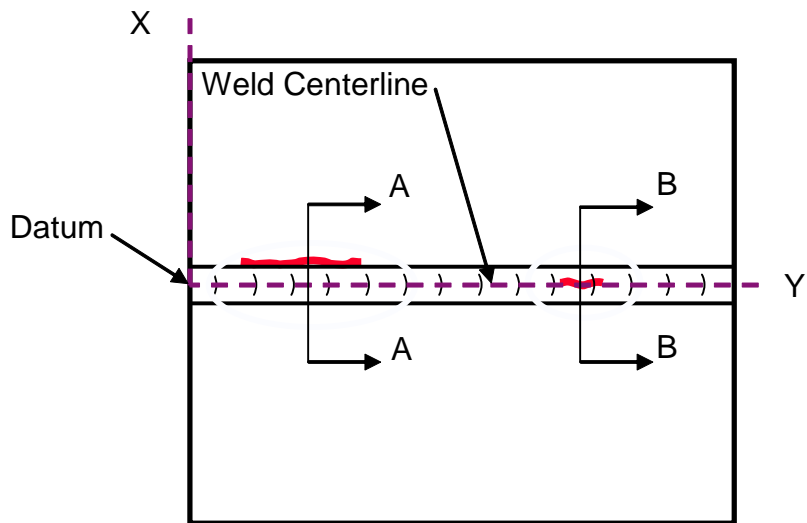


Figure 6. Positioning/setup configuration of MWS-1 scanner on the plate: “Both” configuration describes scanning the weld from both sides of the centerline in a single setup.

System Output

The P-scan system creates and displays the geometry of an indication on three projection planes. To illustrate this, consider laboratory specimen S033 shown schematically in figure 7. This 12.7-mm- (0.5-inch-) thick plate contains two implanted cracks—one at the toe of the weld (figure 8) and one at the root of the weld (figure 9). The appearance of these cracks on a standard radiograph is shown in figure 10. The radiograph shows the entire weld, including the heat-affected zones (HAZ). Figures 11 through 13 show images created by the P-scan system from the inspection of laboratory specimen S033. Figures 11 and 12 display the actual images created by the P-scan system during and after scanning, respectively. Figure 13 illustrates the three projection planes associated with the P-scan images. The geometries of the toe and root cracks are clearly shown in these figures. The region that is inspected by the P-scan and displayed in the P-scan images includes the weld area and the HAZ (i.e., the HAZ is generally taken to be 6.35 mm (0.25 inch) on either side of the weld bevels at the end of the toe). Detailed descriptions of the P-scan images in figures 11 through 13 are as follows:

- **C-Scan (Plan View):** The C-scan image is created from the projection of the indication geometry in the weld onto the horizontal plane. The dashed lines are the representation of the weld bevels. The C-scan image reveals the x-position, the y-position, and the length of the indications. The C-scan image is analogous to the standard radiographic film.
- **B-Scan (Cumulative or Noncumulative End-View Image):** The B-scan image is created from the projection of the indication geometry in the weld onto the vertical plane perpendicular to the centerline. The solid lines represent the weld bevels. The B-scan image reveals the orientation of the indications.
- **Side View:** The side view image is created from the projection of the indication geometry in the weld onto the vertical plane along the weld centerline. The side view image reveals the depth of the indications.
- **Amplitude Profile:** The bottom two images in figures 11 and 12 display the amplitude of the echo detected by the transducer in decibels. The positive decibel (+dB) readings in figures 11 and 12 indicate that the echoes from the indications have exceeded the calibration reference-level echo. Conversely, the negative decibel (-dB) readings indicate that the echoes from the indications are below the calibration reference-level echo. Generally, large indications are positive, while small indications are negative. The horizontal line marked as the threshold level for imaging is set up solely for imaging purposes by the P-scan system. Any echoes crossing this line will create colored pixels in the three projection images (i.e., C-scan, B-scan, and side view). The threshold level for imaging is generally selected based on the plate thickness and the UT acceptance-rejection criteria in tables 6.3 and 6.4 from the AASHTO/AWS D1.5M/D1.5: 2002 Bridge Welding Code.⁽¹⁾ In this report, the color bars in figures 11 and 12 associate decibel levels with specific colors. Specifically, the bars and corresponding images contain nine colors (i.e., red, orange, light yellow, dark yellow, light green, dark green, light blue, dark blue, and purple), with red being the highest amplitude and purple being the lowest amplitude responses.



**Figure 7. Laboratory specimen S033:
Schematic diagram showing two
implanted cracks.**

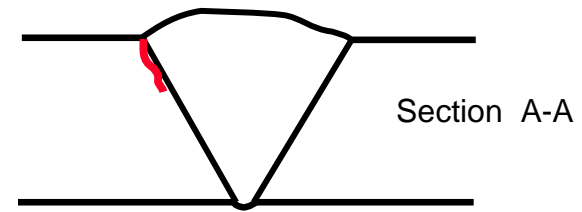


**Figure 8. Laboratory specimen S033:
Schematic diagram of toe crack.**

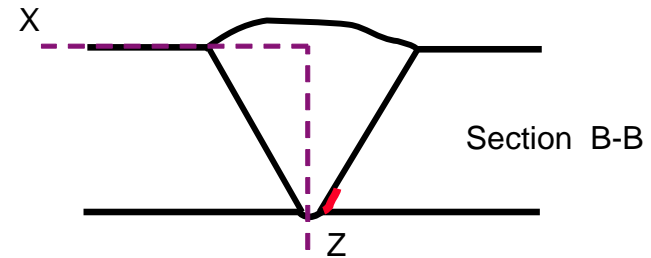


**Figure 9. Laboratory specimen S033:
Schematic diagram of root crack.**

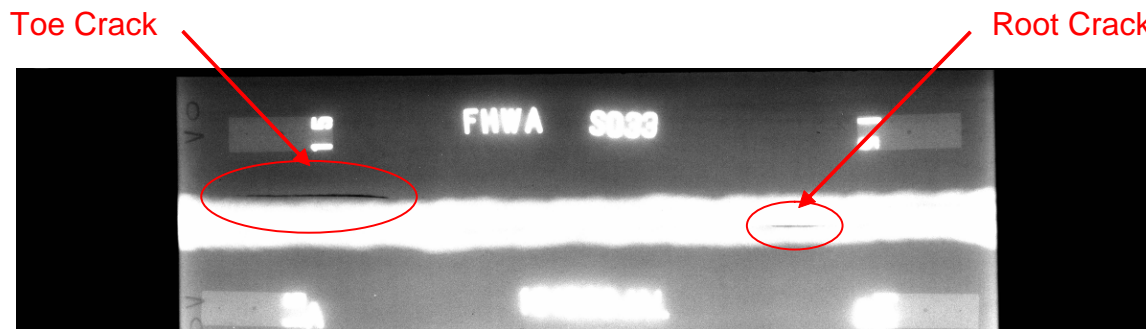


**Figure 10. Laboratory specimen S033: Radiographic image
shows the two implanted cracks.**

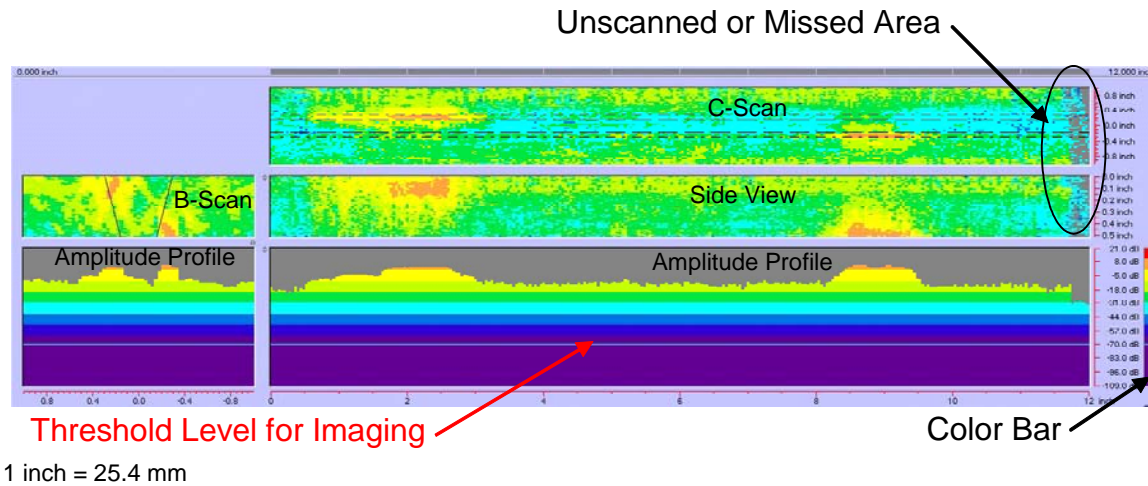


Figure 11. P-scan images of laboratory specimen S033: Displayed in logarithmic mode during scanning to ensure full coverage of the weld.

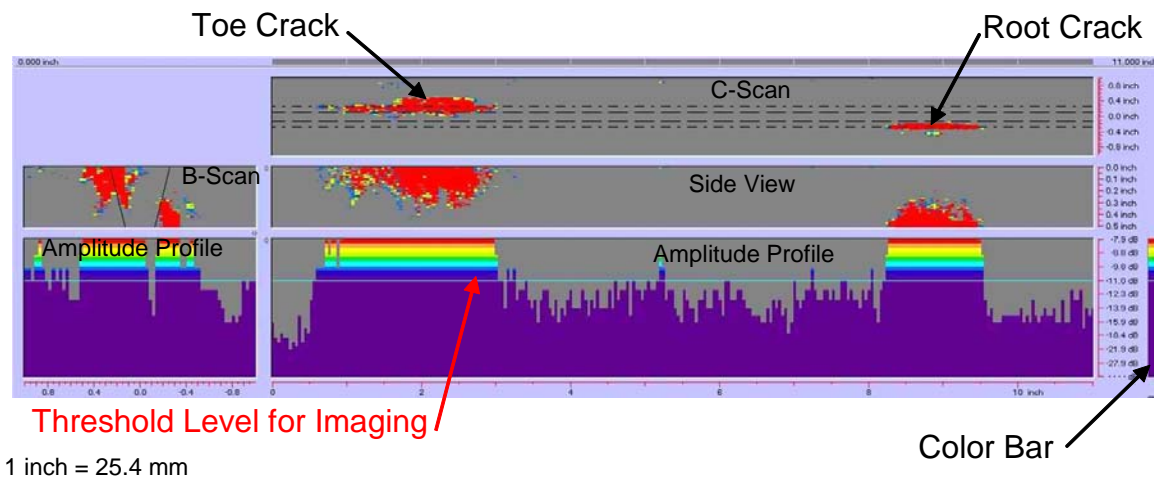


Figure 12. P-scan images of laboratory specimen S033: Displayed in linear mode after scanning (highlighting only the indications in the weld).

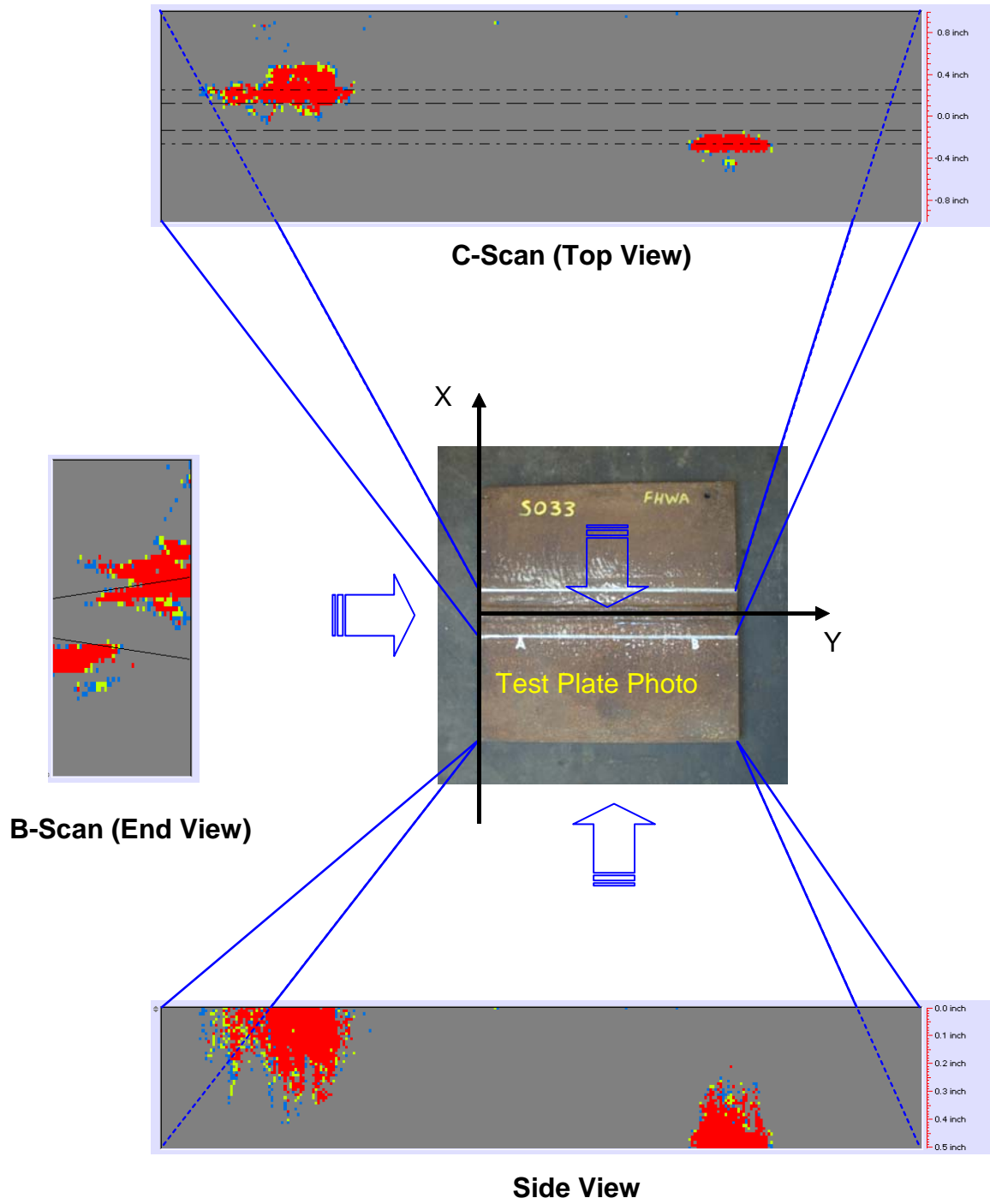


Figure 13. P-scan images on three projection planes.

As mentioned earlier, figures 11 and 12 show the P-scan images created during and after scanning, respectively. The logarithmic mode for imaging is selected during scanning, and the linear mode for imaging is selected after scanning. The logarithmic mode can display a wide range of echo amplitudes (160 dB), while the linear mode can only display an echo amplitude range of 20 dB. In the logarithmic mode, the threshold level for imaging can be lowered so that smaller amplitude echoes received by the transducer are used to create a carpet of colored pixels over the gray background color (figure 11). The use of the logarithmic mode ensures full inspection coverage of the entire weld with the region not colored being either missed or not yet inspected. This scenario is clearly shown in the right end of the C-scan and side view images in figure 11. These uncolored areas should be scanned to provide full inspection coverage of the weld. It is important to note that the P-scan system saves the highest amplitude echo received even if the same point or region is scanned multiple times. Once scanning of the weld is completed, the collected data can be displayed in the linear mode (figure 12), highlighting indications only. The threshold level for imaging in the linear mode can be determined using the plate thickness and the UT acceptance-rejection criteria in tables 6.3 and 6.4 from the AASHTO/AWS D1.5M/D1.5: 2002 Bridge Welding Code.⁽¹⁾ In the linear mode, only indications exceeding the threshold level for imaging are displayed. Note that the threshold level for imaging in the linear mode is chosen to be the indication level for the class D indication or slightly below. Also, the regions of the weld without indications are displayed using the gray background color.

The indication rating (d) and the geometric dimensions of a defect in the weld can be determined using marker lines in the P-scan images. The indication rating is the decibel reading relative to the zero reference level after having been corrected for sound attenuation (sections 6.19.6.3 through 6.19.6.5 of the AASHTO/AWS D1.5M/D1.5: 2002 Bridge Welding Code).⁽¹⁾ To illustrate this, P-scan images of laboratory specimen S033 in figures 12 and 14 are used as an example. The amplitude profile image in figure 12 shows that the peak amplitudes from the root and toe cracks are off the screen. Therefore, manually increasing the amplitude level will bring the peak amplitudes back onto the screen as shown in figure 14. The indication rating is read from the amplitude profile image in figure 14 by placing the solid horizontal marker line on the peak amplitude obtained from the defect. The numerical decibel value for the indication rating, which is designated as “A” in the P-scan system, appears in the P-scan’s marker window. The x-position of the defect is measured from the weld centerline, while the y-position is measured with respect to the datum. The y-position and the length of the defect are determined by moving the horizontal dotted marker to the 50-percent drop in the maximum amplitude as shown in figure 14. Then, the solid and dotted vertical markers are moved to the intersection of the horizontal dotted marker and the amplitude profile of the root crack. The numerical value for the y-position and the length of the root crack appear on the marker window as Y and ΔY , respectively. Similarly, the depth (Z) and the x-position of the root crack are determined using markers in the side view and C-scan, respectively.

The P-scan processor unit is equipped with a built-in logarithmic amplifier for the ultrasonic receiver. The amplifier ensures the accuracy of the echo signal. Unlike linear amplifiers that are used in traditional UT systems, logarithmic amplifiers have amplitude-dependant gain with logarithmic transfer characteristics. This means that the weak part of a signal is highly amplified, whereas the strong part is only slightly amplified. As a consequence, the P-scan system has no manual gain. Note that the echo signal displayed in a logarithmic amplifier scale appears to have

a different amplitude from the conventional linear echo signal. Therefore, the P-scan system must have an internal conversion routine that displays a linear echo signal on the screen instead of the logarithmic signal.

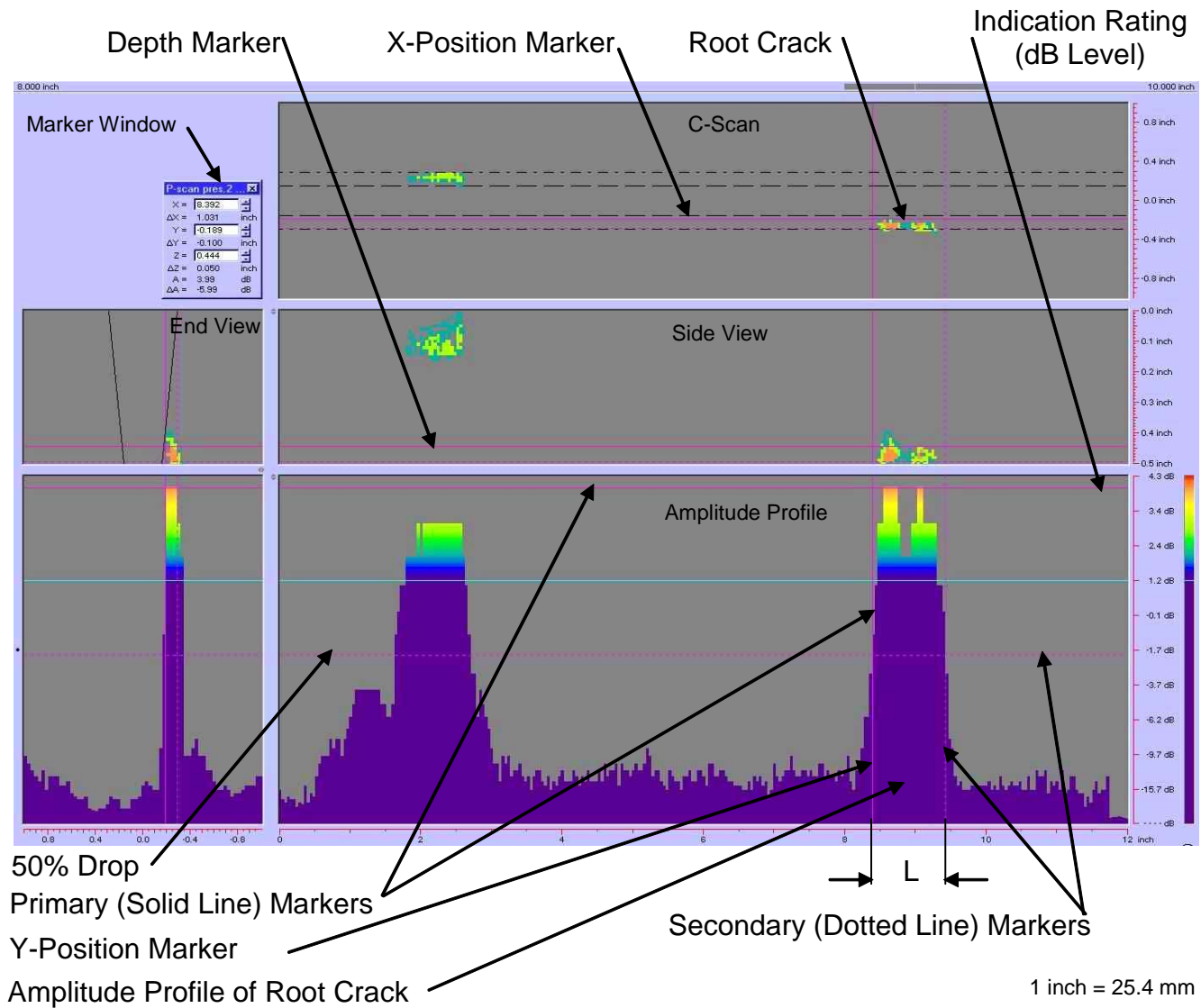


Figure 14. Flaw-sizing scheme of the P-scan system for the root crack in laboratory specimen S033.

ANALOGY OF INDICATION RATING IN AUT VERSUS TRADITIONAL UT

The ratings of indications in AUT and traditional UT are analogous; however, in practice, they are executed differently. Note that the final indication ratings measured by AUT and traditional UT are the same. The differences between the AUT and traditional UT systems stem from different signal amplification concepts. The AUT systems have built-in logarithmic amplifiers with no manual gain control. The traditional UT systems have manual gain control knobs where the operator may manually increase or decrease energy from the received echo. This difference in hardware design creates similar outputs, but displays the output differently for each system. A positive amplitude rating will appear as a negative rating using the P-scan system, while a negative amplitude rating will appear as a positive rating using the P-scan system. Care must be taken when comparing and interpreting the AUT output versus traditional UT output.

UT Indication Rating Procedures

The indication rating procedures for the traditional UT systems described in section 6.19.6.5 of the AASHTO/AWS D1.5M/D1.5: 2002 Bridge Welding Code⁽¹⁾ are summarized as follows:

- The reference level (b) is measured from the echo off of a 1.5-mm- (0.06-inch-) diameter hole in the International Institute of Welding (IIW) reference block. The echo signal is recorded after maximizing it to an 80-percent full-screen (FS) level using manual gain control.
- The indication level (a) is measured from a feature in the weld. The echo from the feature is maximized to an 80-percent FS level using manual gain control. Obviously, the smaller the feature, the more gain that is required to maximize it to an 80-percent FS level and, conversely, the larger the feature, the smaller the gain that is required to get to an 80-percent FS level. Thus, $a > b$ for smaller features and $a < b$ for larger features.
- The attenuation factor (c) is determined from the sound path.
- The indication rating (d) may be computed using the formula given in section 6.19.6.5, d equals a minus b minus c .⁽¹⁾ It is obvious that the indication rating (d) becomes a positive number when the feature is smaller than the 1.5-mm- (0.06-inch-) diameter reference hole and it becomes negative when the feature is larger than the reference hole.

AUT Indication Rating Procedures

The indication rating procedures for AUT are calculated differently. Unlike traditional UT, which displays the indication level (a) on the scope's screen, AUT systems display the indication rating (d) on all of the displays and plots. The following outline summarizes the indication rating procedures for AUT systems:

- The reference level (b) is measured from the echo off of a 1.5-mm- (0.06-inch-) diameter hole in the IIW reference block. The echo signal is maximized to an 80-percent FS level by varying the resolution of the ordinate in the amplitude profile plot. The reference level

(b) is automatically analyzed by the AUT software, causing the 80-percent FS level tick mark to reset itself to zero. Now, the 80-percent FS level tick mark becomes a reference for measuring the indication rating (d). Obviously, the smaller the feature, the less energy that is reflected back, so the signal falls below the reference line. The larger the feature, the more energy that is reflected back, so the signal falls above the reference line. In other words, the indication level (d) is a negative number for smaller features and a positive number for larger features.

- The attenuation factor (c) is automatically accounted for in all of the P-scan data when the attenuation function is turned on in the software during calibration (i.e., 2 dB per 25.4 mm (1 inch) of sound-path distance after the first 25.4 mm (1 inch)).

4. EQUIPMENT QUALIFICATION AND CALIBRATION

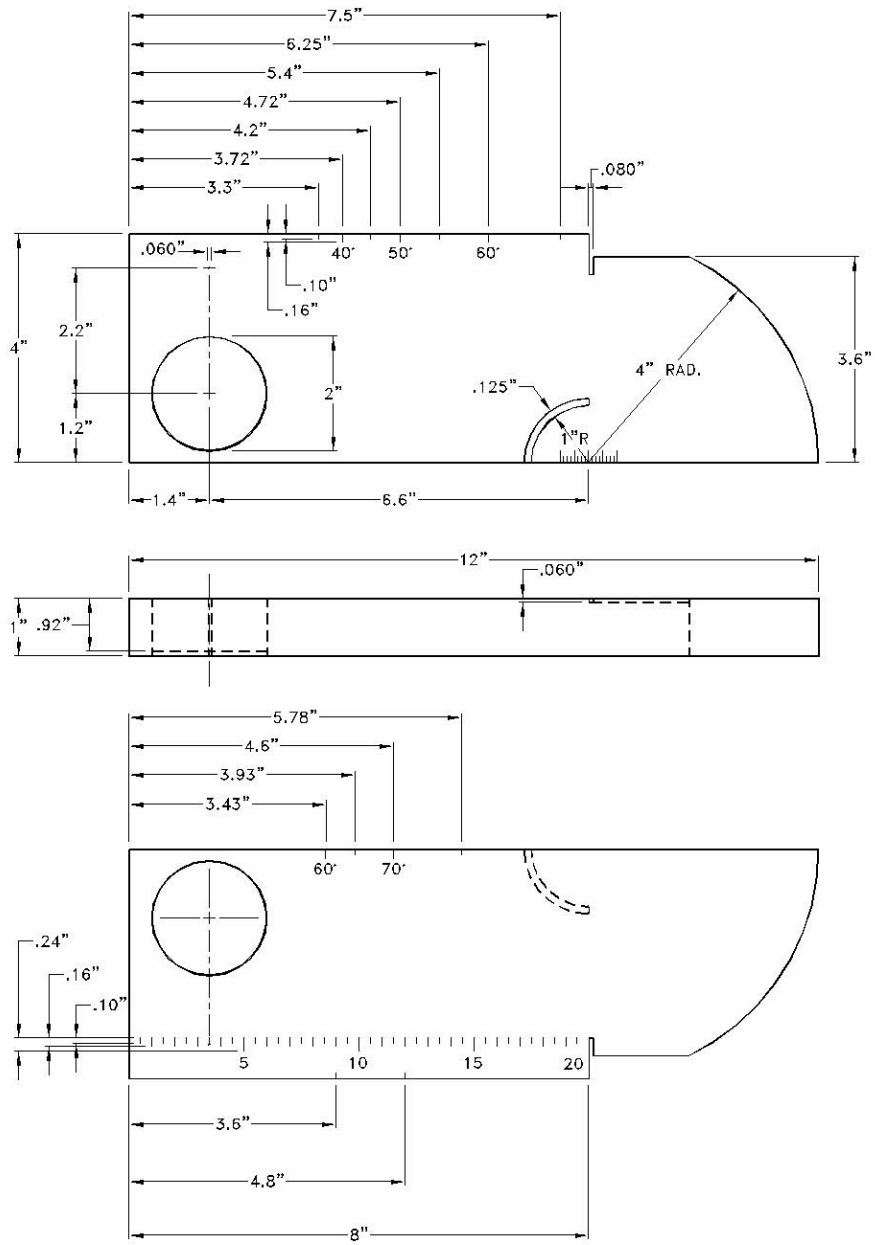
According to section 6.15 of the AASHTO/AWS D1.5M/D1.5: 2002 Bridge Welding Code,⁽¹⁾ every ultrasonic unit shall be calibrated prior to inspection. Therefore, the P-scan system was calibrated by a qualified P-scan operator using approved standard reference blocks. Because the calibration procedures for the P-scan system and the traditional UT systems are alike, the calibration procedures for ultrasonic inspection outlined in section 6.21 of the AASHTO/AWS D1.5M/D1.5: 2002 Bridge Welding Code⁽¹⁾ were applied to the P-scan equipment. Note that IIW or any other standard reference block suggested by the code may be used for equipment qualification and calibration. Figures 15 through 17 show the IIW type I, IIW type Resolution Calibration (RC), and IIW type Distance/Sensitivity Calibration (DSC) reference blocks used during calibration.

EQUIPMENT QUALIFICATION PROCEDURES

The equipment qualification procedures outlined in section 6.15 of the AASHTO/AWS D1.5M/D1.5: 2002 Bridge Welding Code⁽¹⁾ were closely followed for the qualification of the P-scan system. The equipment qualification procedures are summarized as follows:

- **Pulse-Echo Type Equipment Qualification:** Section 6.15.1⁽¹⁾ states that the instrument shall be a pulse-echo type capable of using transducers with frequency ranges of 1 to 6 MHz. The instrument shall be capable of displaying an A-scan rectified trace. In general, the pulse-echo instrument is an ultrasonic instrument that generates ultrasonic pulses at a regular interval and measures the time taken for the pulses to pass through the test object and return to the transceiver. The P-scan system (shown in figure 2) is a pulse-echo system that uses transducers for transmission and reception of ultrasound at frequency ranges of 1 to 15 MHz. The P-scan is capable of displaying an A-scan rectified trace.
- **Horizontal Linearity Qualification:** Section 6.15.2⁽¹⁾ states that the horizontal linearity of the test instrument shall be qualified over the full sound-path distance being used during testing. For this qualification, a straight-beam search unit creating longitudinal waves is used. Since the velocity of a longitudinal wave is almost double that of a shear wave, a 250-mm (10-inch) screen calibration for shear waves would require a 500-mm (20-inch) screen calibration for longitudinal waves. The procedures for horizontal linearity qualification are outlined as follows:
 - Couple a straight-beam transducer on the surface of the IIW type I reference block at the position shown in figure 18 to obtain five backwall reflections.
 - Adjust the first and fifth backwall reflections to their proper locations by use of the distance calibration and zero delay adjustments.
 - Each indication shall be adjusted to the reference level with the gain or attenuation control for horizontal location examination.

- Each intermediate trace deflection location shall be correct within ± 2 percent of the screen width. This qualification is not applicable to the P-scan system because the position of the echo is indicated by the peak amplitude rather than the leading edge where the position of the peak remains the same for all values of echo height.
- **Signal Stability Check After Warmup:** Section 6.15.3⁽¹⁾ states that the instrument shall be internally stabilized after warmup so that no variation in response greater 1 dB occurs with a nominal supply voltage change of 15 percent for a battery-operated instrument within the charge operating life. The P-scan system satisfies this qualification. The P-scan system houses two rechargeable batteries (one battery is used at a time to operate the system). When a battery's capacity falls below 10 percent, the system will automatically switch to the second battery, allowing the discharged battery to be exchanged ("hot swapped"). If both batteries fall below a 10 percent capacity, the system will give a warning and will shut off automatically.
- **Gain Control, Attenuation, and Decibel Accuracy Qualification:** Section 6.15.4⁽¹⁾ states that the instrument shall have a calibrated gain control adjustable in discrete 1- or 2-dB steps over a range of 60 dB. The accuracy of the gain control setting shall be within ± 1 dB. This qualification is not applicable to the P-scan system because the P-scan has a logarithmic amplifier. There is no manual gain control in the P-scan system.
- **Dynamic Range Accuracy Check:** Section 6.15.5⁽¹⁾ states that the dynamic range of the instrument's display shall be such that a difference of 1 dB of amplitude can be easily detected on the display. The P-scan's scope window can be set up to have a resolution such that a difference of 1 dB of amplitude can be easily detected.



1 inch = 25.4 mm

Figure 15. IIW reference block used for the P-scan calibration: Type I.

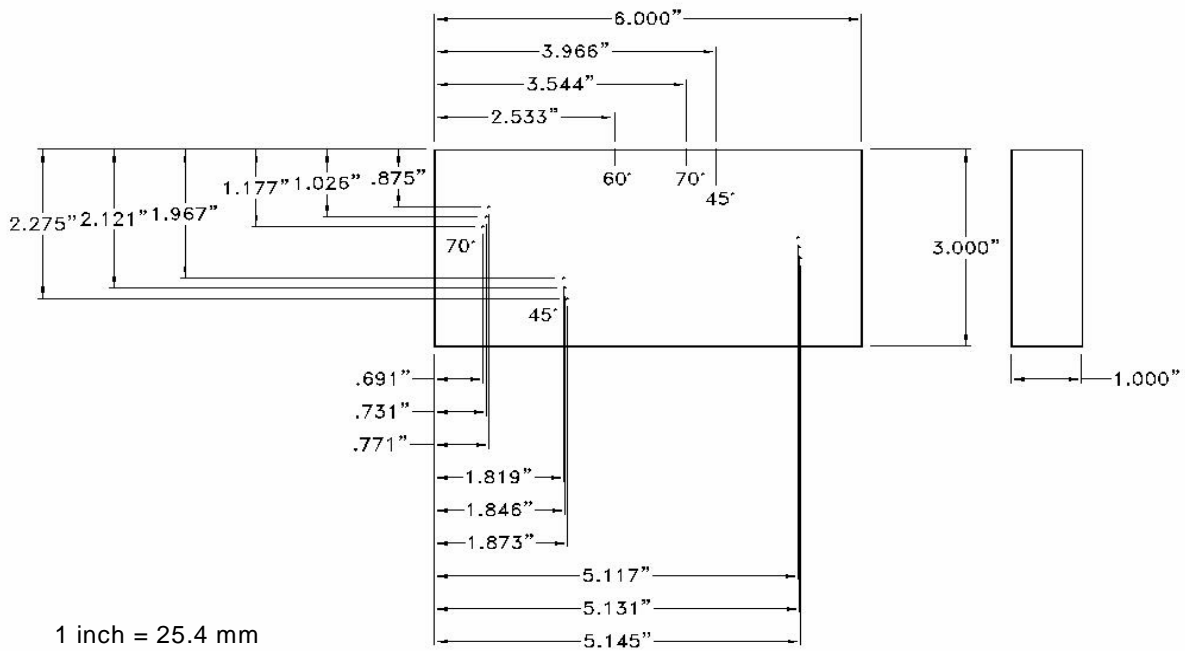


Figure 16. IIW reference block used for the P-scan calibration: Type RC.

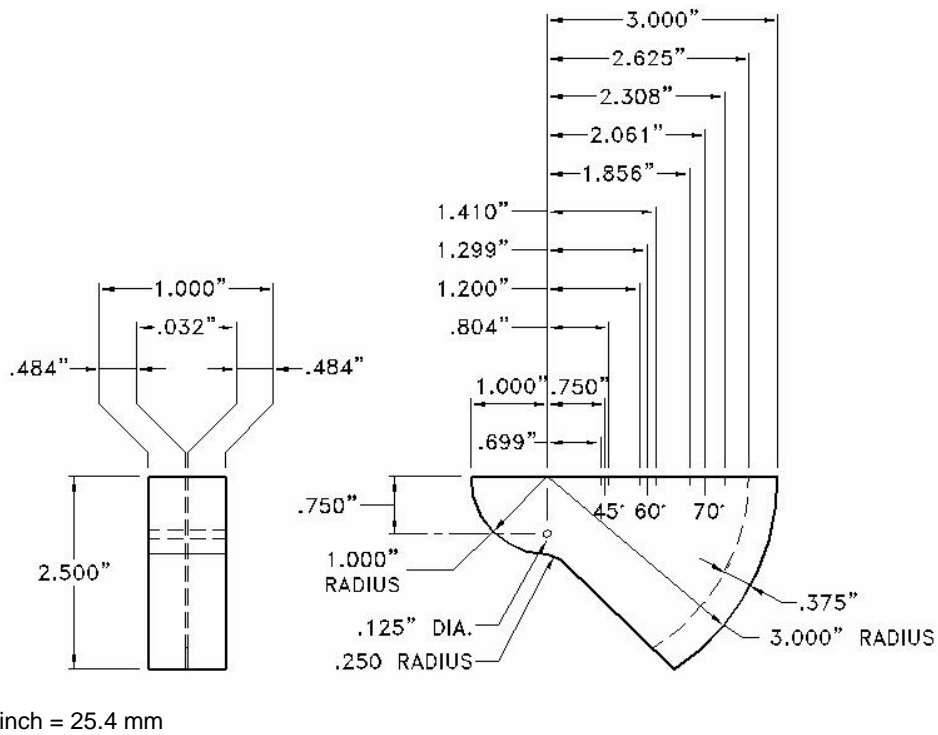


Figure 17. IIW reference block used for the P-scan calibration: Type DSC.

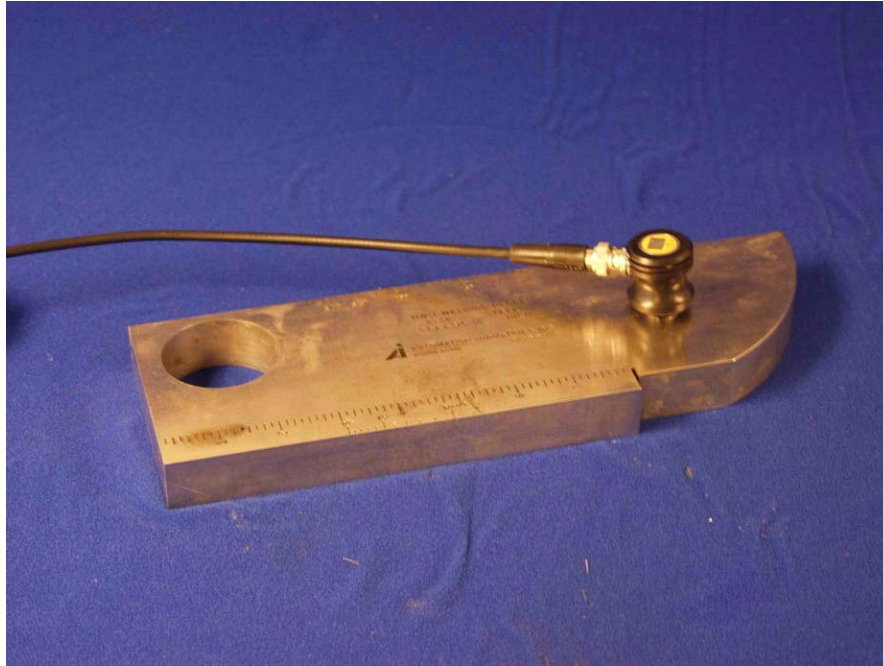


Figure 18. Horizontal linearity check using a straight-beam transducer and IIW type I reference block.

CALIBRATION PROCEDURES

The calibration procedures in sections 6.18 and 6.21 of the AASHTO/AWS D1.5M/D1.5: 2002 Bridge Welding Code⁽¹⁾ were closely followed to calibrate the AUT system for angle beam transducers. The calibration procedures were completed as follows:

- **Sound Entry Point (Index Point) Check:** The sound entry point is the point at which sound exits the wedge or shoe that the transducer is mounted on and enters the test object. The manufacturer always marks the sound entry point on the wedge. However, its position may shift because of wear in the lower surface of the wedge. Section 6.21.2.1⁽¹⁾ states that the following procedures shall be used to check the sound entry point of the wedge to be used in testing:
 - Couple the angle transducer on the IIW type I reference block at the position shown in figure 19.
 - Maximize the echo signal from the 100-mm (4-inch) radius circular reflector in the reference block (figure 20).
 - Mark the point on the wedge that aligns with the radius line of the circular reflector on the calibration block.

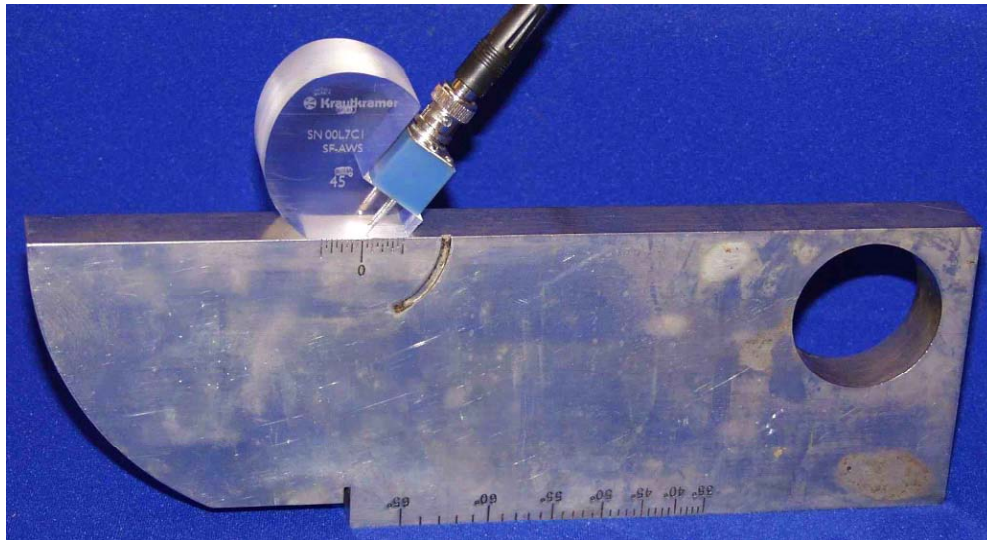
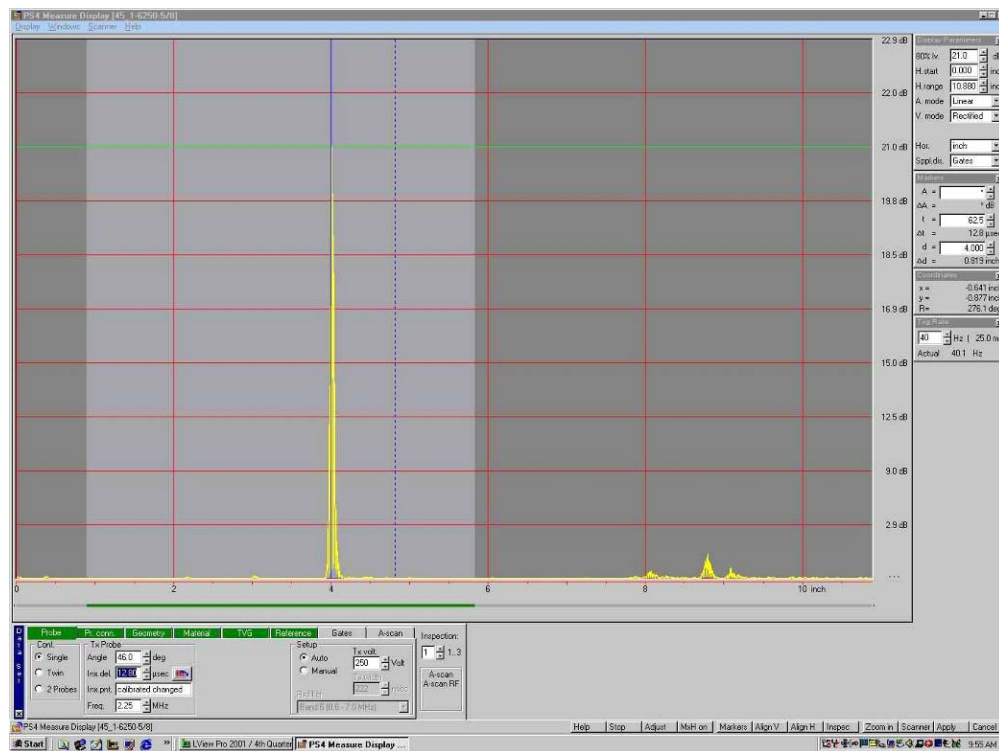


Figure 19. Sound entry point check: Photograph shows the transducer position on the IIW reference block.



1 inch = 25.4 mm

Figure 20. Sound entry point check: A-scan screen displays the echo reflected from the 100-mm (4-inch) radius circular reflector on the IIW type I reference block.

- **Sound-Path Angle (Beam Angle) Check:** An angle transducer is characterized by the angle of refraction of the sound wave in the object being tested. Wedges are manufactured to carry longitudinal sound waves to the interface of the object being tested. As a result of mode conversion at the interface, a shear wave is produced in the object being tested. The angle of refraction is generally marked on the wedge. However, the angle may change because of wear on the lower surface of the wedge, so calibration is required to ensure that the correct angle is being implemented during inspection. Section 6.21.2.2⁽¹⁾ states that the following procedures shall be followed to check the sound-path angle:
 - Couple the selected angle transducer on the IIW type I reference block at the position shown in figure 21, where the angle of the wedge is the same angle marked on the IIW reference block.
 - Maximize the echo signal from the 50-mm (2-inch) diameter hollow circular reflector in the IIW reference block by moving the transducer back and forth over the line indicating the wedge angle on the reference block (figure 22).
 - Compare the sound entry point on the wedge with the angle mark on the IIW calibration block. If the sound entry point is within ± 2 degrees of the angle mark, the transducer is acceptable.

- **Resolution Check:** The resolution is a measure of an instrument's ability to resolve echo signals reflected from neighboring objects. The resolution check for an angle transducer may be accomplished by the use of the IIW type RC reference block. The instrument shall be able to identify the three 1.5-mm- (0.06-inch-) diameter side-drilled holes. Section 6.21.2.5⁽¹⁾ states that the following procedures shall be followed to check resolution:
 - Couple the selected angle transducer on the IIW type RC reference block at the position shown in figure 23. Note that the angle of the wedge corresponds to the angle markings on the reference block.
 - Resolve the echo signal to distinguish between the peak associated with each of the three 1.5-mm- (0.06-inch-) diameter holes (figure 24).

- **Distance Calibration Check:** Section 6.21.2.3⁽¹⁾ states that the following procedures shall be followed to check distance calibration:
 - Couple the angle transducer on the IIW type I reference block at the position shown in figure 25, where the transducer's sound entry point aligns with the radius line of the 100-mm (4-inch) radius circular reflector.
 - Adjust the instrument to attain indications at 100 mm (4 inches) and 225 mm (9 inches) (figure 26).

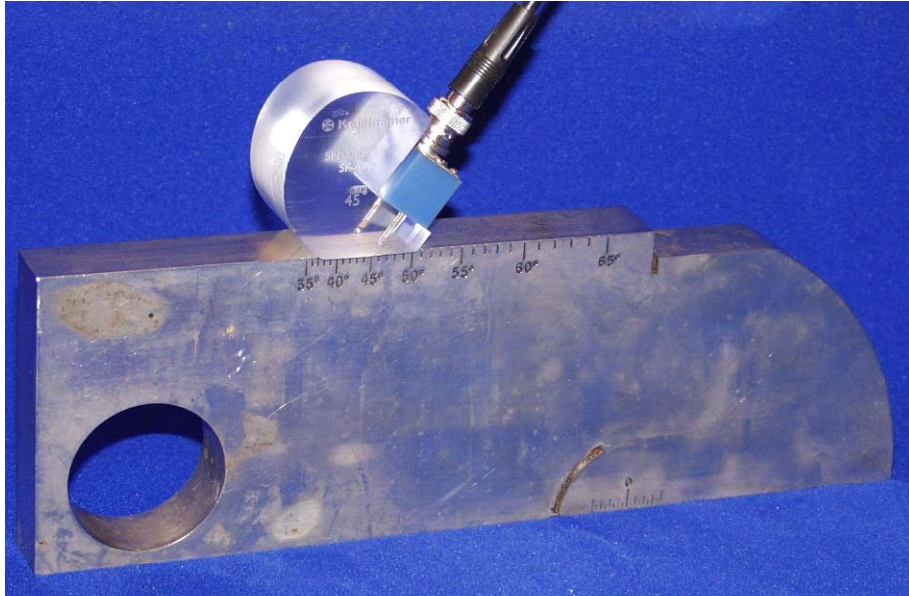
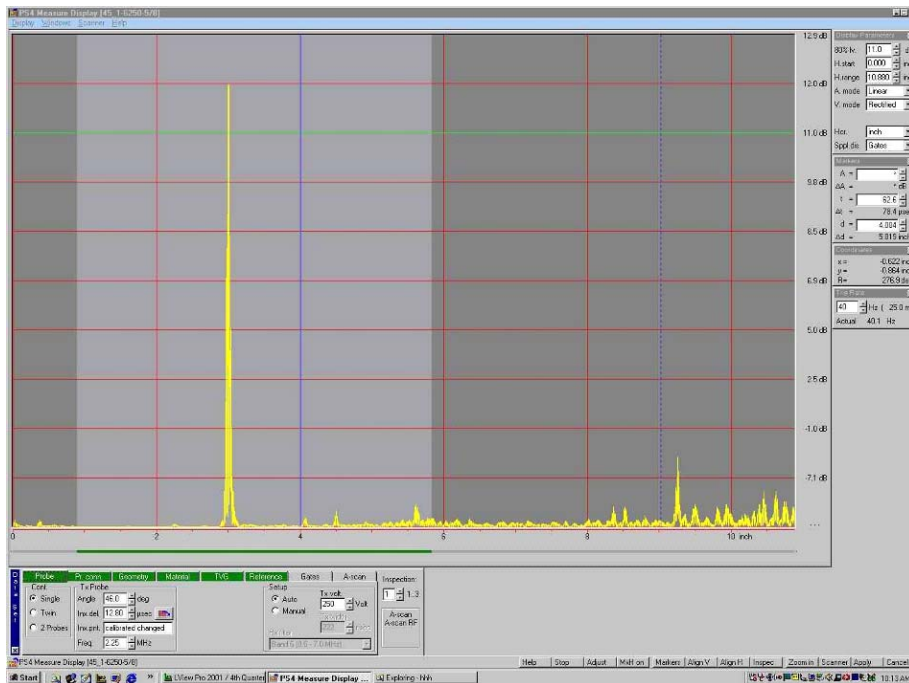
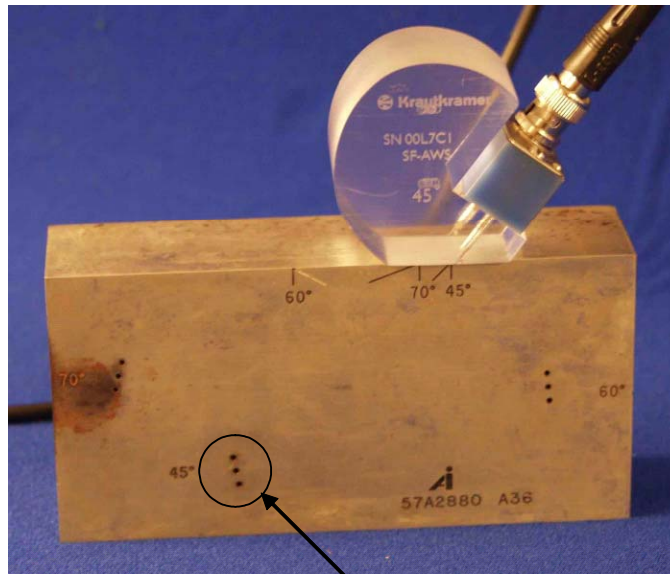


Figure 21. Sound-path angle check: Photograph shows that the selected angle transducer is positioned on the IIW type I reference block over the line indicative of the transducer angle.



1 inch = 25.4 mm

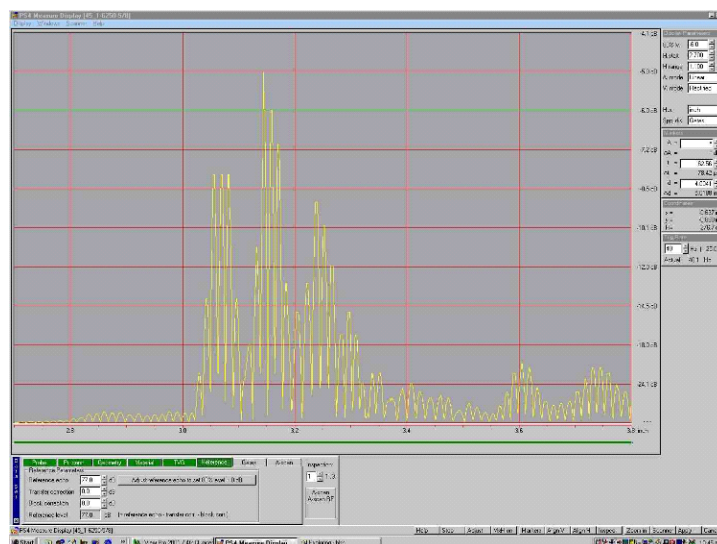
Figure 22. Sound-path angle check: A-scan screen displays the echo reflected from the 50-mm (2-inch) diameter hollow-disk reflector in the reference block.



1 inch = 25.4 mm

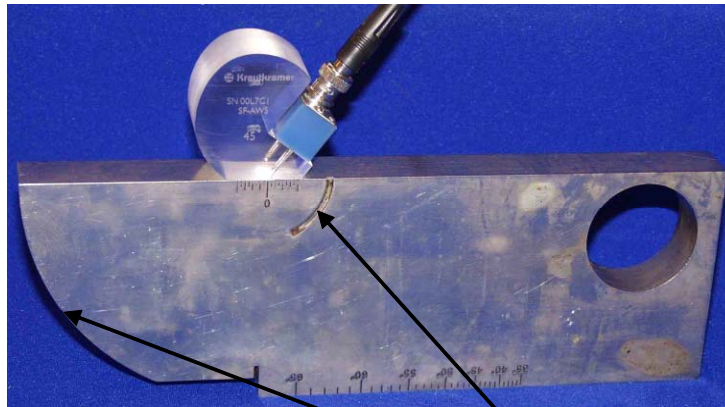
Three 0.06-inch diameter Holes

Figure 23. Resolution check: Photograph shows that the selected angle transducer is positioned on the IIW type RC reference block over the line indicative of the transducer angle.



1 inch = 25.4 mm

Figure 24. Resolution check: A-scan screen displays the three distinguishable signals reflected from the three holes.

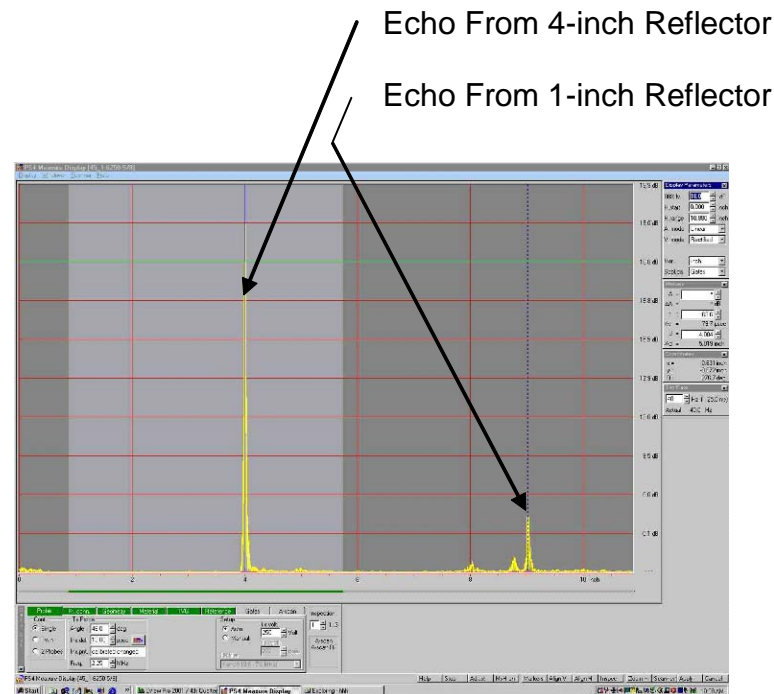


1 inch = 25.4 mm

1-inch Reflector

4-inch Reflector

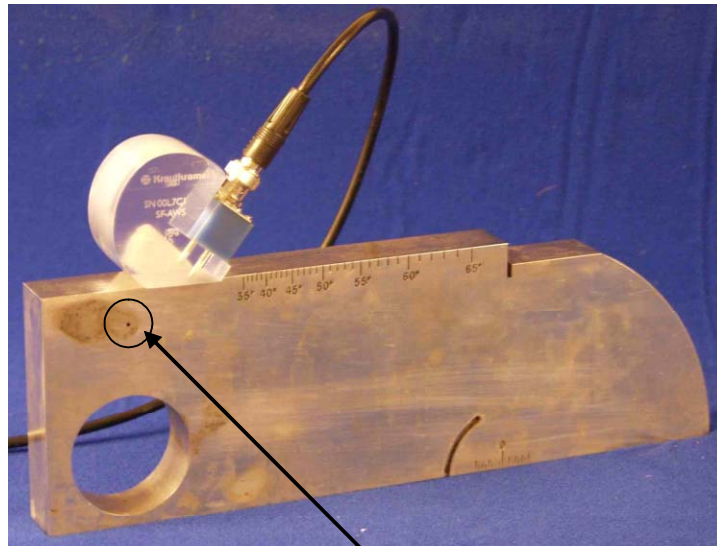
Figure 25. Distance calibration check: Photograph shows that the angle transducer is positioned on the IIW type I reference block so that the transducer's sound entry point aligns with the radius line of the 100-mm (4-inch) reflector.



1 inch = 25.4 mm

Figure 26. Distance calibration check: A-scan screen displays the signals reflected back and forth from the 100-mm (4-inch) radius circular reflector and 25.4-mm (1-inch) radius groove reflector.

- **Amplitude, Sensitivity, or Reference-Level Calibration:** Section 6.21.2.4⁽¹⁾ states that the following procedures shall be followed for sensitivity calibration:
 - Couple the angle transducer on the IIW type I reference block at the position shown in figure 27.
 - Maximize the signal from the 1.5-mm (0.06-inch) side-drilled hole in the IIW type I reference block by moving the transducer back and forth (figure 28).
 - Adjust the instrument to attain a horizontal reference line (i.e., an 80 percent FS level).

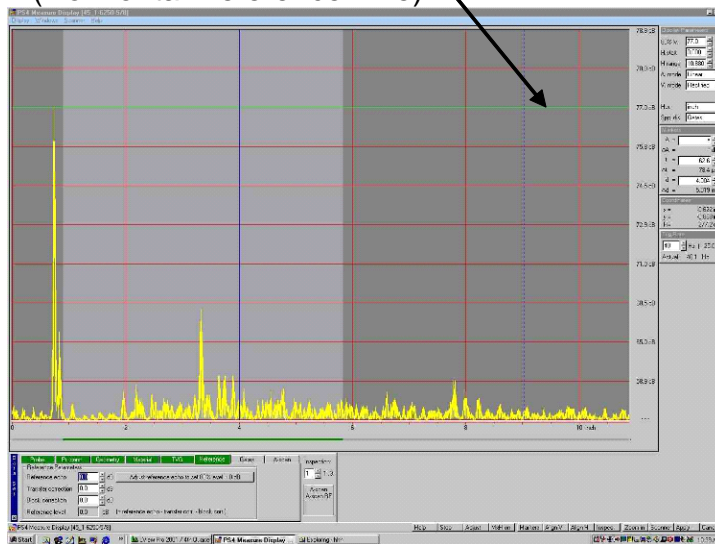


0.06-inch Sidewall Hole

1 inch = 25.4 mm

Figure 27. Amplitude, sensitivity, or reference-level calibration: Photograph shows that the angle transducer is positioned on the IIW type I reference block.

80-Percent Full-Screen Level
(Horizontal Reference Line)



1 inch = 25.4 mm

Figure 28. Amplitude, sensitivity, or reference-level calibration: A-scan screen displays the signal reflected from the 1.5-mm (0.06-inch) sidewall hole that is maximized to attain a horizontal reference-line (i.e., green line) height indication.

5. TESTING AND EVALUATION PLAN

Testing and evaluation of the AUT technique included both laboratory testing and inline field testing. The laboratory evaluation assessed the viability of AUT under controlled laboratory conditions. The inline field testing assessed the practicality of the AUT technique and system for use in the fabrication shop environment.

The AUT laboratory study was conducted at FHWA's Nondestructive Evaluation Validation Center (NDEVC) laboratory. The laboratory specimens consisted of professionally manufactured plates with implanted artificial flaws and plates fabricated in a steel bridge fabrication shop that contained volumetric defects.

AUT field testing and evaluation was performed at fabrication plants in Lancaster, PA, and Bowling Green, KY. The field specimens were flange and web plates commonly fabricated for use in steel bridge girders.

In the laboratory and field studies, the P-scan system was not configured to inspect the weld for transverse defects (defects perpendicular to the weld centerline) or defects in the weld at width transitions (width transitions will be described in the Description of Specimens section below). To inspect these defects and regions, special gates, different setups, and different data files are required in order to account for and mask the sidewall reflections. Since the research objectives focused on the AUT process rather than on the internal processing associated with AUT, no special gates, etc., were used. Consequently, testing could not include the previously mentioned defects or regions.

DESCRIPTION OF SPECIMENS

All specimens were butt-welded steel plates with full-penetration groove welds. Some of the specimens had thickness transitions and/or width transitions at the butt joints as shown in figures 29 and 30, respectively. Welding at thickness transitions is generally performed on two plates of unequal thickness. Welding at width transitions is generally performed on two plates of unequal width. The defects common in full-penetration butt welds generally fall into two categories: planar defects and volumetric defects. The planar defects consist of cracks and lack of fusion, while volumetric defects include slag inclusions, porosity, and incomplete penetration.

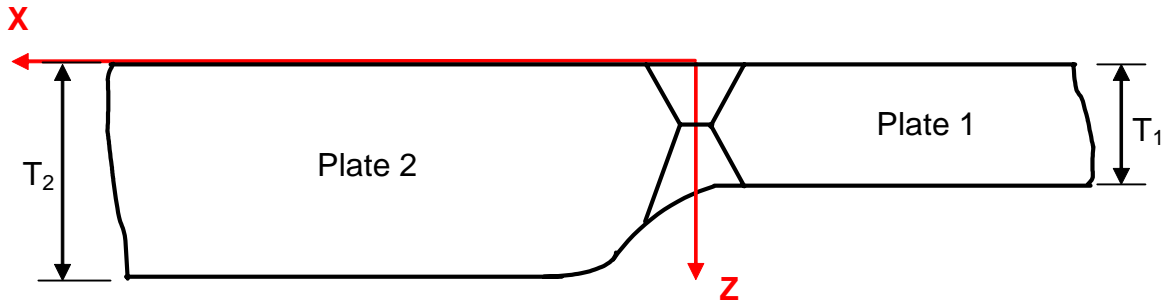


Figure 29. Schematic diagram of specimen: Thickness transition at butt joint.

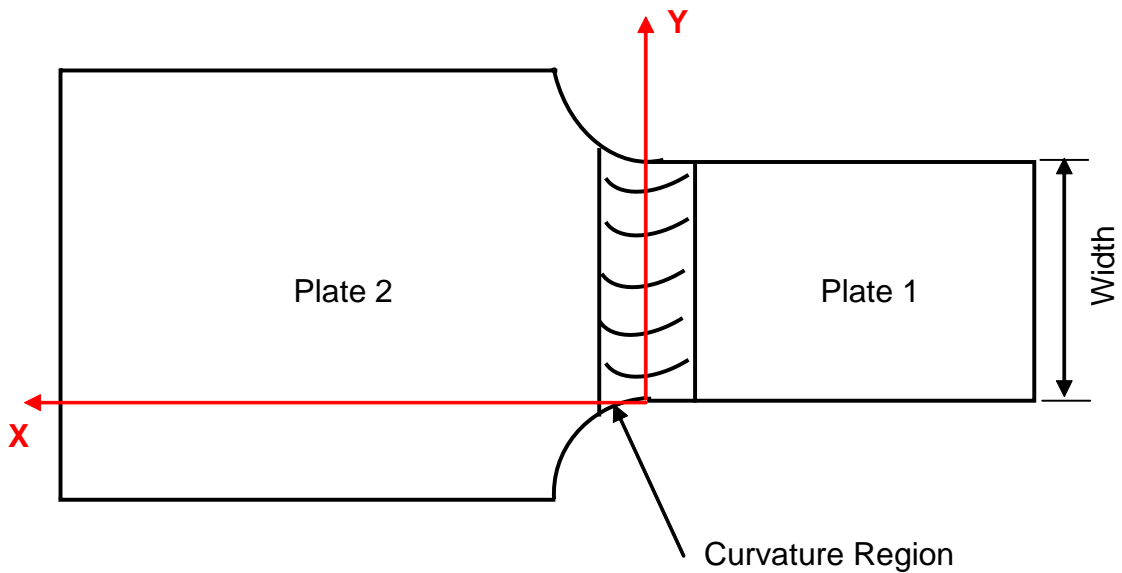


Figure 30. Schematic diagram of specimen: Width transition at butt joint.

Laboratory Specimens

The laboratory specimens were obtained from two different sources. The first source is a flaw manufacturing company specializing in the production of welded steel plates with artificially induced, crack-like defects in the weld. Two of the 10 laboratory specimens were made by this company and were designated as category 1 laboratory specimens, while the remaining eight specimens were made by another company and were designated as category 2 laboratory specimens. The thicknesses of the laboratory specimens ranged from 12.7 to 38.1 mm (0.5 to 1.5 inches). Widths ranged from 142.875 to 454.025 mm (5.625 to 17.875 inches). To simulate typical flange plates and avoid encountering spurious backwall echoes during the AUT inspections, the laboratory specimens were approximately 508 mm (20 inches) long. The descriptions of the laboratory specimens are contained in table 1. The first column in table 1 indicates the different categories of laboratory specimens. The second column indicates the specimen identification code. The third and fourth columns indicate the thicknesses of plate 1

(T₁) and plate 2 (T₂), respectively. Different values for T₁ and T₂ indicate that the weld is located at a thickness transition. The fifth column of table 1 indicates the plate width. For welds located at flange width transitions, the width is equal to the width of the narrowest plate (figure 30). The number of scan segments used to effectively inspect the entire weld is shown in column six. Column seven indicates the transducer's refracted angle (i.e., the wedge angle).

Table 1. Description of laboratory specimens.

Category	Specimen ID	Thickness	Thickness	Width	AUT Scan	Probe Angle
		T ₁ (inch)	T ₂ (inch)	(inch)	Segments	θ°
1	S033	0.5	0.5	12	1	70
	S034	0.5	0.5	12	1	70
2	S125	1	1	15	1	70
	S126	1	1	15	1	70
	S131	1.5	1.5	12	1	70
	S132	1.5	1.5	12	1	70
	S133	1.5	1.5	5.625	1	70
	S134	1.5	1.5	7.375	1	70
	S135 ¹	1	1.5	17.875	2	70
	S136 ¹	1	1.5	17.875	2	70

¹Thickness transition at butt joints

1 inch = 25.4 mm

Category 1 Specimens

The category 1 laboratory specimens were 12.7 mm (0.5 inch) thick, 304.8 mm (12 inches) wide, and contained crack-like defects with known characteristics. The weld reinforcement was not ground flush in either specimen. Table 2 describes the physical characteristics of the defects in each specimen. The first column of table 2 indicates the specimen identification code, the second column describes the type of defect induced in the weld, the third column shows the length of each defect, and the fourth column indicates the Y location of each defect measured from the datum. Specimen S033 contained two longitudinal cracks (one at the toe and one at the root of the weld), while specimen S034 contained one longitudinal crack and one transverse crack.

Table 2. Description of manufactured defects in the category 1 laboratory specimens.

Specimen ID	Defect Type	Defect Length L (inch)	Y-Position Y (inch)
S033	Toe Indication	2.40	0.90
	Root Indication	0.94	8.66
S034	Centerline Indication	1.45	3.93
	Transverse Indication	0.43	11.02

1 inch = 25.4 mm

Category 2 Specimens

The thicknesses of the category 2 laboratory specimens ranged from 25.4 to 38.1 mm (1 to 1.5 inches) and the widths ranged from 142.875 to 454.025 mm (5.625 to 17.875 inches). The specimens were fabricated to include lack of fusion, slag inclusions, and/or porosity. The fabricator performed manual UT inspection on the category 2 specimens and the characteristics of the defects found in the weld are indicated in table 3. The first column of table 3 indicates the specimen identification code, the second column describes the number of indications detected in the weld, the third column specifies the angle (θ) of the transducer, the fourth column indicates the length (L) of each indication, the fifth column indicates the depth (Z) of each indication measured from face A (face A is shown in table 6.2 in the AASHTO/AWS D1.5M/D1.5: 2002 Bridge Welding Code⁽¹⁾), the sixth column indicates the indication rating (d), the seventh column shows the location of each indication measured from the weld centerline (X), and the eighth column shows the location of each indication measured along the weld centerline from the datum (Y).

Table 3. Description of defects found by manual UT in the category 2 laboratory specimens.

Specimen ID	Ind. No.	Probe Angle θ°	Indication Length L (inch)	Indication Depth Z (inch)	Indication Rating d (dB)	X-Position X (inch)	Y-Position Y (inch)
S125	1	70	0.38	0.63	-1	-0.38	2.25
	2	70	0.50	0.50	+6	0.00	7.50
	3	70	0.25	0.33	+7	0.00	13.38
S126	1	70	1.25	0.82	-2	-0.25	2.50
	2	70	0.63	0.69	+5	+0.25	6.88
	3	70	0.50	0.25	+11	-0.38	8.63
	4	70	0.50	0.88	-2	-0.13	11.25
S131	None	None	None	None	None	None	None
S132	1	70	12.00	1.00	+9	+0.56	0.00
S133	1	70	5.75	0.94	+8	-0.56	0.00
S134	None	None	None	None	None	None	None
S135	1	70	2.25	0.38	-2	+0.13	3.50
	2	70	2.38	0.19	+9	+0.25	8.13
	3	70	1.25	0.56	+1	+0.25	11.75
S136	1	70	2.00	0.38	+2	+0.13	2.00
	2	70	2.38	0.25	+6	0.00	0.50

1 inch = 25.4 mm

Field Specimens

The field specimens were 25.4 to 83.82 mm (1 to 3.3 inches) thick, 279.4 to 1092.2 mm (11 to 43 inches) wide, and on the order of 30.48 meters (m) (100 feet (ft)) long. There were a total of 46 field specimens tested in the fabrication plants using the AUT system.

In one fabrication plant (High Steel Structures, Inc. (HSS)), 42 field specimens were tested. One specimen was a web plate, 2 were company procedural test plates, and the remaining 39 were flange plates. Some of the specimens had thickness transitions at the butt joints, width transitions at the butt joints, or both. The two company procedural test plates (i.e., TP2 and AWS-FCM-02-6A-TP) were similar to the laboratory specimens and typically were used by the fabricator's quality assurance and quality control division for in-house training and practice. The thicknesses of the field specimens tested at HSS ranged from 25.4 to 83.82 mm (1 to 3.3 inches) and the widths ranged from 279.4 to 1092.2 mm (11 to 43 inches). Table 4 provides a description of the field specimens from the first fabrication plant. The first column in table 4 indicates the period in which field testing was conducted, while the second column indicates the specimen identification code. The identification codes are always stamped on the plates outside of the HAZ to identify both the plate and the weld. The third and fourth columns indicate the thicknesses of each joined plate (as shown in figure 29). Different values for T_1 and T_2 indicate that the weld is located at a thickness transition. The fifth column indicates the plate width. For welds located at width transitions, the width is equal to the width of the narrowest plate (figure 30). The number of

AUT scan segments used to effectively inspect the entire weld is shown in column six, while column seven indicates the transducer's refracted angle (i.e., the wedge angle).

Table 4. Description of field specimens tested at HSS.

Field Test No.	Specimen ID	Thickness T ₁ (inch)	Thickness T ₂ (inch)	Width (inch)	AUT Scan Segments	Probe Angle θ°
1	G20A-TF2-BottF	1.378	1.378	20	1	70
	G21A-TF2-BottF	1.378	1.378	20	1	70
2	G3F-CF1-BottF ¹	1.25	1.75	24	1	70
	G3F-CF2-BottF ¹	1.25	1.75	24	1	70
	G3F-TF1-TopF ¹	1.125	1.75	20.0625	1	70
	G3F-TF2-TopF ¹	1.125	1.75	20.0625	1	70
	G4F-TF1-TopF ¹	1.125	1.75	20.0625	1	70
	G4F-TF2-TopF ¹	1.125	1.75	20.0625	1	70
	G5G-TF1-TopF ¹	1	1.75	20	1	70
	G3J-TF1-TopF ¹	1	1.75	20.0625	1	70
	G3J-CF1-BottF ¹	1.25	1.75	24.0625	1	70
	G2G-CF1-BottF-FCM ^{1,2}	3.15	3.937	43.3	1	45
	G2A-CF1-TopF ¹	1.0625	3.3125	16.25	1	70
	G2A-CF2-TopF ²	3.3125	3.3125	16.25	1	70
	G2A-CF3-TopF ²	3.3125	3.3125	16.25	1	70
	G2A-CF4-TopF ¹	1.0625	3.3125	16.25	1	70
	3	FG4A-TF1-BottF-FCM	1.75	1.75	16.0625	1
FG1A-TF1-BottF-FCM		1.75	1.75	16.0625	1	70
FG2A-TF1-BottF-FCM		1.75	1.75	15.875	1	70
FG3A-TF1-BottF-FCM		1.75	1.75	15.875	1	70
FG26G-TF2-BottF-FCM		1.75	1.75	11.875	1	70
FG16D-TF1-BottF-FCM		2	2	12	1	70 60
FG36K-TF2-TopF-FCM ²		3	3	33.75	3	45
FG37K-TF2-TopF-FCM ²		3	3	34	4	70 45
FG37K-TF3-BottF-FCM		3	3	31.5	4	45
FG38K-TF3-BottF-FCM		3	3	31.5	4	70 45
FG38K-TF1-TopF-FCM ²		3	3	33.75	3	45
FG38K-TF2-TopF-FCM ²		3	3	33.75	3	45
AWS-FCM-02-6A-TP		1.5	1.5	36	4	70
TP2		1	1	11.75	1	70

1 inch = 25.4 mm

Table 4. Description of field specimens tested at HSS (continued).

Field Test No.	Specimen ID	Thickness T ₁ (inch)	Thickness T ₂ (inch)	Width (inch)	AUT Scan Segments	Probe Angle θ°
4	FG40M-TF1-Curved-FCM ¹	3	3.4375	39.125	4	45
	FBG80-TF1-BottF-FCM	2.5	2.5	39.4375	6	70
	FG1E-TF2-TopF-FCM ^{1,2}	1	2.25	15.75	1	70
	FG2E-TF2-TopF-FCM ^{1,2}	1	2.25	15.75	1	70
	FG1A-TF2-BottF-FCM	2	2	19.5	1	70 60
	G3VHW-CF1-BottF ¹	1.75	2.75	26.5	2	70
	G5VHW-CF1-BottF ¹	1.75	2.75	26.25	4	70 45
	G7UHW-CF1-TopF ¹	1.125	1.25	18	1	70
	G11THW-CF1-BottF ^{1,2}	2.75	3.0625	21.875	2	70
	G11THW-CF2-BottF ^{1,2}	2.75	3.0625	22.875	2	70 45

¹Transition of thickness at butt joint parts

²Transition of width at butt joint parts

BottF: Bottom flange

CF: Compression flange

FCM: Fracture-critical member

TF: Tension flange

TopF: Top flange

TP: Test plate

1 inch = 25.4 mm

In the other bridge fabrication plant (Stupp), four field specimens were tested. The description of each of these specimens is tabulated in table 5. All of the specimens were flange plates. The thicknesses of these specimens ranged from 50.8 to 66.675 mm (2 to 2.625 inches) and the typical width was 609.6 mm (24 inches).

Table 5. Description of field specimens tested at Stupp.

Field Test No.	Specimen ID	Thickness T ₁ (inch)	Thickness T ₂ (inch)	Width (inch)	AUT Scan Segments	Probe Angle θ°
1	FS32B1&2-BottF, Joint B015	2.625	2.625	24	3	70
	FS45A1&2, Joint T019	2.5	2.5	24	3	70
	FS46A1&2, Joint T021	2	2	24	3	70 60
	FS31B1&2, Joint B011	2.5	2.5	24	3	70 60

BottF: Bottom flange

1&2: Joint between splices 1 and 2

1 inch = 25.4 mm

LABORATORY TESTING

FHWA's NDEVC laboratory was used to test and evaluate the AUT system under controlled conditions. For each test, an appropriate angle transducer was selected based on the thickness of the joined plates. According to table 6.2 in the AASHTO/AWS D1.5M/D1.5: 2002 Bridge Welding Code,⁽¹⁾ plates with thicknesses from 12.7 to 38.1 mm (0.5 to 1.5 inches) require a 70-degree angle transducer. Thus, all laboratory specimens were tested using a 70-degree angle transducer operating at 2.25 MHz.

The category 1 laboratory specimens containing crack-like flaws of known physical characteristics were inspected by the P-scan system. The welds were scanned from both sides of the centerline using the Both configuration.

The category 2 laboratory specimens that were fabricated to include discontinuities such as lack of fusion, slag inclusions, and/or porosity were inspected by the P-scan system. The BSC and TSC scanner configurations were used in inspecting specimens S125, S126, S135, and S136. The remaining category 2 specimens were inspected using the Both configuration.

All laboratory specimens were inspected by RT. The RT inspection was performed at the fabrication plant by American Society for Nondestructive Testing (ASNT)-certified RT inspectors. The inspection documents and reports, including the radiographic films, are available.

FIELD TESTING

Field testing was conducted during four visits to HSS and one visit to Stupp. These field-testing sessions ranged from 3 days to 2 weeks. Figures 31 and 32 illustrate activities during a typical field test. Four weeks in advance of the field tests, work plans were prepared and sent to the resident inspection engineer for review and comment. In the weeks before a field test, details and logistics were finalized and the appropriate work plans were established to avoid or minimize any interruption to regular plant operations. Note that the AUT inspections were not used to accept or reject any of the welds. Instead, the AUT inspections were solely used for research purposes.

During each testing period, the P-scan system was set up, calibrated, and placed adjacent to the RT and manual UT systems. FHWA's NDEVC staff was responsible for P-scan operations, while resident inspection engineers from the fabrication plants performed RT and manual UT.

All three scanner configurations (TSC, BSC, and Both) were implemented during testing. Since the field specimens were generally thicker than 12.7 mm (0.5 inch) and wider than 304.8 mm (12 inches), the specimens were generally segmented into two or more AUT scan segments. Thus, the P-scan system required a total of 106 scans to inspect the 46 field specimens.



Figure 31. AUT field testing: High Steel Structures, Inc.



Figure 32. AUT field testing: Stupp Bridge Company.

6. RESULTS

Laboratory evaluation and field testing of the P-scan system in parallel with both RT and manual UT was performed on 10 laboratory specimens and 46 field specimens. The results produced from this testing illustrate the potential benefits of implementing AUT.

LABORATORY RESULTS

The results of the laboratory evaluation are summarized in table 6. The first column of table 6 indicates the specimen identification code. The second, third, and fourth columns indicate the inspection method performed on each specimen. “Rejected” or “Accepted” indicates that the specimen was either rejected or accepted, respectively, by the employed inspection method. “Ind.” stands for indication, and the angle (θ) indicates the transducer’s refracted angle. The indication characteristics in the fourth column (i.e., indication rating (d), length (L), depth (Z), x-position, and y-position) are obtained from P-scan images. These characteristics are compared with the UT acceptance-rejection criteria in tables 6.3 and 6.4 from the AASHTO/AWS D1.5M/D1.5: 2002 Bridge Welding Code⁽¹⁾ to determine whether the indication should be accepted or rejected.

The category 1 laboratory specimens were rejected by all three inspection methods (table 6). Figure 10 shows the radiographic image of laboratory specimen S033. Figure 12 shows the P-scan images of the toe and root cracks in specimen S033. The radiographic image provides the spatial dimensions of the defects (i.e., length and position), while the P-scan images provide three-dimensional information (including length, depth, and global position). Specimen S034 (figure 33) contained two manufactured cracks. This 12.7-mm- (0.5-inch-) thick plate contains a longitudinal crack in the weld (figure 34) and a transverse crack in the weld (figure 35). Both cracks were detected by RT and manual UT. Figure 36 shows the radiographic image of specimen S034. The two cracks can be seen clearly. The transverse crack in specimen S034 was detected by manual UT when the weld was inspected in the transverse direction. The P-scan system detected only the longitudinal/centerline crack in specimen S034 (figures 37 and 38). The photographs, radiographic images, and P-scan images of the remaining laboratory specimens that contained rejectable defects are shown in figures 39 through 71.

The results provided in table 6 showed that the indication rating (d) given by the P-scan system varied from the conventional UT rating in some cases. This variance may be caused by one of the following parameters:

- High sensitivity of P-scan system.
- Manual versus computer determination of spatial characteristics of defects (including sound path and time of flight).
- Attenuation.
- Slightly varying scanning patterns.
- Operator variability.

Table 6. Inspection results of laboratory specimens.

Specimen ID	RT	Manual UT	AUT
S033	Rejected Ind. 1: Toe Crack Ind. 2: Root Crack	Rejected Ind. 1: Toe Crack Ind. 2: Root Crack	Rejected Ind.1: Toe Crack d = -3 dB L = 2.45", Z = 0" X = +0.13", Y = 0.57" Ind. 2: Root Crack d = -4 dB L = 1.03", Z = 0.44" X = -0.19", Y = 8.39"
S034	Rejected Ind. 1: Centerline Crack Ind. 2: Transverse Crack	Rejected Ind. 1: Centerline Crack Ind. 2: Transverse Crack	Rejected* Ind. 1: Centerline Crack d = 0 dB L = 1.37", Z = 0.02" X = +0.07", Y = 3.94"

*AUT is not configured to detect transverse cracks.

1 inch = 25.4 mm

Table 6. Inspection results of laboratory specimens (continued).

Specimen ID	RT	Manual UT	AUT
S125	Rejected	Rejected Ind. 1: $\theta = 70^\circ$ d = -1 dB L = 0.38", Z = 0.63" X = -0.38", Y = 2.25" Ind. 2: $\theta = 70^\circ$ d = +6 dB L = 0.50", Z = 0.50" X = 0", Y = 7.50" Ind. 3: $\theta = 70^\circ$ d = +7 dB L = 0.25", Z = 0.33" X = 0", Y = 13.38"	Rejected Ind. 1: $\theta = 70^\circ$ d = +3 dB L = 0.55", Z = 0.65" X = -0.34", Y = 2.29" Ind. 2: $\theta = 70^\circ$ d = +6 dB L = 0.47", Z = 0.35" X = +0.053", Y = 7.81" Ind. 3: $\theta = 70^\circ$ d = +8 dB L = 0.23", Z = 0.39" X = +0.09", Y = 13.32"
S126	Rejected	Rejected Ind. 1: $\theta = 70^\circ$ d = -2 dB L = 1.25", Z = 0.82" X = -0.25", Y = 2.5" Ind. 2: $\theta = 70^\circ$ d = +5 dB L = 0.63", Z = 0.69" X = +0.25", Y = 6.88" Ind. 3: $\theta = 70^\circ$ d = +11 dB L = 0.50", Z = 0.25" X = -0.38", Y = 8.63" Ind. 4: $\theta = 70^\circ$ d = -2 dB L = 0.50", Z = 0.88" X = -0.13", Y = 11.25"	Rejected Ind. 1: $\theta = 70^\circ$ d = -6 dB L = 1.51", Z = 0.67" X = -0.25", Y = 2.46" Ind. 2: $\theta = 70^\circ$ d = +7 dB L = 0.87", Z = 0.47" X = +0.09", Y = 6.85" Ind. 3: $\theta = 70^\circ$ d = +4 dB L = 0.55", Z = 0.33" X = -0.15", Y = 8.84" Ind. 4: $\theta = 70^\circ$ d = -5 dB L = 1.17", Z = 0.91" X = +0.04", Y = 11.23"

1 inch = 25.4 mm

Table 6. Inspection results of laboratory specimens (continued).

Specimen ID	RT	Manual UT	AUT
S131	Accepted	Accepted	Accepted
S132	Rejected	Rejected Ind. 1: $\theta = 70^\circ$ $d = +9$ dB $L = 12''$, $Z = 1.00''$ $X = +0.56''$, $Y = 0''$	Rejected [†] Ind. 1A: BSC, $\theta = 70^\circ$ $d = +8$ dB $L = 0.60''$, $Z = 1.0''$ $X = +0.52''$, $Y = 0''$ Ind. 1B: BSC, $\theta = 70^\circ$ $d = +9$ dB $L = 1.2''$, $Z = 0.72''$ $X = +0.53''$, $Y = 2.6''$ Ind. 1C: BSC, $\theta = 70^\circ$ $d = +7$ dB $L = 0.48''$, $Z = 0.72''$ $X = +0.48''$, $Y = 4.52''$ Ind. 1D: BSC, $\theta = 70^\circ$ $d = +5$ dB $L = 0.56''$, $Z = 0.86''$ $X = +0.50''$, $Y = 5.88''$ Ind. 1E: $\theta = 70^\circ$ $d = +9$ dB $L = 1.1''$, $Z = 1.49''$ $X = +0.25''$, $Y = 9.10''$ Ind. 1F: TSC, $\theta = 70^\circ$ $d = +5$ dB $L = 7''$, $Z = 0.133''$ $X = +0.44''$, $Y = 0''$ Ind. 1G: TSC, $\theta = 70^\circ$ $d = +4$ dB $L = 0.80''$, $Z = 0''$ $X = +0.42''$, $Y = 7.0''$ Ind. 1H: TSC, $\theta = 70^\circ$ $d = +4$ dB $L = 0.95''$, $Z = 0.36''$ $X = +0.42''$, $Y = 8.93''$

[†]Under the provisions of table 6.3 in the AASHTO/AWS D1.5: 2002 Bridge Welding Code (i.e., class B and class C flaws shall be separated by at least 2L), Ind. 1A, Ind. 1B, ... are considered as a single defect, Ind. 2A, Ind. 2B, ... are considered as a single defect, etc.

1 inch = 25.4 mm

Table 6. Inspection results of laboratory specimens (continued).

Specimen ID	RT	Manual UT	AUT
S133	Rejected	Rejected Ind. 1: $\theta = 70^\circ$ d = +8 dB L = 5.75", Z = 0.94" X = -0.56", Y = 0"	Rejected [†] Ind. 1A: $\theta = 70^\circ$ d = 0 dB L = 0.28", Z = 0.21" X = +0.39", Y = 0" Ind. 1B: $\theta = 70^\circ$ d = +6 dB L = 1.28", Z = 0.29" X = +0.32", Y = 2.77" Ind. 1C: $\theta = 70^\circ$ d = +6 dB L = 0.88", Z = 0.21" X = +0.32", Y = 4.28"
S134	Accepted	Accepted	Accepted

[†]Under the provisions of table 6.3 in the AASHTO/AWS D1.5: 2002 Bridge Welding Code (i.e., class B and class C flaws shall be separated by at least 2L), Ind. 1A, Ind. 1B, ... are considered as a single defect, Ind. 2A, Ind. 2B, ... are considered as a single defect, etc.

1 inch = 25.4 mm

Table 6. Inspection results of laboratory specimens (continued).

Specimen ID	RT	Manual UT	AUT
S135	Rejected	Rejected Ind. 1: $\theta = 70^\circ$ $d = -2$ dB $L = 2.25''$, $Z = 0.38''$ $X = +0.13''$, $Y = 3.50''$ Ind. 2: $\theta = 70^\circ$ $d = +9$ dB $L = 2.38''$, $Z = 0.19''$ $X = +0.25''$, $Y = 8.13''$ Ind. 3: $\theta = 70^\circ$ $d = +1$ dB $L = 1.25''$, $Z = 0.56''$ $X = +0.25''$, $Y = 11.75''$	Rejected [†] Ind. 1A: BSC, $\theta = 70^\circ$ $d = +6$ dB $L = 1.76''$, $Z = 0.47''$ $X = +0.09''$, $Y = 3.72''$ Ind. 1B: TSC, $\theta = 70^\circ$ $d = -11$ dB $L = 0.72''$, $Z = 0.39''$ $X = +0.09''$, $Y = 4.44''$ Ind. 2A: BSC, $\theta = 70^\circ$ $d = +1$ dB $L = 0.79''$, $Z = 0.35''$ $X = -0.35''$, $Y = 9.57''$ Ind. 2B: TSC, $\theta = 70^\circ$ $d = +2$ dB $L = 1.07''$, $Z = 0.30''$ $X = -0.05''$, $Y = 9.95''$ Ind. 3A: BSC, $\theta = 70^\circ$ $d = 0$ dB $L = 1.13''$, $Z = 0.65''$ $X = +0.30''$, $Y = 12.20''$ Ind. 3B: TSC, $\theta = 70^\circ$ $d = -4$ dB $L = 0.89''$, $Z = 0.50''$ $X = +0.42''$, $Y = 12.27''$

[†]Under the provisions of table 6.3 in the AASHTO/AWS D1.5: 2002 Bridge Welding Code (i.e., class B and class C flaws shall be separated by at least 2L), Ind. 1A, Ind. 1B, ... are considered as a single defect, Ind. 2A, Ind. 2B, ... are considered as a single defect, etc.

1 inch = 25.4 mm

Table 6. Inspection results of laboratory specimens (continued).

Specimen ID	RT	Manual UT	AUT
S136	Rejected	Rejected Ind. 1: $\theta = 70^\circ$ $d = +2$ dB $L = 2.0''$, $Z = 0.38''$ $X = +0.13''$, $Y = 2.0''$ Ind. 2: $\theta = 70^\circ$ $d = +6$ dB $L = 2.38''$, $Z = 0.25''$ $X = 0''$, $Y = 9.5''$	Rejected [†] Ind. 1A: BSC, $\theta = 70^\circ$ $d = -7$ dB $L = 0.96''$, $Z = 0.30''$ $X = +0.96''$, $Y = 2.21''$ Ind. 1B: TSC, $\theta = 70^\circ$ $d = -4$ dB $L = 1.12''$, $Z = 0.35''$ $X = -0.45''$, $Y = 2.61''$ Ind. 2A: BSC, $\theta = 70^\circ$ $d = -2$ dB $L = 0.641''$, $Z = 0.73''$ $X = -0.65''$, $Y = 9.16''$ Ind. 2B: BSC, $\theta = 70^\circ$ $d = +3$ dB $L = 1.23''$, $Z = 0.13''$ $X = -0.65''$, $Y = 10.53''$

[†]Under the provisions of table 6.3 in the AASHTO/AWS D1.5: 2002 Bridge Welding Code (i.e., class B and class C flaws shall be separated by at least 2L), Ind. 1A, Ind. 1B, ... are considered as a single defect, Ind. 2A, Ind. 2B, ... are considered as a single defect, etc.

1 inch = 25.4 mm

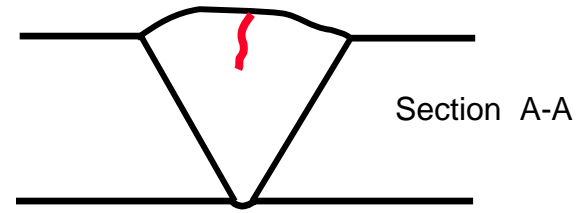
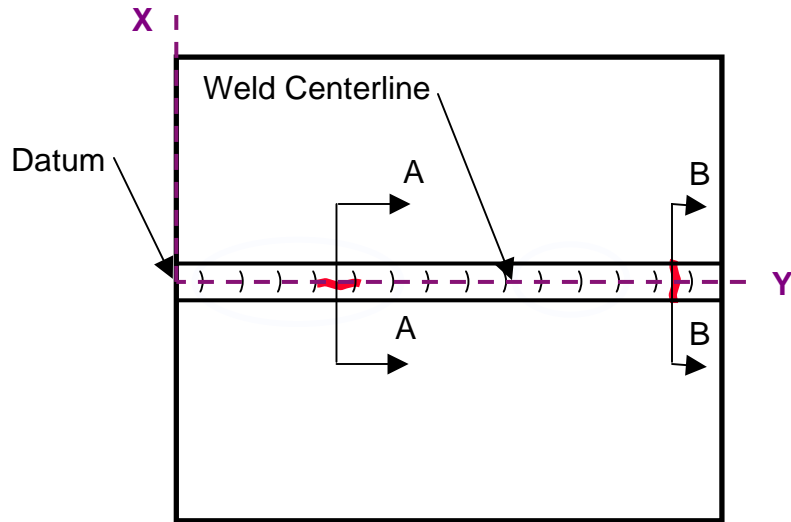


Figure 34. Laboratory specimen S034: Schematic diagram of longitudinal/centerline crack.

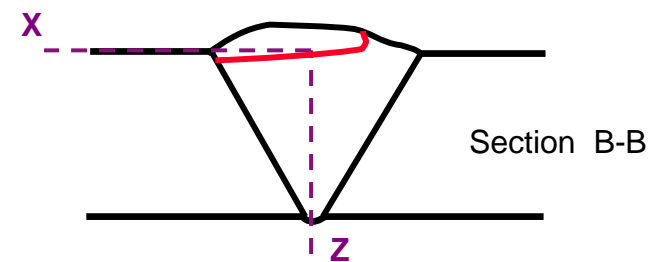
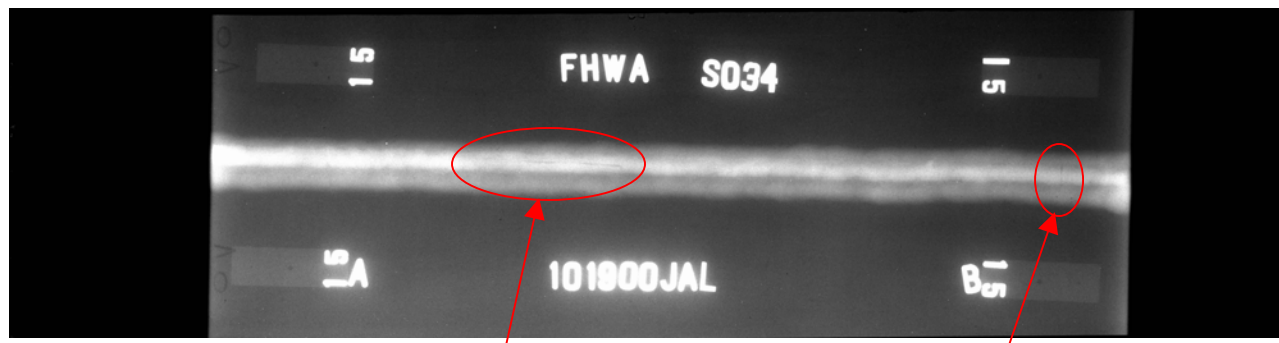


Figure 35. Laboratory specimen S034: Schematic diagram of transverse crack.



Longitudinal/Centerline Indication

Transverse Indication

Figure 36. Laboratory specimen S034: Radiographic image showing the two implanted cracks.

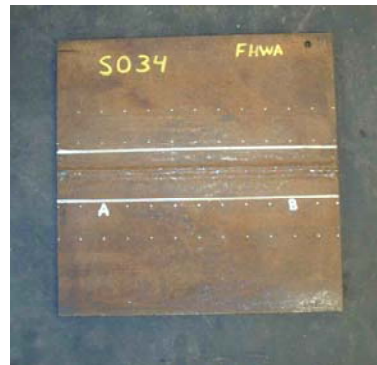
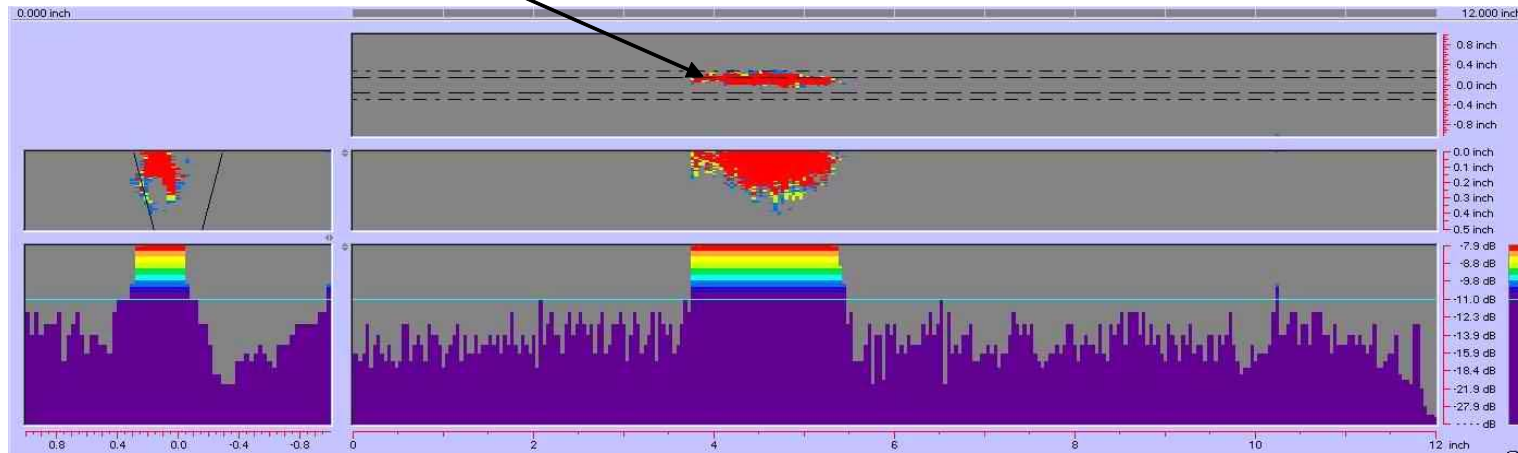


Figure 37. Laboratory specimen S034: Top view of joint.

55

Longitudinal/Centerline Crack



1 inch = 25.4 mm

Figure 38. P-scan images of laboratory specimen S034: Images of longitudinal/centerline indication in the weld.

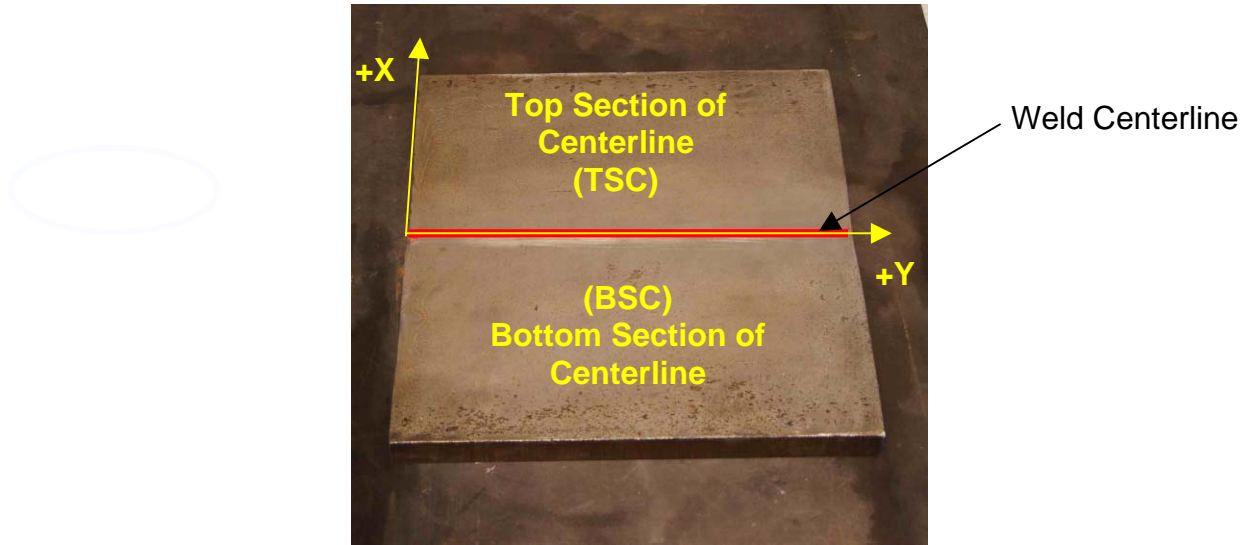


**Figure 39. Laboratory specimen S125:
Top view of joint.**

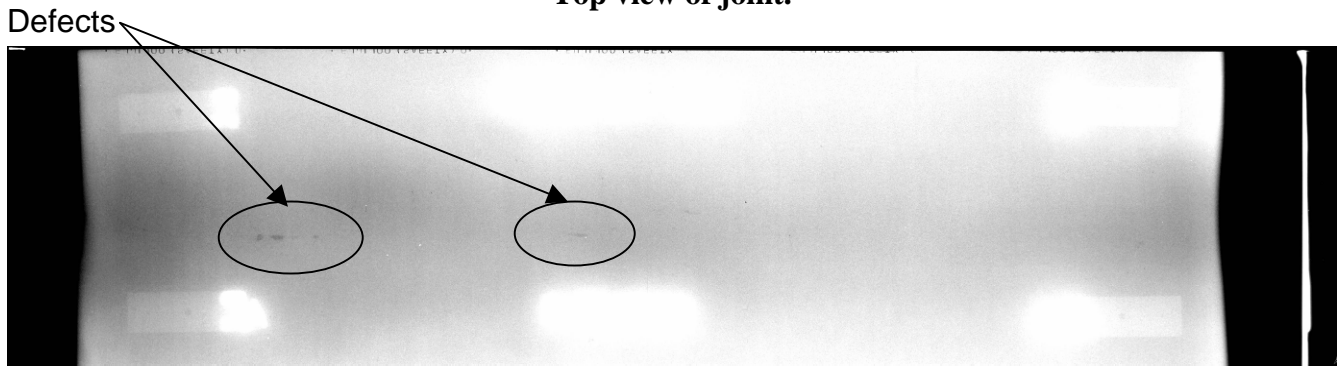


**Figure 40. Laboratory specimen S125: Radiographic image
showing discontinuities in the weld.**

Rejectable Indications

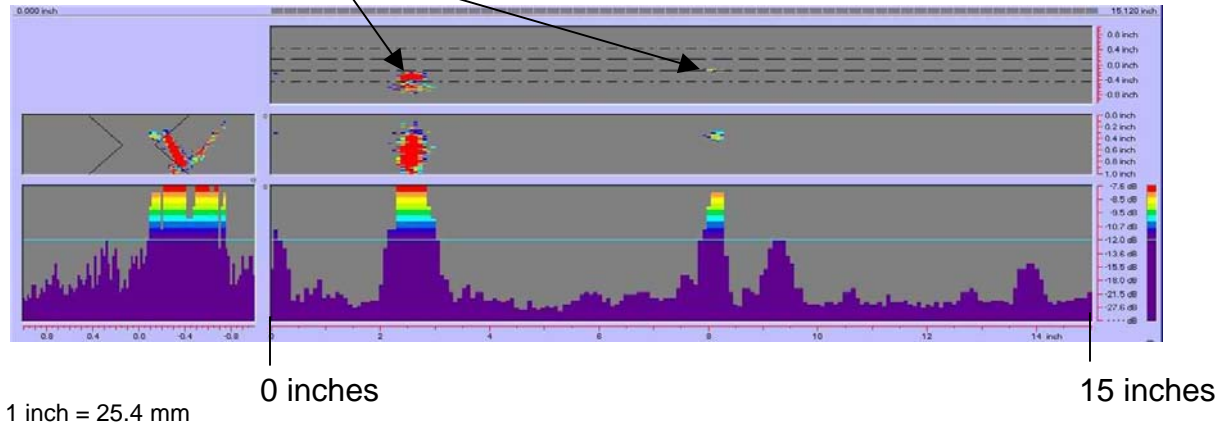


Figure 41. P-scan images of laboratory specimen S125: From TSC side of centerline.

Rejectable Indications

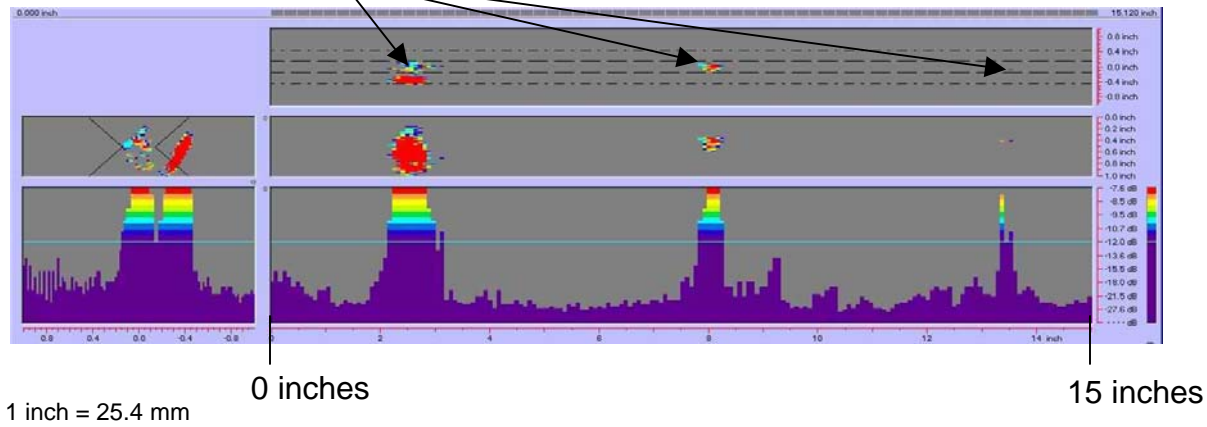
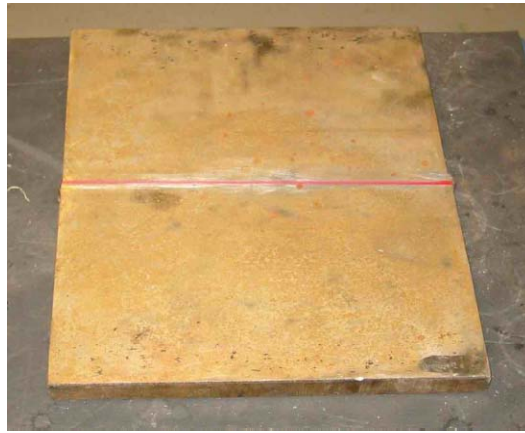
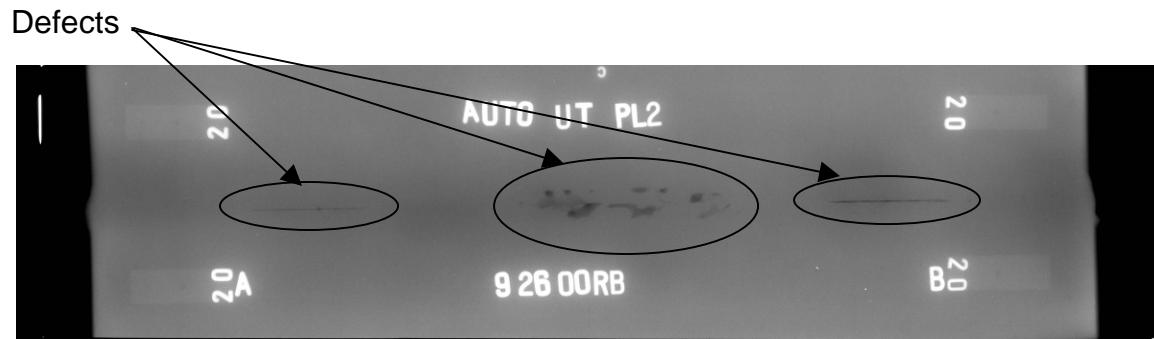


Figure 42. P-scan images of laboratory specimen S125: From BSC side of centerline.



**Figure 43. Laboratory specimen S126:
Top view of joint.**



**Figure 44. Laboratory specimen S126: Radiographic image
showing discontinuities in the weld.**

Rejectable Indications

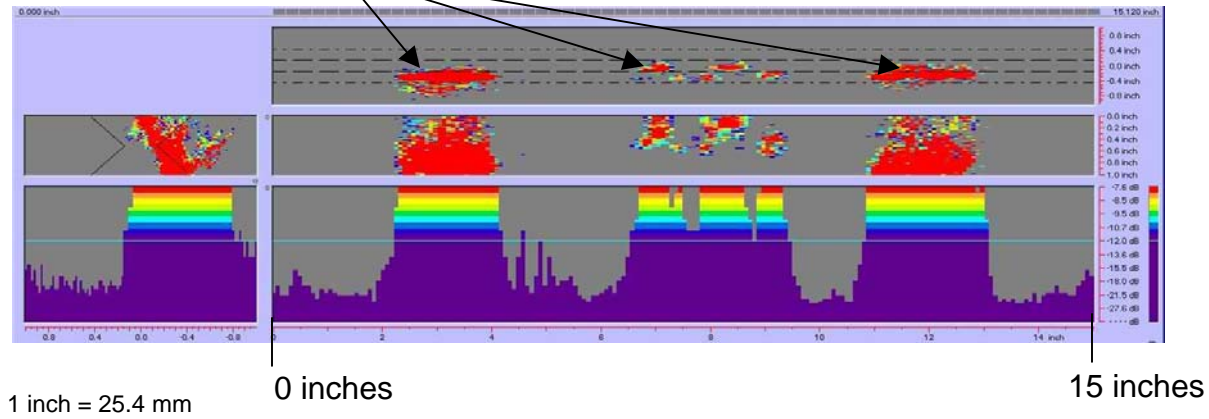


Figure 45. P-scan images of laboratory specimen S126: From TSC side of centerline.

Rejectable Indications

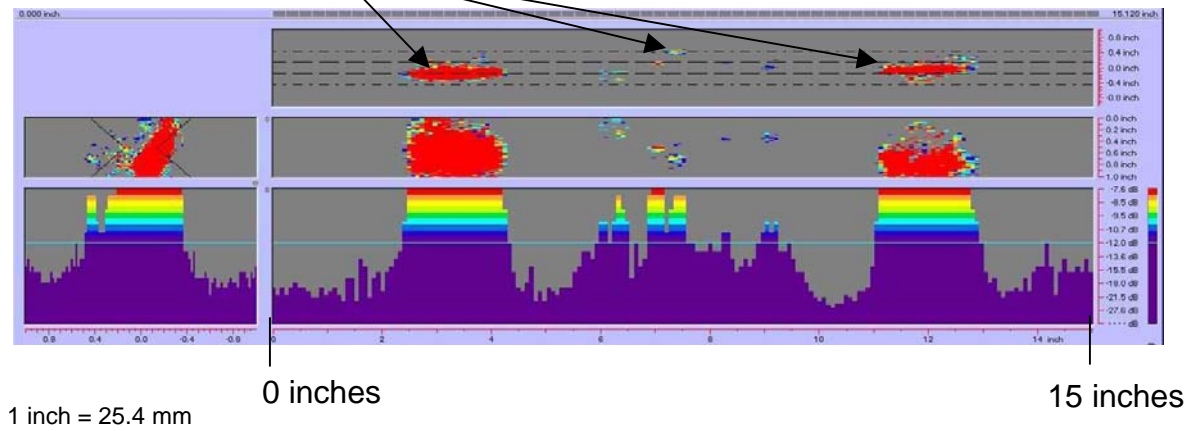


Figure 46. P-scan images of laboratory specimen S126: From BSC side of centerline.

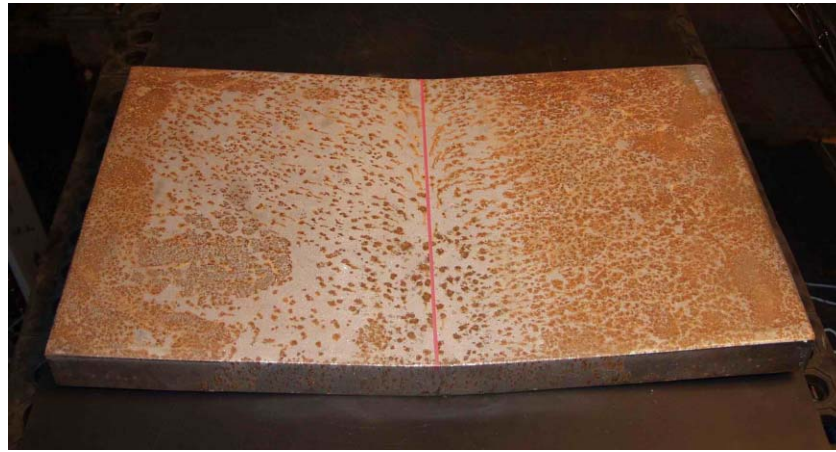


Figure 47. Laboratory specimen S132: View of joint.

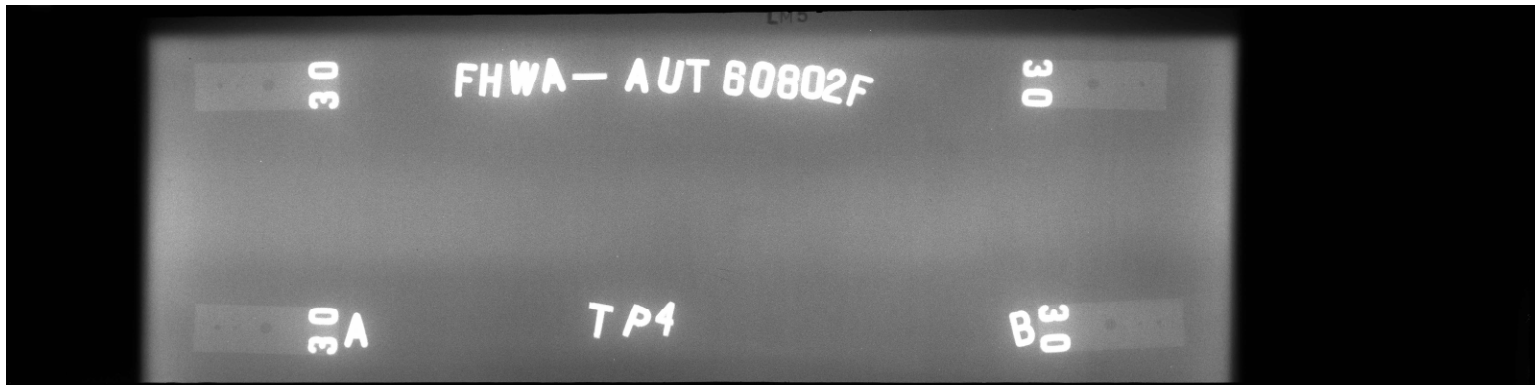


Figure 48. Laboratory specimen S132: Radiographic image showing discontinuities in the weld.

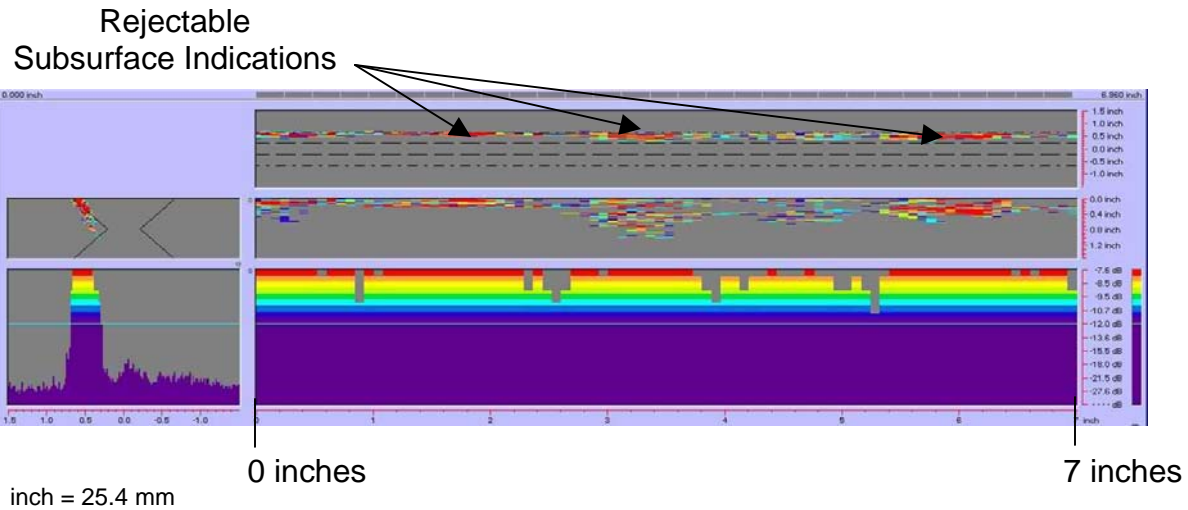


Figure 49. P-scan images of laboratory specimen S132: From TSC side of centerline between 0 and 177.8 mm (0 and 7 inches).

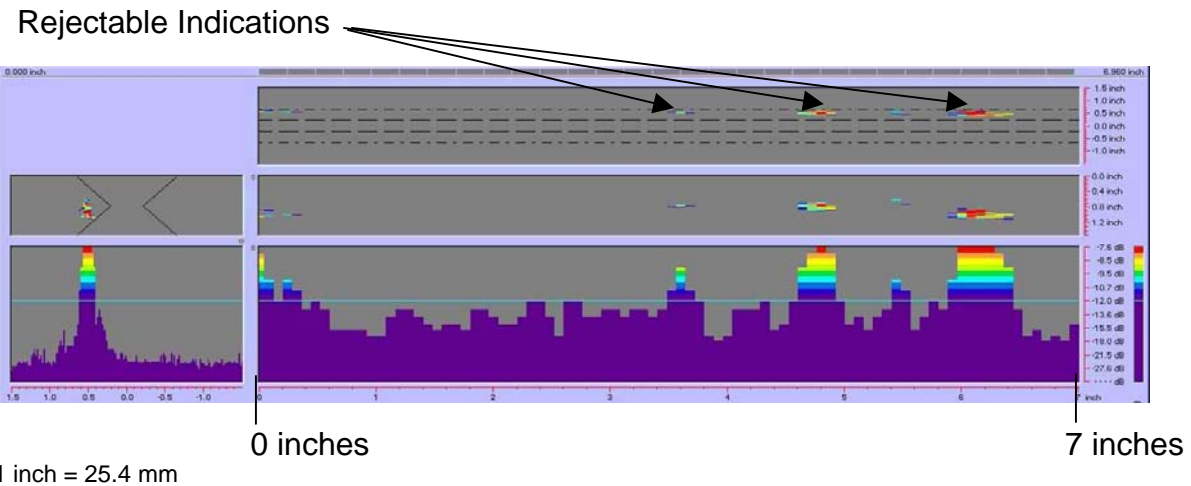
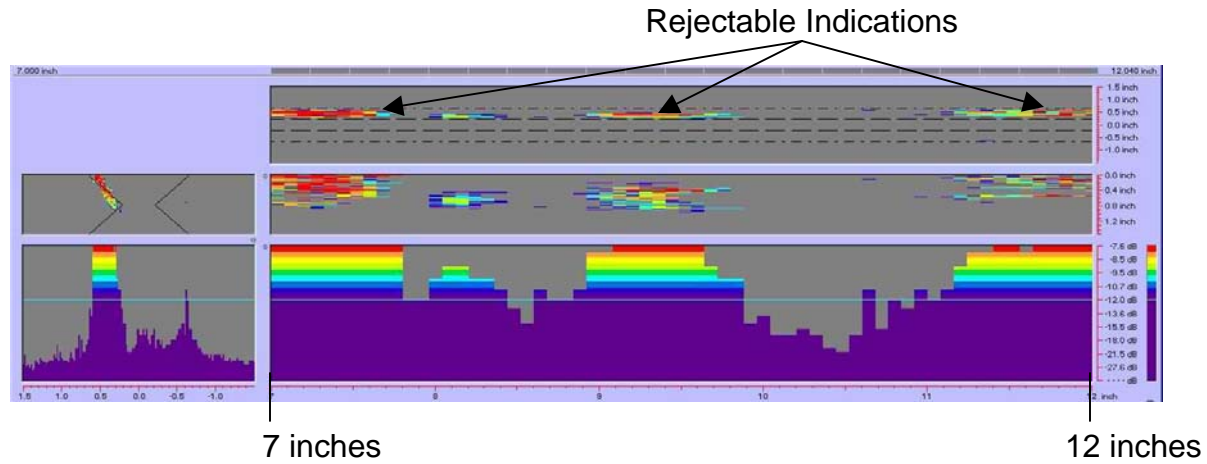
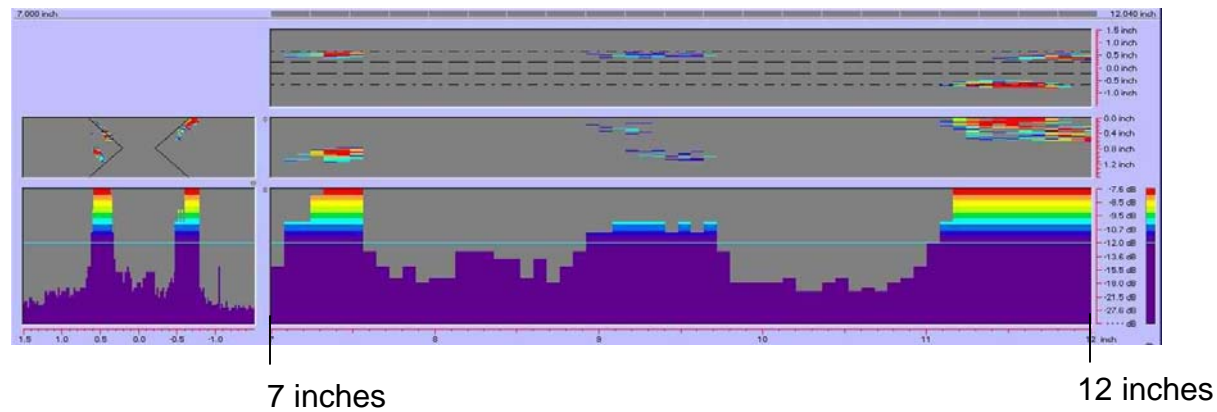


Figure 50. P-scan images of laboratory specimen S132: From BSC side of centerline between 0 and 177.8 mm (0 and 7 inches).



1 inch = 25.4 mm

Figure 51. P-scan images of laboratory specimen S132: From TSC side of centerline between 177.8 and 304.8 mm (7 and 12 inches).



1 inch = 25.4 mm

Figure 52. P-scan images of laboratory specimen S132: From BSC side of centerline between 177.8 and 304.8 mm (7 and 12 inches).

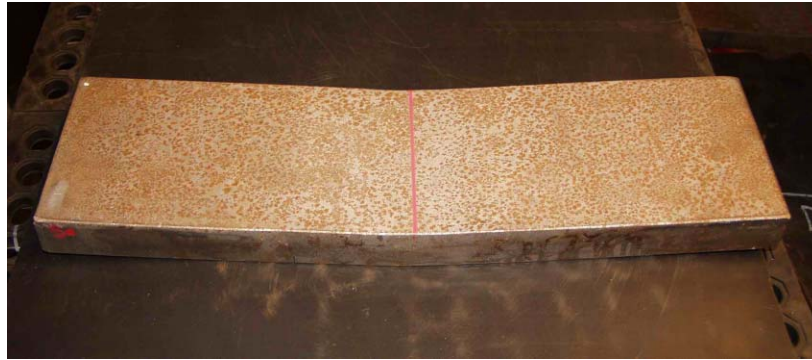


Figure 53. Laboratory specimen S133: Top view of joint.

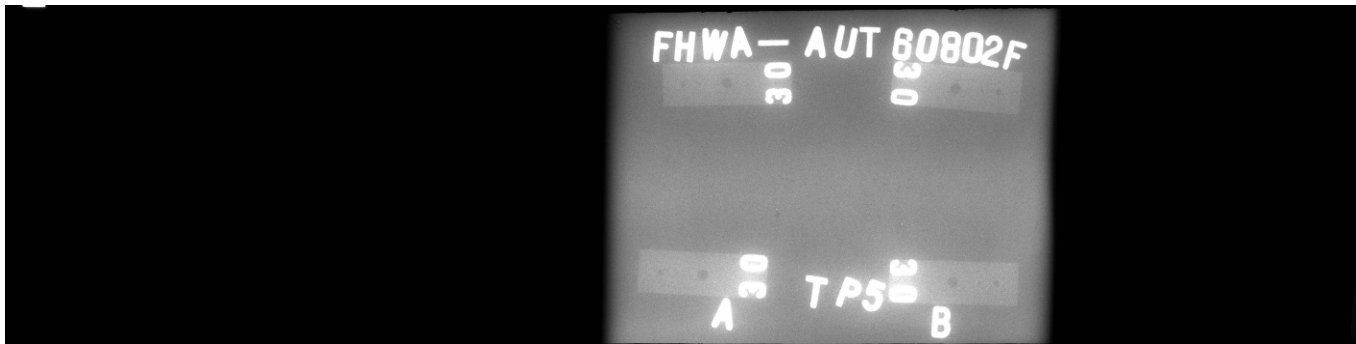


Figure 54. Laboratory specimen S133: Radiographic image showing discontinuities in the weld.

Rejectable Indications

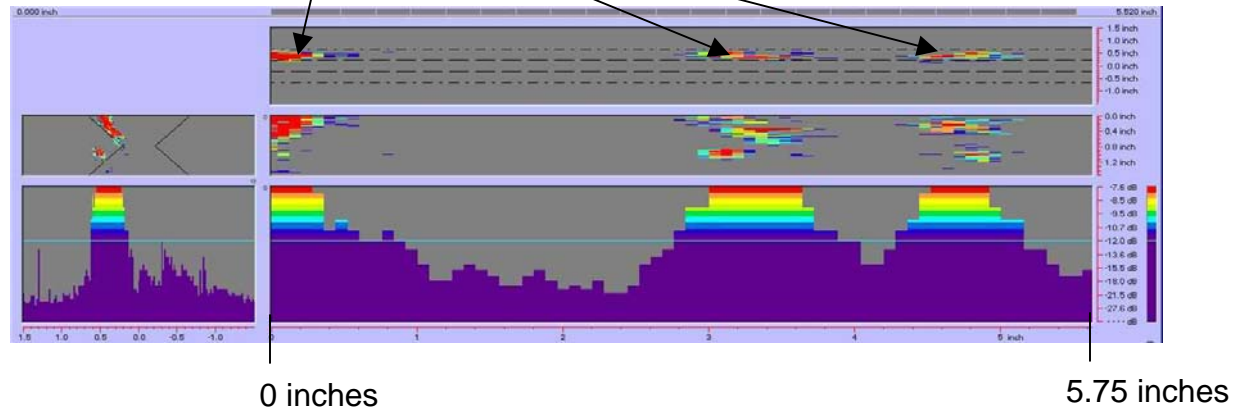
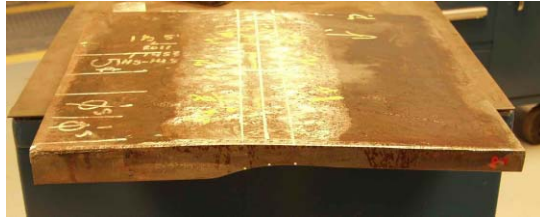
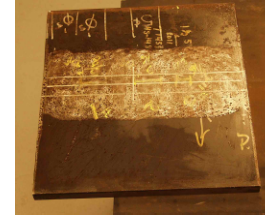


Figure 55. P-scan images of laboratory specimen S133.



**Figure 56. Laboratory specimen S135:
Side view of joint.**



**Figure 57. Laboratory specimen S135:
Top view of joint.**

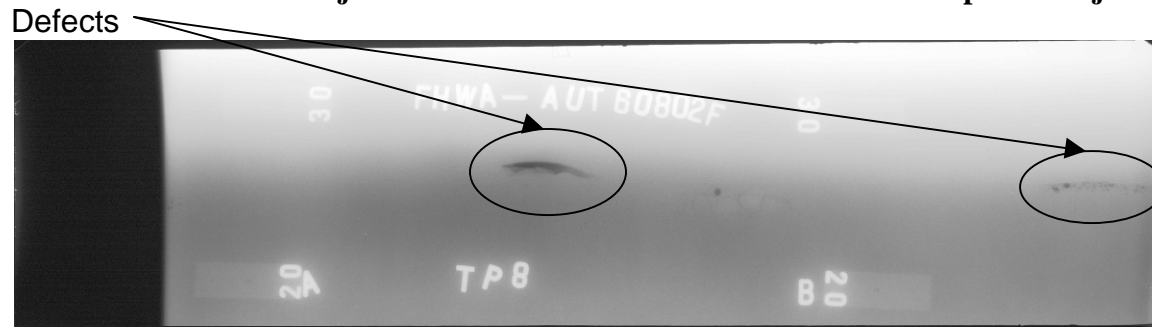


**Figure 58. Laboratory specimen S135: Radiographic image
showing discontinuities in the weld between markers A and B.**

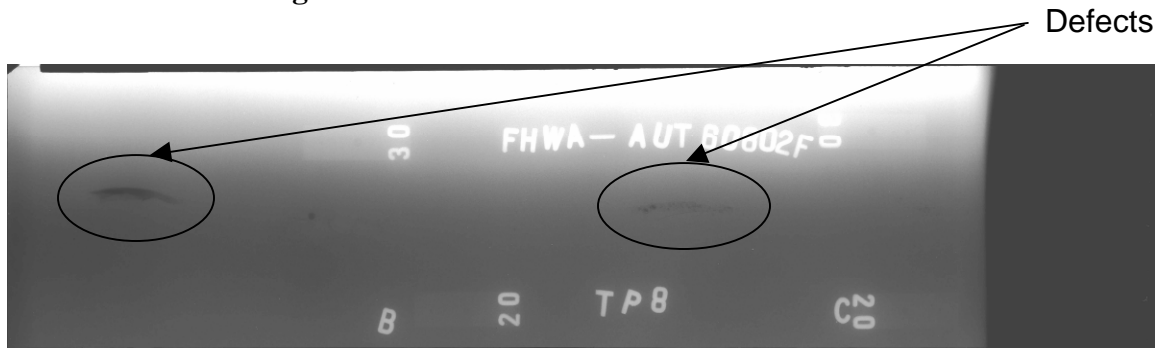


**Figure 59. Laboratory specimen S135: Radiographic image
showing discontinuities in the weld between markers B and C.**

Rejectable Indication

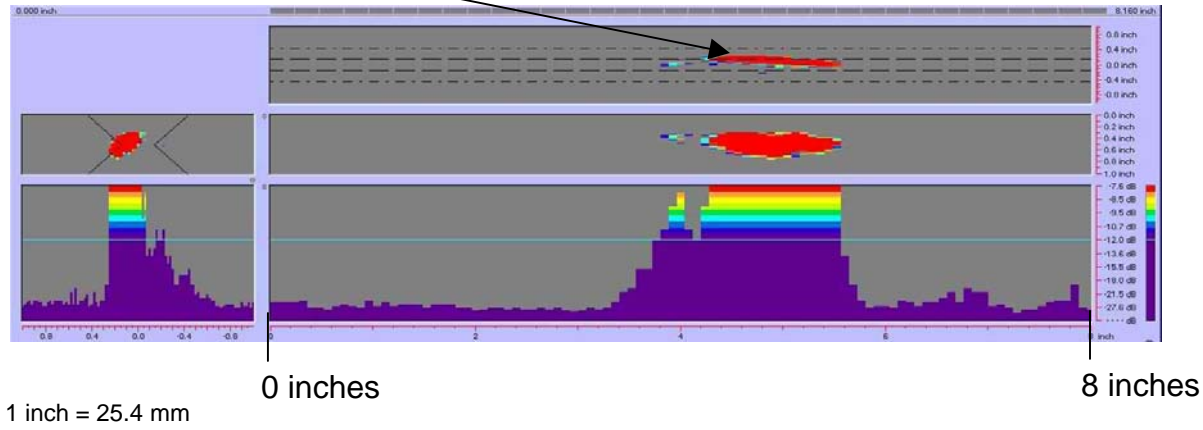


Figure 60. P-scan images of laboratory specimen S135: From TSC side of centerline between 0 and 203.2 mm (0 and 8 inches).

Rejectable Indication

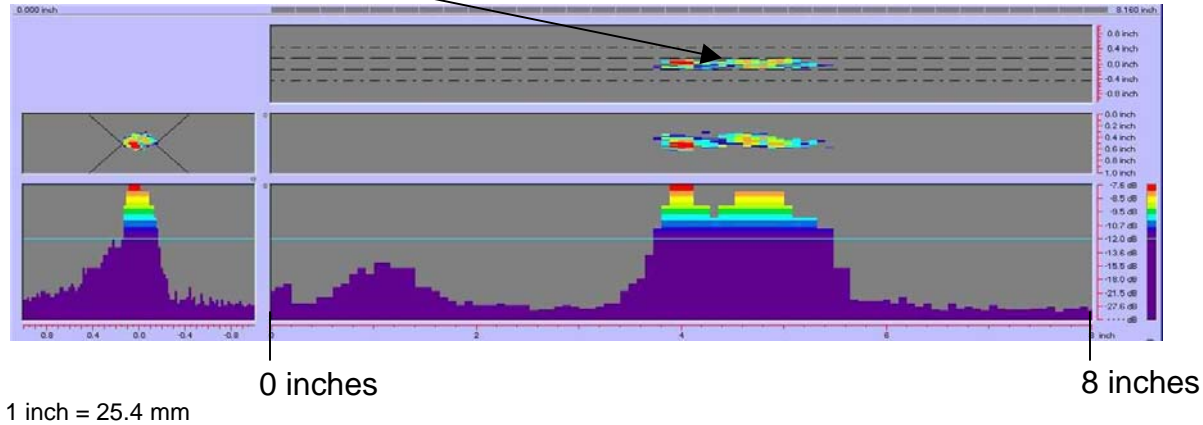


Figure 61. P-scan images of laboratory specimen S135: From BSC side of centerline between 0 and 203.2 mm (0 and 8 inches).

Rejectable Indications

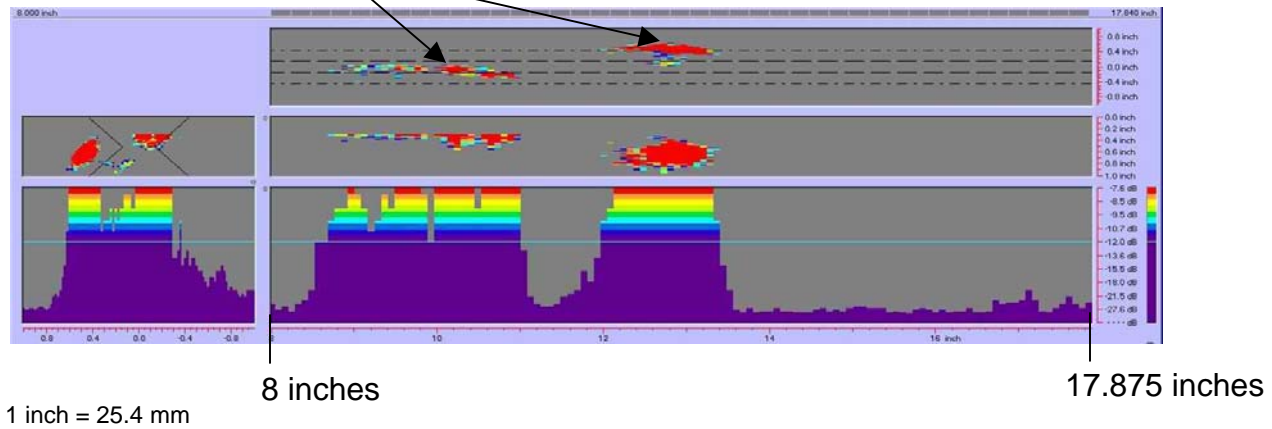


Figure 62. P-scan images of laboratory specimen S135: From TSC side of centerline between 203.2 and 454 mm (8 and 17.875 inches).

Rejectable Indications

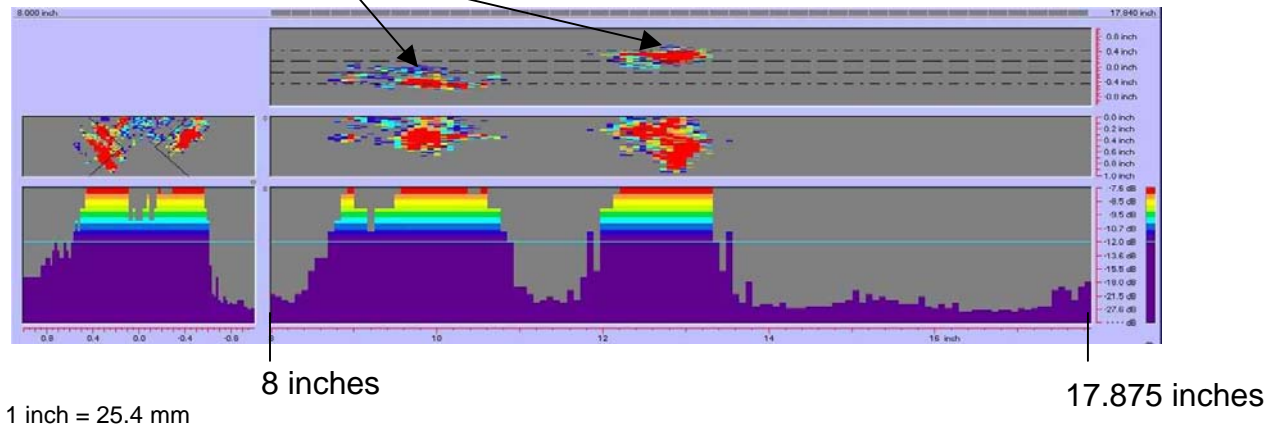
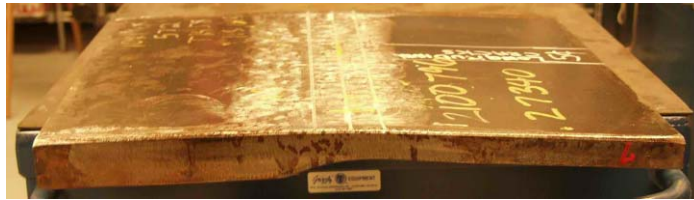
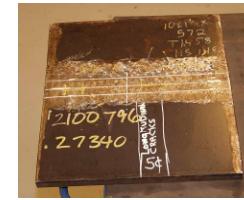


Figure 63. P-scan images of laboratory specimen S135: From BSC side of centerline between 203.2 and 454 mm (8 and 17.875 inches).



**Figure 64. Laboratory specimen S136:
Side view of joint.**



**Figure 65. Laboratory specimen S136:
Top view of joint.**

Defect

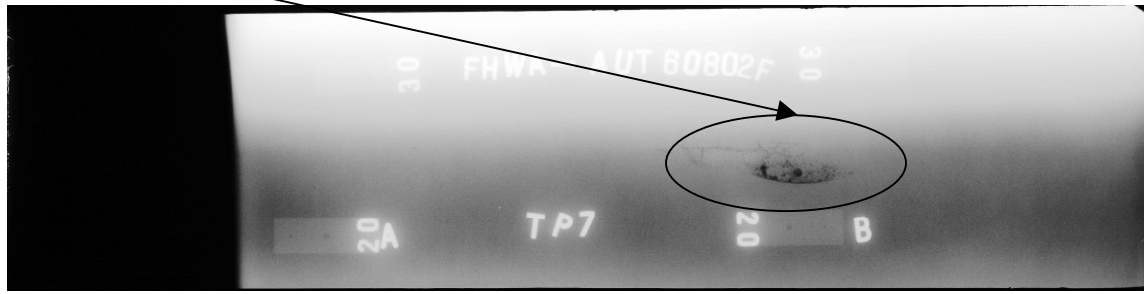


**Figure 66. Laboratory specimen S136: Radiographic image
showing discontinuities in the weld between markers A and B.**

Defects

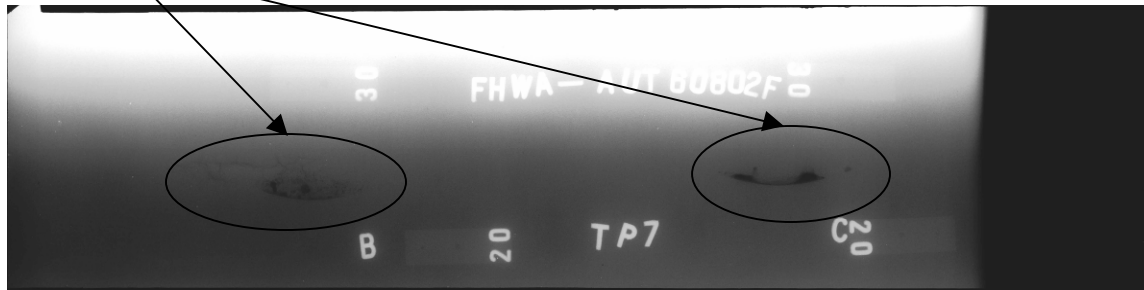


**Figure 67. Laboratory specimen S136: Radiographic image
showing discontinuities in the weld between markers B and C.**

Rejectable Indication

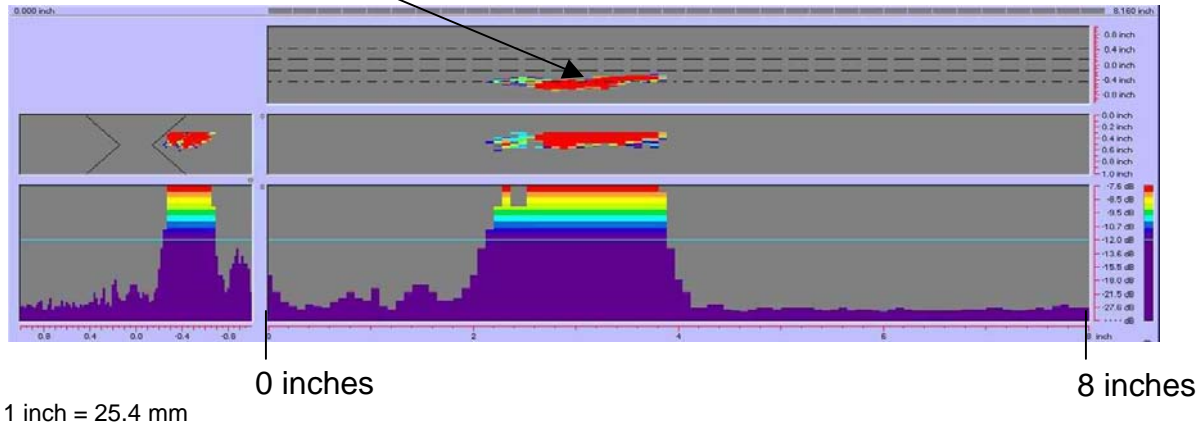


Figure 68. P-scan images of laboratory specimen S136: From TSC side of centerline between 0 and 203.2 mm (0 and 8 inches).

Rejectable Indication

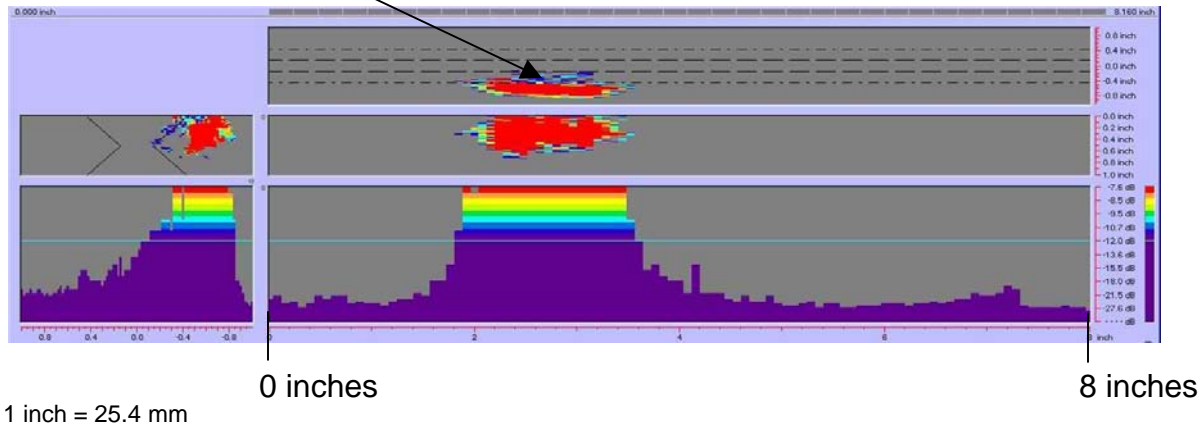


Figure 69. P-scan images of laboratory specimen S136: From BSC side of centerline between 0 and 203.2 mm (0 and 8 inches).

Rejectable Indication

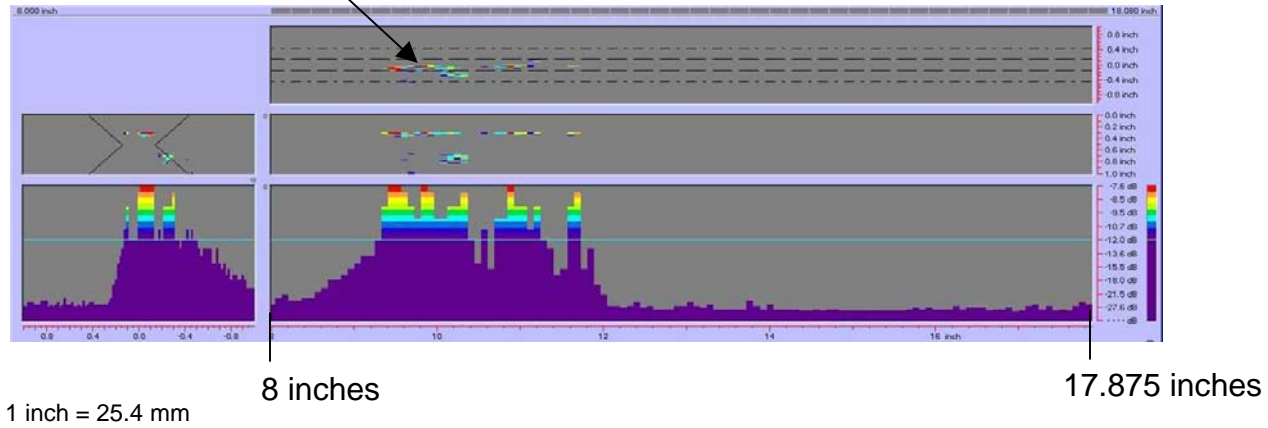


Figure 70. P-scan images of laboratory specimen S136: From TSC side of centerline between 203.2 and 454 mm (8 and 17.875 inches).

Rejectable Indications

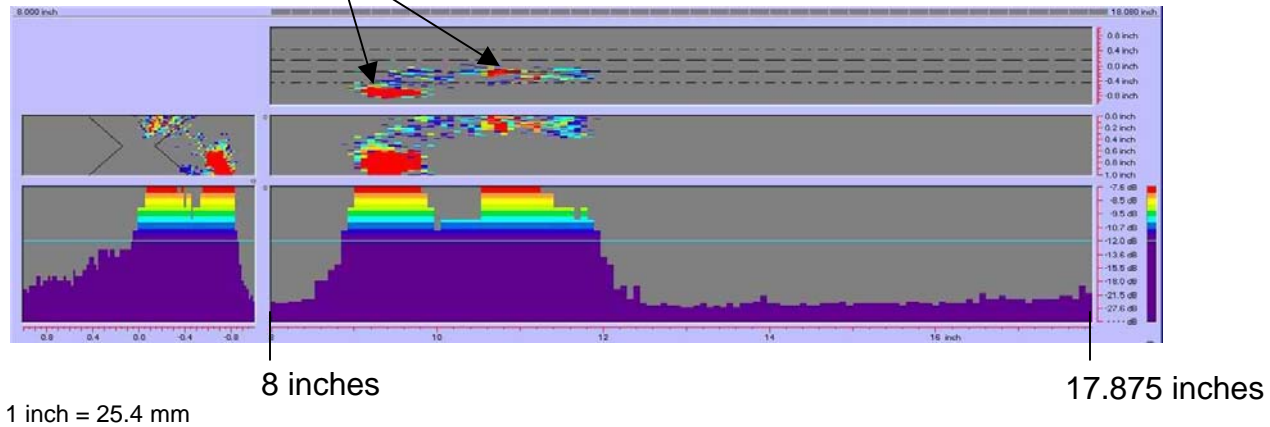


Figure 71. P-scan images of laboratory specimen S136: From BSC side of centerline between 203.2 and 454 mm (8 and 17.875 inches).

BLIND FIELD-TESTING RESULTS

During the course of the AUT field study, it was not convenient to conduct blind testing because of fabrication plant logistics and scheduling. However, one blind test was conducted successfully. The purpose of blind testing was to eliminate bias by performing AUT inspection before RT and manual UT inspection.

The specimen (selected at random) for blind testing was FG38K-TopF-FCM. Specimen FG38K-TopF-FCM was composed of two welded butt joints designated as FG38K-TF1-TopF-FCM and FG38K-TF2-TopF-FCM, each having a width transition. Specimen FG38K-TopF-FCM was 76.2 mm (3 inches) thick, 857.25 mm (33.75 inches) wide, and was designated as a fracture-critical member (FCM). Plates designed as FCMs must be inspected by both RT and manual UT according to section 6.7.1.2 of the AASHTO/AWS D1.5M/D1.5: 2002 Bridge Welding Code.⁽¹⁾ Table 6.2 in the AASHTO/AWS D1.5M/D1.5: 2002 Bridge Welding Code⁽¹⁾ indicates that plates with thicknesses ranging from greater than 60 to 90 mm (2.5 to 3.5 inches) must be inspected by UT using 45-degree and 70-degree probes. The 45-degree probe inspects the top quarter of the weld thickness, while the 70-degree probe inspects the remainder of the weld thickness. Unfortunately, the AUT inspection was only performed using a 45-degree probe because of time constraints.

For convenience, the width of each butt joint was divided into three segments: 280 mm (11 inches), 280 mm (11 inches), and 300 mm (11.75 inches) long. The P-scan results indicated that specimen FG38K-TF1-TopF-FCM passed the AUT inspection with no rejectable defects in the weld. However, specimen FG38K-TF2-TopF-FCM (figures 72 and 73) was diagnosed with defects and was rejected. The P-scan images of specimen FG38K-TF2-TopF-FCM are shown in figures 74 through 79. Figures 74 and 75 show the P-scan images of the first segment of the weld. At location $Y = 27.686$ mm (1.09 inches) from the datum, a 20.32-mm- (0.8-inch-) long indication was found. In addition, subsurface indications were detected along face A (i.e., the top surface) and face B (i.e., the bottom surface) of the plate. Figures 76 and 77 show the second segment of the weld with rejectable subsurface indications. Figures 78 and 79 show rejectable subsurface indications in the third segment of the weld. Figures 80 through 82 show the RT results for specimen FG38K-TF2-TopF-FCM in three segments. The first section extends from the left edge of the plate to approximately 304.8 mm (12 inches) from the left edge (figure 80). Fiducial marker B, indicated in figure 80, corresponds to the same marker in figure 81 (the second segment of the radiograph). Fiducial marker C, in figure 81, corresponds to the same marker in figure 82 (the third segment of the radiograph). The radiographic image for specimen FG38K-TF2-TopF-FCM (shown in figure 80) indicates a slag inclusion at location $Y = 19.05$ mm (0.75 inch) from the left edge. No subsurface defects were observed in the other radiographs. Table 7 summarizes the blind field-testing results.

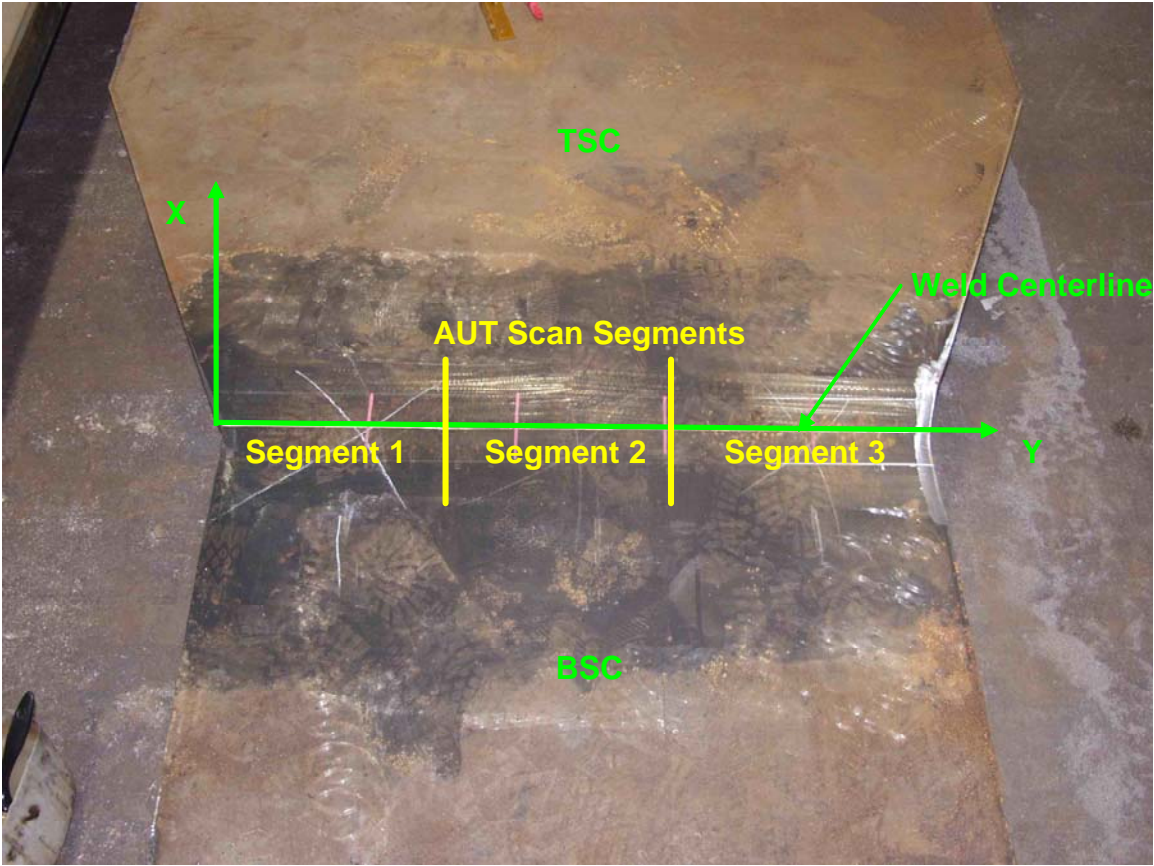


Figure 72. Field specimen FG38K-TF2-TopF-FCM used in blind testing: Top view of joint.



Figure 73. Field specimen FG38K-TF2-TopF-FCM used in blind testing: Side view of joint.

Subsurface Indications

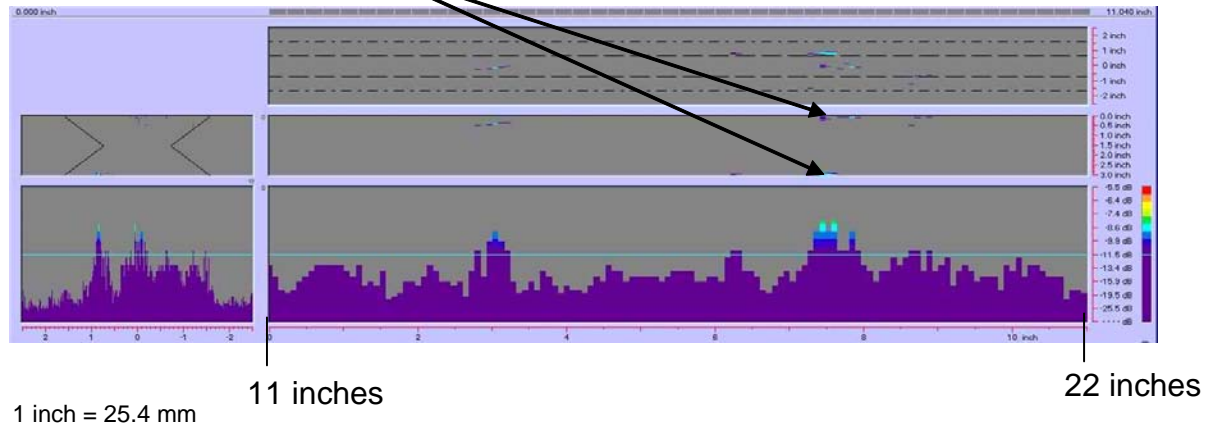


Figure 76. P-scan images of field specimen FG38K-TF2-TopF-FCM using 45-degree probe: From TSC side of centerline between 279.4 and 558.8 mm (11 and 22 inches).

74

Subsurface Indications



Figure 77. P-scan images of field specimen FG38K-TF2-TopF-FCM using 45-degree probe: From BSC side of centerline between 279.4 and 558.8 mm (11 and 22 inches).

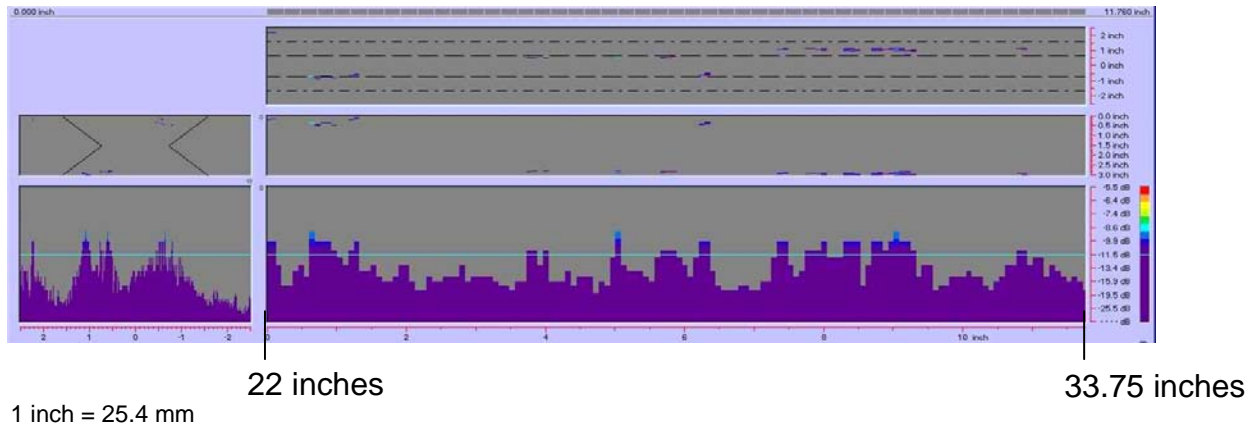


Figure 78. P-scan images of field specimen FG38K-TF2-TopF-FCM using 45-degree probe: From TSC side of centerline between 558.8 and 857.25 mm (22 and 33.75 inches).

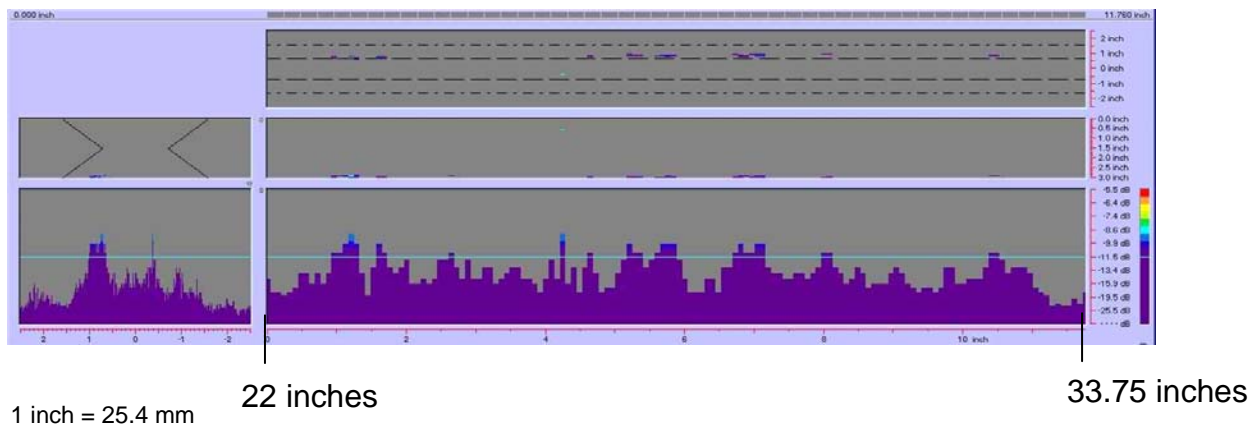


Figure 79. P-scan images of field specimen FG38K-TF2-TopF-FCM using 45-degree probe: From BSC side of centerline between 558.8 and 857.25 mm (22 and 33.75 inches).

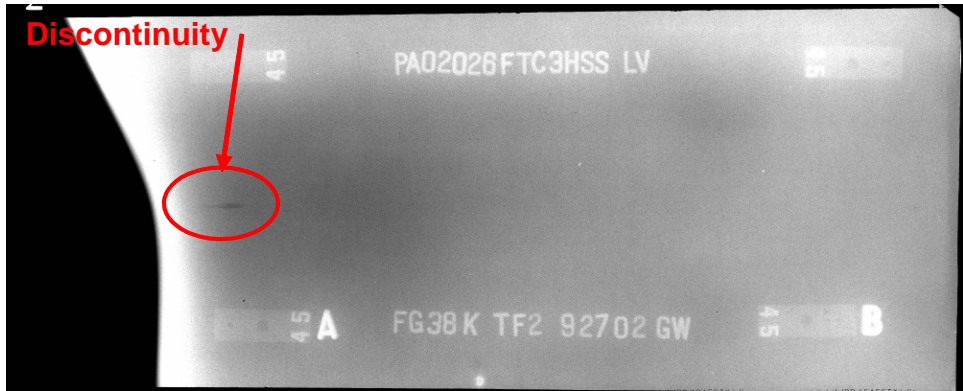


Figure 80. Radiographic image of field specimen FG38K-TF2-TopF-FCM: Section A-B.

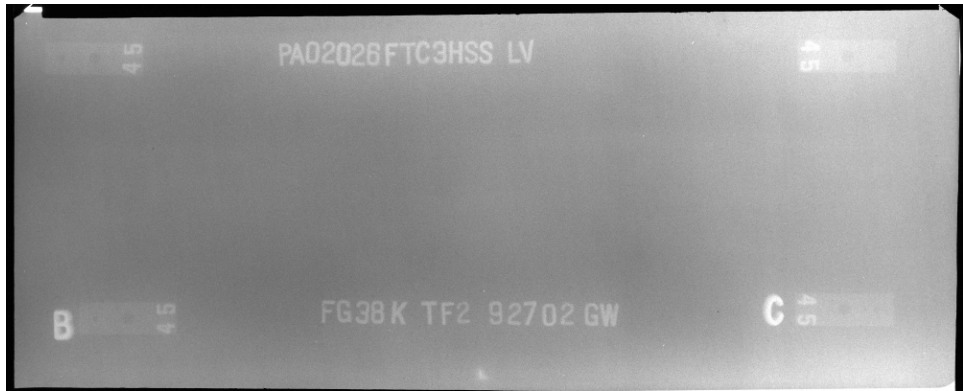


Figure 81. Radiographic image of field specimen FG38K-TF2-TopF-FCM: Section B-C.



Figure 82. Radiographic image of field specimen FG38K-TF2-TopF-FCM: Section C-D.

Table 7. Inspection results of blind field testing.

Specimen ID	RT	Manual UT	AUT
FG38K-TF2- TopF-FCM	Rejected Ind. 1: A-B, Slag 0.75" From A Edge (i.e., Y = 0.75")	Rejected Ind. 1: $\theta = 45^\circ$ L = 0.80" Y = 1.00" Ind. 2: Subsurface Indications	Rejected [†] Ind. 1A: BSC, $\theta = 45^\circ$ d = -2 dB L = 0.55", Z = 1.72" X = -0.40", Y = 1.09" Ind. 1B: TSC, $\theta = 45^\circ$ d = +3 dB L = 0.25", Z = 1.82" X = -0.08", Y = 1.79" Ind. 2A: TSC, $\theta = 45^\circ$ d = +9 dB L = 1.86", Z = 0.08" X = -2.06", Y = 4.68" Ind. 2B: BSC, $\theta = 45^\circ$ d = +10 dB L = 0.15", Z = 0.05" X = -0.04", Y = 6.45" Ind. 3: BSC, $\theta = 45^\circ$ d = +8 dB L = 1.10", Z = 2.82" X = -0.49", Y = 6.68" Ind. 4: BSC, $\theta = 45^\circ$ d = +9 dB L = 4.44", Z = 2.883" X = +0.56", Y = 11" Ind. 5: BSC, $\theta = 45^\circ$ d = +7 dB L = 1.45", Z = 2.85" X = -1.08", Y = 16.41"

[†]Under the provisions of table 6.3 in the AASHTO/AWS D1.5: 2002 Bridge Welding Code (i.e., class B and class C flaws shall be separated by at least 2L), Ind. 1A, Ind. 1B, ... are considered as a single defect, Ind. 2A, Ind. 2B, ... are considered as a single defect, etc.

1 inch = 25.4 mm

Table 7. Inspection results of blind field testing (continued).

Specimen ID	RT	Manual UT	AUT
FG38K-TF2- TopF-FCM (continued)			Ind. 6: BSC, $\theta = 45^\circ$ d = +8 dB L = 0.31", Z = 0.07" X = -0.56", Y = 20.01" Ind. 7: BSC, $\theta = 45^\circ$ d = +9 dB L = 1.19", Z = 2.88" X = +0.69", Y = 22.86" Ind. 8: BSC, $\theta = 45^\circ$ d = +10 dB L = 2.42", Z = 2.9" X = +0.84", Y = 27"
FG38K-TF1- TopF-FCM	Accepted	Accepted	Accepted

1 inch = 25.4 mm

FIELD-TESTING RESULTS

The field testing results are summarized in tables 8 through 12. The first column of tables 8 through 12 indicates the specimen identification code. The second, third, and fourth columns indicate the inspection method performed on each specimen. "Rejected" or "Accepted" indicates that the specimen was either rejected or accepted, respectively, by the employed inspection method. "Not Required" indicates that the owners did not prescribe the particular inspection method for the specimen. In the cases where the specimens were rejected by RT and the owners did not require manual UT inspection, the fabricators used manual UT to determine the defect depth so that efficient repairs could be performed. In tables 8 through 12, "Ind." stands for indication, and the angle (θ) indicates the transducer's refracted angle. The indication characteristics in the fourth column (i.e., indication rating (d), length (L), depth (Z), x-position, and y-position) are obtained from P-scan images. These characteristics are compared with the UT acceptance-rejection criteria in tables 6.3 and 6.4 from the AASHTO/AWS D1.5M/D1.5: 2002 Bridge Welding Code⁽¹⁾ to determine whether the indications are accepted or rejected.

Tables 8 through 12 show that RT was performed on the remaining 44 field specimens according to the owner's requirements. Note that section 6.7.1.2 of the AASHTO/AWS D1.5M/D1.5: 2002 Bridge Welding Code⁽¹⁾ indicates that 100 percent of each joint subjected to calculated tension or stress reversal and 25 percent of each joint subjected to compression or shear should be inspected by manual UT or RT. The P-scan and radiographic images of the rejected field specimens are provided in figures 83 through 96.

The results from the first field test set at HSS are summarized in table 8. Only two specimens were tested in the first set using RT and AUT. Manual UT was not required. RT and AUT accepted both specimens with no rejectable defects.

Table 8. Inspection results of the first field testing at HSS.

Specimen ID	RT	Manual UT	AUT
G20A-TF2-BottF	Accepted	Not Required	Accepted
G21A-TF2-BottF	Accepted	Not Required	Accepted

Table 9. Inspection results of the second field testing at HSS.

Specimen ID	RT	Manual UT	AUT
G3F-CF1-BottF	Accepted	Not Required	Accepted
G3F-CF2-BottF	Accepted	Not Required	Accepted
G3F-TF1-TopF	Accepted	Not Required	Accepted
G3F-TF2-TopF	Accepted	Not Required	Accepted
G4F-TF1-TopF	Accepted	Not Required	Accepted
G4F-TF2-TopF	Accepted	Not Required	Accepted
G3J-TF1-TopF	Accepted	Not Required	Accepted
G3J-CF1-BottF	Accepted	Not Required	Accepted
G2A-CF1-TopF	Accepted	Not Required	Accepted
G2A-CF2-TopF	Accepted	Not Required	Accepted
G2A-CF3-TopF	Accepted	Not Required	Accepted
G2A-CF4-TopF	Accepted	Not Required	Accepted
G5G-TF1-TopF	Rejected Ind. 1: A–B, 0.13” Slag 0.94” From Edge (i.e., L = 0.13”, Y = 0.94”) Ind. 2: B–C, 0.25” Slag 0.82” From Edge (i.e., L = 0.25”, Y = 19.19”)	Not Required (Accepted <i>Within Code</i>) Ind.1: L = 0.5”, Z = 0.56” X = 0, Y = 0 Ind. 2: L = 0.5”, X = 0, Y = 19.0”)	Accepted <i>Within Code</i> Ind. 1: TSC, $\theta = 70^\circ$ d = +14 dB L = 0.52”, Z = 0.81” X = -0.05”, Y = 0” Ind. 2: BSC, $\theta = 70^\circ$ d = +14 dB L = 1.12”, Z = 0.11” X = -0.22”, Y = 18.4”
G2G-CF1-BottF-FCM	Accepted	Rejected	Rejected [†] Ind. 1A: TSC, $\theta = 45^\circ$ d = +5 dB L = 0.58”, Z = 1.12” X = -0.06”, Y = 26.21” Ind. 1B: TSC, $\theta = 45^\circ$ d = 0 dB L = 1.50”, Z = 1.12” X = +0.01”, Y = 26.93”

[†]Under the provisions of table 6.3 in the AASHTO/AWS D1.5: 2002 Bridge Welding Code (i.e., class B and class C flaws shall be separated by at least 2L), Ind. 1A, Ind. 1B, ... are considered as a single defect, Ind. 2A, Ind. 2B, ... are considered as a single defect, etc.

1 inch = 25.4 mm

Table 10. Inspection results of the third field testing at HSS.

Specimen ID	RT	Manual UT	AUT
FG4A-TF1-BottF-FCM	Accepted	Accepted	Accepted
FG1A-TF1-BottF-FCM	Accepted	Accepted	Accepted
FG2A-TF1-BottF-FCM	Accepted	Accepted	Accepted
FG3A-TF1-BottF-FCM	Accepted	Accepted	Accepted
FG37K-TF2-TopF-FCM	Accepted	Accepted	Accepted
FG38K-TF3-BottF-FCM	Accepted	Accepted	Accepted
FG26G-TF2-BottF-FCM	Rejected Ind. 1: A-B, 0.12" Slag 0.59" From B Edge (i.e., L = 0.12", Y = 11.29")	Accepted <i>Within Code</i>	Accepted <i>Within Code</i> Ind. 1: BSC, $\theta = 70^\circ$ d = +7 dB L = 0.39", Z = 0.76" X = 0.45", Y = 9.97"
FG16D-TF1-BottF-FCM	Rejected Ind. 1: A-B, <i>Within Code</i> 0.04" Slag at A (i.e., L = 0.04", Y = 0") Ind. 2: A-B, 0.12" Slag 0.98" From B Edge (i.e., L = 0.12", Y = 11.02")	Accepted <i>Within Code</i>	Accepted <i>Within Code</i> Ind. 1: BSC, $\theta = 70^\circ$ d = +14 dB L = 1.74", Z = 0.69" X = -0.24", Y = 0.61" Ind. 2: BSC, $\theta = 70^\circ$ d = +9 dB L = 0.72", Z = 0.32" X = -0.14", Y = 9.56"

1 inch = 25.4 mm

Table 10. Inspection results of the third field testing at HSS (continued).

Specimen ID	RT	Manual UT	AUT
FG36K-TF2- TopF-FCM	Rejected Ind. 1: C-D, Edge of Plate (i.e., Y = 33.75")	Rejected Ind. 1: $\theta = 70^\circ$ L = 2", Z = 0.5" X = -0.75", Y = 33.5" Ind. 2: Subsurface Indications	Rejected [†] Ind. 1: BSC, $\theta = 45^\circ$ d = +7 dB L = 0.83", Z = 0.04" X = +1.2", Y = 22.55" Ind. 2A: TSC, $\theta = 45^\circ$ d = +9 dB L = 1.31", Z = 0" X = -0.85", Y = 25.55" Ind. 2B: TSC, $\theta = 45^\circ$ d = +3 dB L = 0.70", Z = 0.04" X = -0.53", Y = 27.60" Ind. 3A: BSC, $\theta = 45^\circ$ d = -2 dB L = 1.31", Z = 0.02" X = -0.67", Y = 31.18" Ind. 3B: TSC, $\theta = 45^\circ$ d = -3 dB L = 1.43", Z = 0.02" X = -0.58", Y = 31.78"
FG37K-TF3- BottF-FCM	Accepted	Rejected Ind. 1: $\theta = 45^\circ$ L = 1.0", Z = 2.0" X = +0.50", Y = 26"	Rejected Ind. 1: BSC, $\theta = 45^\circ$ d = +6 dB L = 0.41", Z = 1.85" X = +0.54", Y = 26.67"

[†]Under the provisions of table 6.3 in the AASHTO/AWS D1.5: 2002 Bridge Welding Code (i.e., class B and class C flaws shall be separated by at least 2L), Ind. 1A, Ind. 1B, ... are considered as a single defect, Ind. 2A, Ind. 2B, ... are considered as a single defect, etc.

1 inch = 25.4 mm

Table 10. Inspection results of the third field testing at HSS (continued).

Specimen ID	RT	Manual UT	AUT
TP2	Rejected Slags Ind. 1: L = 0.50", Y = 0.25" Ind. 2: L = 0.75", Y = 3.50" Ind. 3: L = 1.13", Y = 7.0" Ind. 4: L = 1", Y = 10.5"	Rejected Ind. 1: d = +5 dB L = 0.38", Z = 0.92" X = -0.50", Y = 0" Ind. 2: d = +2 dB L = 0.50", Z = 0.18" X = +0.31", Y = 3.63" Ind. 3: d = -1 dB L = 0.75", Z = 0.95" X = -0.13", Y = 7.13" Ind. 4: d = +1 dB L = 0.50", Z = 0.09" X = -0.38", Y = 10.5"	Rejected Ind. 1: d = +4 dB L = 0.46", Z = 0.97" X = -0.53", Y = 0" Ind. 2: d = +2 dB L = 0.88", Z = 0.01" X = +22", Y = 3.17" Ind. 3: d = -3 dB L = 1.12", Z = 0.93" X = -0.19", Y = 7.0" Ind. 4: d = +1 dB L = 0.89", Z = 0" X = -0.30", Y = 10.19"
AWS-FCM-02-6A	Rejected	Rejected	Rejected

1 inch = 25.4 mm

Table 11. Inspection results of the fourth field testing at HSS.

Specimen ID	RT	Manual UT	AUT
FBG80-TF1- BottF-FCM	Accepted	Accepted	Accepted
FG1E-TF2- TopF- FCM	Accepted	Accepted	Accepted
FG2E-TF2- TopF-FCM	Accepted	Accepted	Accepted
G11THW-CF1- BottF	Accepted	Not Required	Accepted
G11THW-CF2- BottF	Accepted	Not Required	Accepted
G7UHW-CF1- TopF	Accepted <i>Within Code</i> Ind. 1: B-C, Indication 1.31" Right of A (i.e., Y = 1.31") Ind. 2: B-C, Indication 0.5" Left of B (i.e., Y = 17.5")	Not Required	Accepted

1 inch = 25.4 mm

Table 11. Inspection results of the fourth field testing at HSS (continued).

Specimen ID	RT	Manual UT	AUT
FG40M-TF1-Curved-FCM	Accepted	Rejected Ind. 1: $\theta = 45^\circ$ d = +1 dB L = 1.75", Z = 2" X = +0.38", Y = 12" Ind. 2: $\theta = 45^\circ$ d = +5 dB L = 0.75", Z = 1.38" X = +0.63", Y = 16"	Rejected [†] Ind. 1A: BSC, $\theta = 45^\circ$ d = +8 dB L = 1.29", Z = 2" X = +0.49", Y = 10.68" Ind. 1B: TSC, $\theta = 45^\circ$ d = +1 dB L = 1.02", Z = 1.37" X = +1.10", Y = 11.17"
FG1A-TF2-BottF-FCM	Rejected Ind. 1: A-B, Slag	Rejected	Rejected [†] Ind. 1A: TSC, $\theta = 60^\circ$ d = -1 dB L = 0.97", Z = 0.49" X = -1.40", Y = 3.0" Ind. 1B: TSC, $\theta = 70^\circ$ d = +6 dB L = 1.11", Z = 0.72" X = -1.50", Y = 3.08"
G3VHW-CF1-BottF	Rejected Ind. 1: A-B, Indication 3.25" Left of B (i.e., Y = 9.88")	Not Required (Accepted <i>Within Code</i>)	Accepted <i>Within Code</i> Ind. 1: TSC, $\theta = 70^\circ$ d = +4 dB L = 0.66", Z = 1.52" X = +1.46", Y = 8.76"
G5VHW-CF1-BottF	Rejected Ind. 1: B-C, 0.25" Slag 1.06 From C Edge (i.e., L = 0.25", Y = 25.19")	Not Required (Accepted <i>Within Code</i>)	Accepted <i>Within Code</i> Ind. 1: TSC, $\theta = 45^\circ$ d = +9 dB L = 0.40", Z = 1.70" X = +0.71", Y = 24.76"

[†]Under the provisions of table 6.3 in the AASHTO/AWS D1.5: 2002 Bridge Welding Code (i.e., class B and class C flaws shall be separated by at least 2L), Ind. 1A, Ind. 1B, ... are considered as a single defect, Ind. 2A, Ind. 2B, ... are considered as a single defect, etc.

1 inch = 25.4 mm

Table 12. Inspection results of field testing at Stupp.

Specimen ID	RT	Manual UT	AUT
FS32B1&2-BottF Joint B015	Accepted	Accepted	Accepted
FS45A1&2 Joint T019	Accepted	Accepted	Accepted
FS46A1&2 Joint T021	Accepted	Accepted	Accepted
FS31B1&2 Joint B011	Accepted <i>Within Code</i>	Accepted	Accepted

The results from the second field test set at HSS are summarized in table 9. There were 14 field specimens in the second set. One specimen was designated as an FCM. RT and AUT inspections were performed on all specimens and an additional manual UT inspection was performed on the FCM specimen. RT and AUT inspection methods accepted the first 12 specimens in table 9. RT rejected field specimen G5G-TF1-TopF based on two slag inclusions found near the edge of the plate. The slag inclusions were 3.302 and 6.35 mm (0.13 and 0.25 inches) long and 23.876 and 487.426 mm (0.94 and 19.19 inches) from the datum, respectively. Figures 83 and 84 show photographs of field specimen G5G-TF1-TopF, with the datum assigned to the left edge of the plate. Figures 85 and 86 show the radiographic images of specimen G5G-TF1-TopF in two segments. The two slag inclusions in specimen G5G-TF1-TopF are not visible in figures 85 and 86 because of loss of resolution in the digitization process. Even though manual UT inspection was not required for specimen G5G-TF1-TopF, the fabricator conducted a manual UT inspection to determine the depth of the defects identified by RT. Again, this information allows for more efficient repairs. Note that the slag inclusions were found to be within code requirements according to the UT and AUT results. Figures 87 and 88 show the P-scan images of the weld in specimen G5G-TF1-TopF. The C-scan, B-scan, and end-view images show no rejectable indications. Therefore, the amplitude profile images in figures 87 and 88 show that the rejectable indications identified by RT are acceptable based on AUT. FCM field specimen G2G-CF1-BottF-FCM (figures 89 and 90) was required to be inspected using both RT and UT. RT accepted the specimen while UT and AUT rejected the specimen. Figures 91 through 94 show the radiographic images of specimen G2G-CF1-BottF-FCM in four segments. The P-scan images in figures 95 and 96 show a rejectable indication at approximately 635 mm (25 inches) from the datum. Manual UT inspection was conducted using 45-degree and 70-degree probes while the P-scan inspection was only performed with a 45-degree probe between Y = 224.8 mm and Y = 795 mm (Y = 8.85 inches and Y = 31.30 inches) due to time constraints.



**Figure 83. Field specimen G5G-TF1-TopF:
Top view of joint.**



**Figure 84. Field specimen G5G-TF1-TopF:
Side view of joint.**



**Figure 85. Radiographic image of field specimen G5G-TF1-TopF:
Section A-B.**

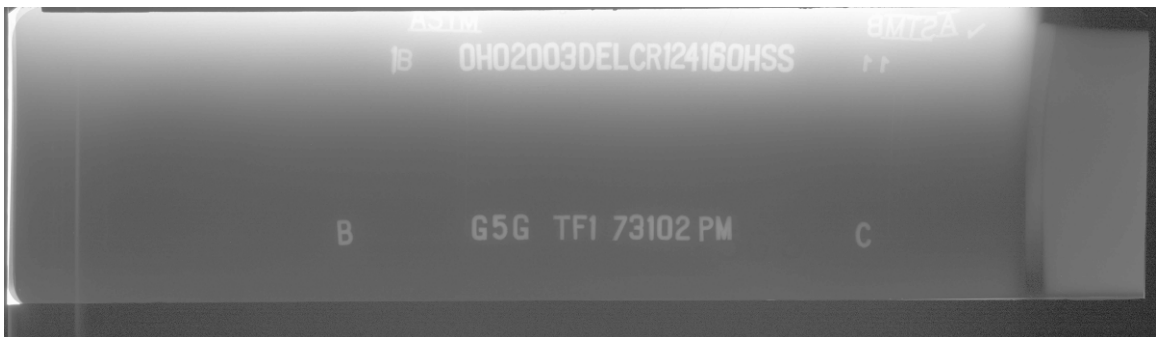


**Figure 86. Radiographic image of field specimen G5G-TF1-TopF:
Section B-C.**

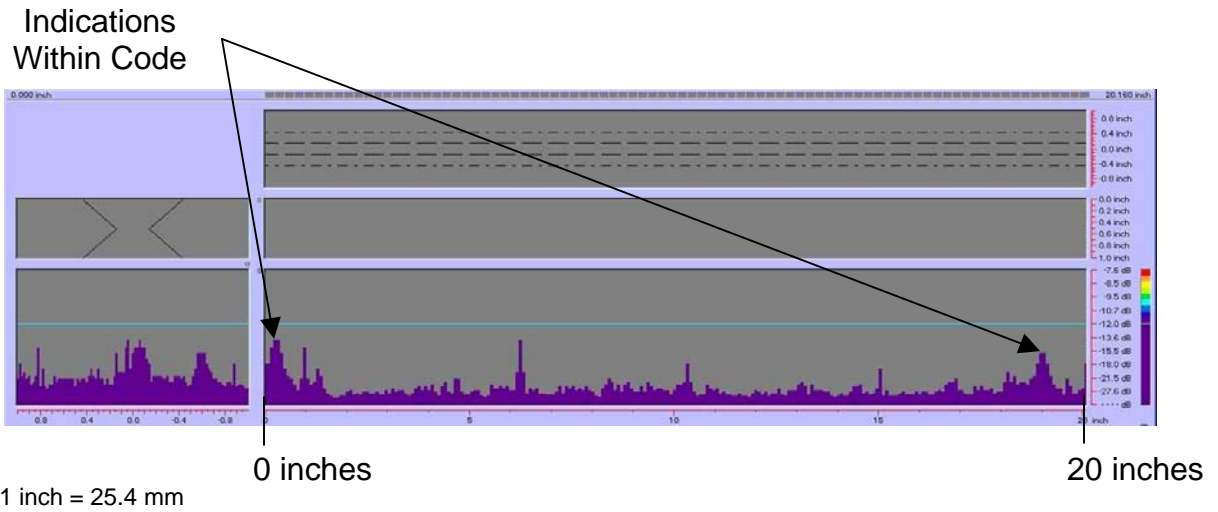


Figure 87. P-scan images of field specimen G5G-TF1-TopF using 70-degree probe: From TSC side of centerline.

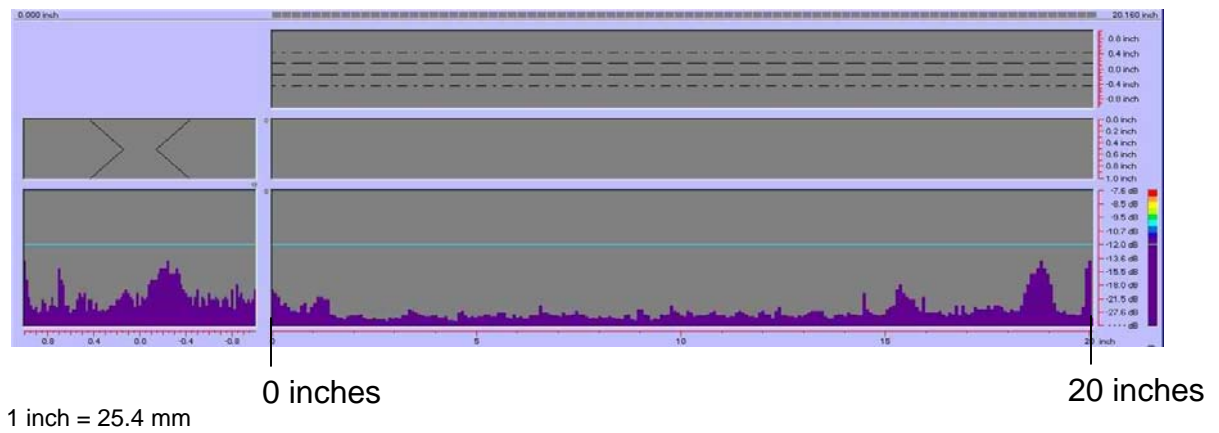
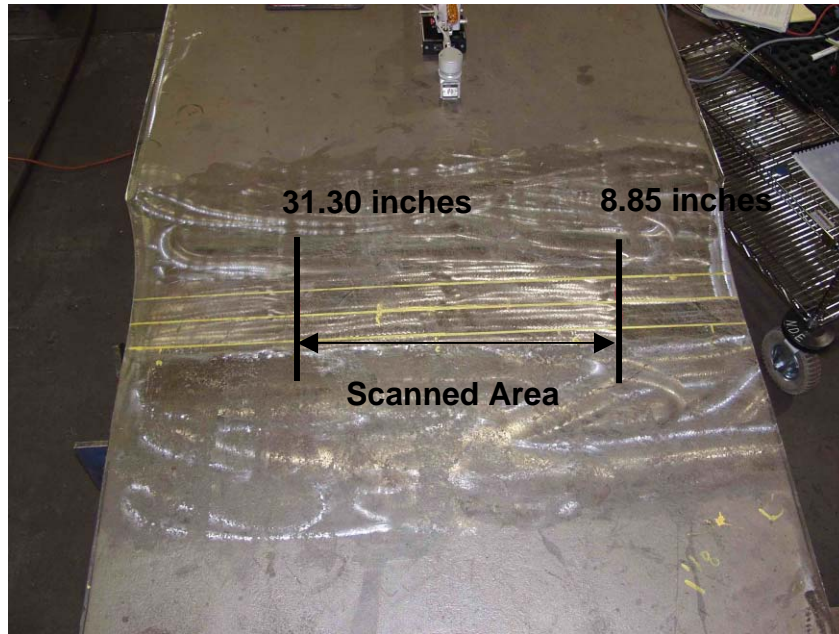


Figure 88. P-scan images of field specimen G5G-TF1-TopF using 70-degree probe: From BSC side of centerline.



1 inch = 25.4 mm

**Figure 89. Field specimen G2G-CF1-BottF-FCM:
Top view of joint.**



**Figure 90. Field specimen G2G-CF1-BottF-FCM:
Side view of joint.**



**Figure 91. Radiographic image of field specimen G2G-CF1-BottF-FCM:
Section A-B.**



**Figure 92. Radiographic image of field specimen G2G-CF1-BottF-FCM:
Section B-C.**

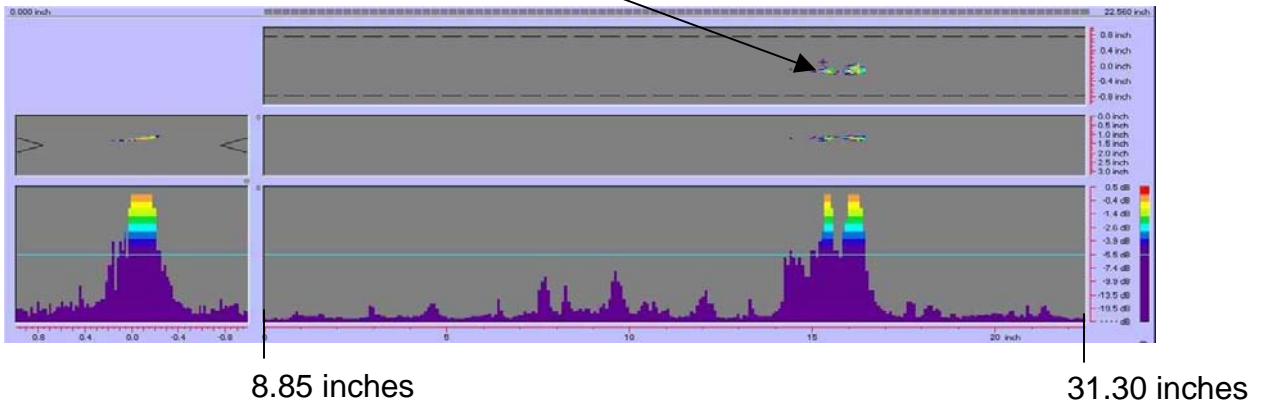


**Figure 93. Radiographic image of field specimen G2G-CF1-BottF-FCM:
Section C-D.**



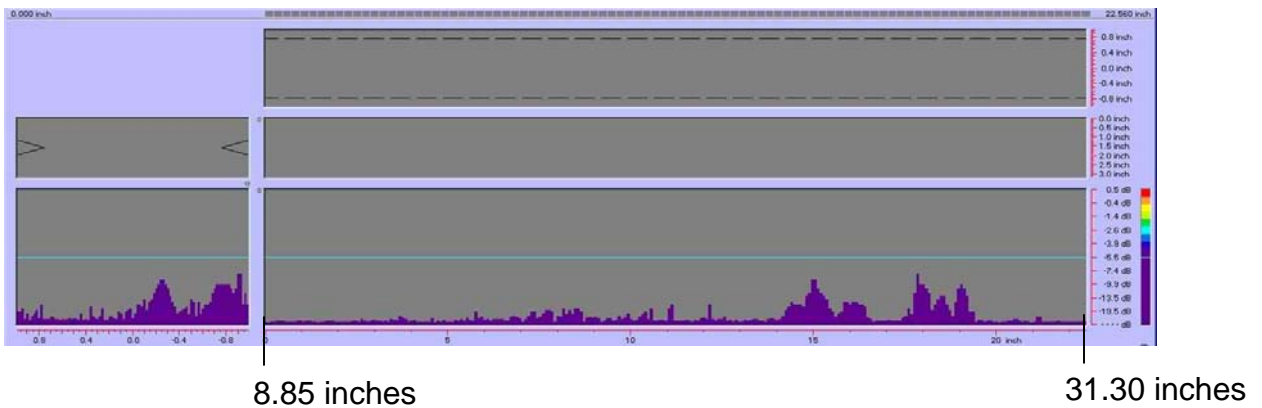
**Figure 94. Radiographic image of field specimen G2G-CF1-BottF-FCM:
Section D-E.**

Rejectable Indication



1 inch = 25.4 mm

Figure 95. P-scan images of field specimen G2G-CF1-BottF-FCM using 45-degree probe: From TSC side of centerline.



1 inch = 25.4-mm

Figure 96. P-scan images of field specimen G2G-CF1-BottF-FCM using 45-degree probe: From BSC side of centerline.

The results from the third set of field tests at HSS are summarized in table 10. The third test set consisted of 10 FCM field specimens and 2 HSS procedural test plates (TP2 and AWS-FCM-02-6A). Each HSS procedural test plate contains multiple realistic defects in the weld. The first six field specimens in table 10 were accepted by all three inspection methods. Specimens FG26G-TF2-BottF-FCM and FG16D-TF1-BottF-FCM were rejected by RT, but were accepted by manual UT and AUT. Photographs of specimen FG26G-TF2-BottF-FCM are shown in figures 97 and 98. Figure 99 shows the radiographic image of the weld with a rejectable 3.048-mm- (0.12-inch-) long slag inclusion at location $Y = 286.77$ mm ($Y = 11.29$ inches). The P-scan images in figures 100 and 101 indicate that the same rejectable slag inclusion identified by RT as rejectable is acceptable using AUT. Specimen FG16D-TF1-BottF-FCM (figures 102 and 103) was rejected by RT. The radiographic image in figure 104 shows that RT detected two slag inclusions. One slag inclusion was acceptable, while the other slag inclusion was rejectable. The P-scan images of specimen FG16D-TF1-BottF-FCM (figures 105 through 107) confirmed the presence of the two slag inclusions that were identified by RT. AUT identified these indications as being acceptable. Field specimen FG36K-TF2-TopF-FCM (figures 108 and 109) was rejected by all three inspection methods. RT detected a rejectable slag inclusion at $Y = 857.25$ mm ($Y = 33.75$ inches). However, the radiographic image of specimen FG36K-TF2-TopF-FCM (figure 110) shows no visible defects because of loss of resolution during the digitization process. Note that the quality and the contrast of the radiographic image decreases for plates greater than 50.8 mm (2 inches) thick. Manual UT results (table 10) and P-scan images (figures 111 and 112) confirmed the presence of a rejectable slag inclusion. In addition, AUT also found multiple rejectable subsurface indications. Field specimen FG37K-TF3-BottF-FCM (figures 113 and 114) was accepted by RT, but was rejected by manual UT and AUT. Figure 115 is the radiographic image of weld section C–D, where a rejectable defect was found. The defect is not clearly visible in the radiograph because of loss of resolution during the digitization process. The P-scan image of weld segment C–D (figure 116) shows a rejectable indication 10.414 mm (0.41 inch) long at $Y = 677.418$ mm ($Y = 26.67$ inches). The defect was 46.99 mm (1.85 inches) deep and was detected using a 45-degree probe. Figure 117 shows that no rejectable indications were found in segment C–D using a 70-degree probe. The first HSS procedural plate (TP2) (figures 118 and 119) was fabricated with four realistic slag inclusions in the weld. RT, manual UT, and AUT confirmed the presence of these rejectable slag inclusions. Unfortunately, a radiographic image was not available for TP2. The P-scan images of TP2 (figure 119) indicate four rejectable indications. The second HSS procedural plate (AWS-FCM-02-6A) was rejected by all three inspection methods. Unfortunately, a radiographic image was not available for this specimen.

Rejectable Slag Inclusion

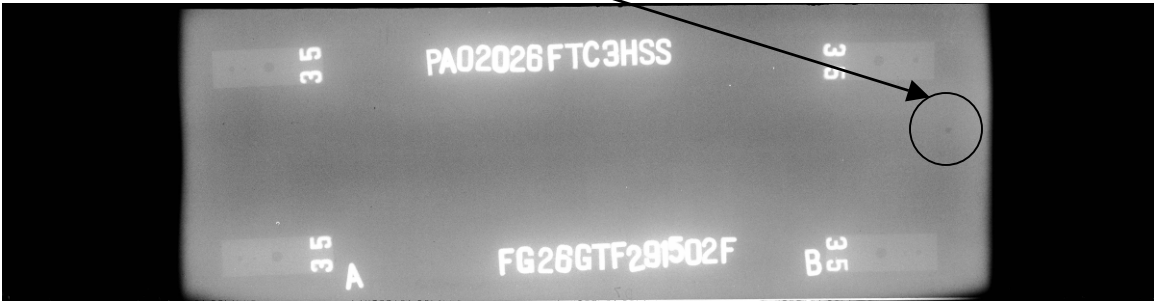
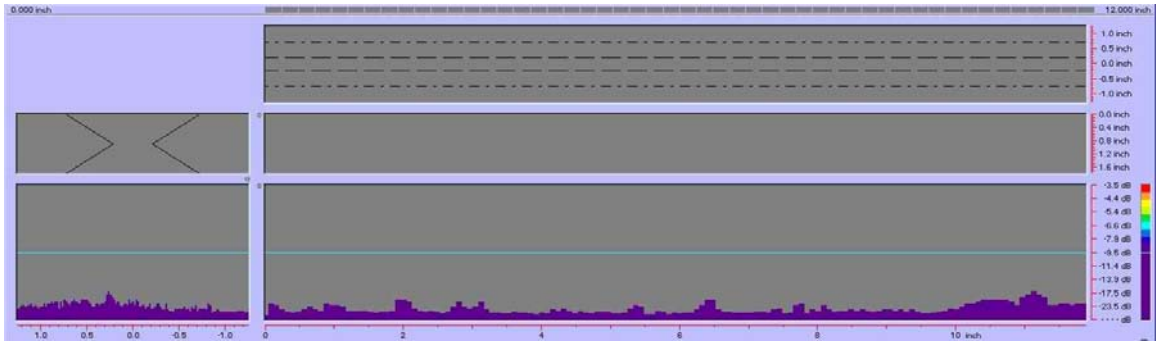


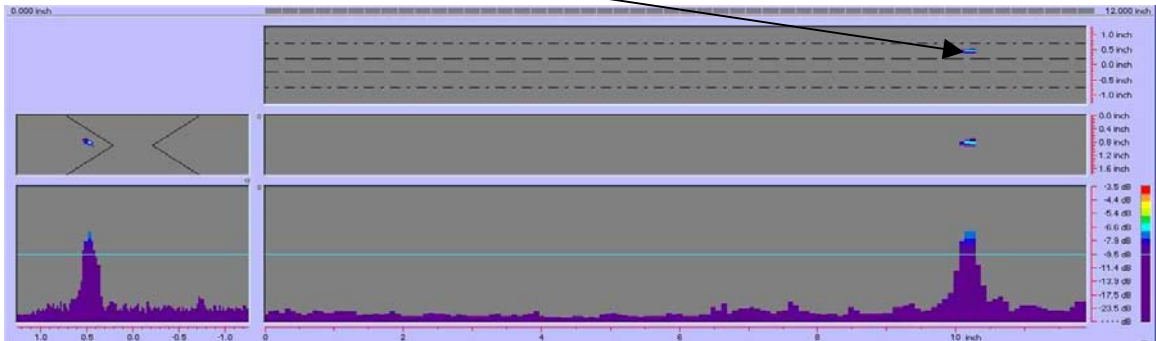
Figure 99. Radiographic image of field specimen FG26G-TF2-BottF-FCM.



1 inch = 25.4 mm

Figure 100. P-scan images of field specimen FG26G-TF2-BottF-FCM using 70-degree probe: From TSC side of centerline.

Indication
Within Code



1 inch = 25.4 mm

Figure 101. P-scan images of field specimen FG26G-TF2-BottF-FCM using 70-degree probe: From BSC side of centerline.



**Figure 102. Field specimen FG16D-TF1-BottF-FCM:
Top view of joint.**



**Figure 103. Field specimen FG16D-TF1-BottF-FCM:
Side view of joint.**

Rejectable Slag Inclusion

Slag Inclusion
Within Code

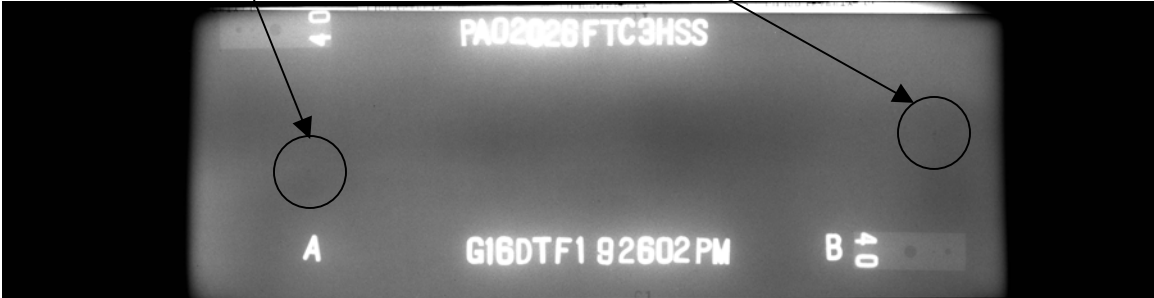
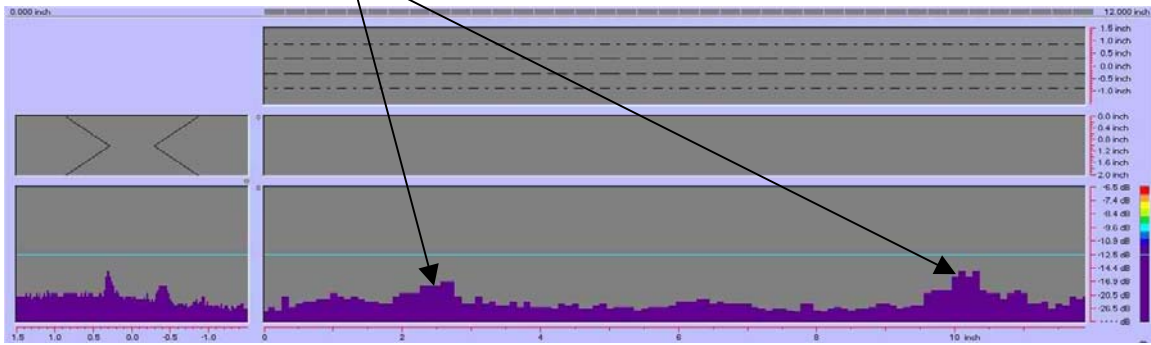


Figure 104. Radiographic image of field specimen FG16D-TF1-BottF-FCM.

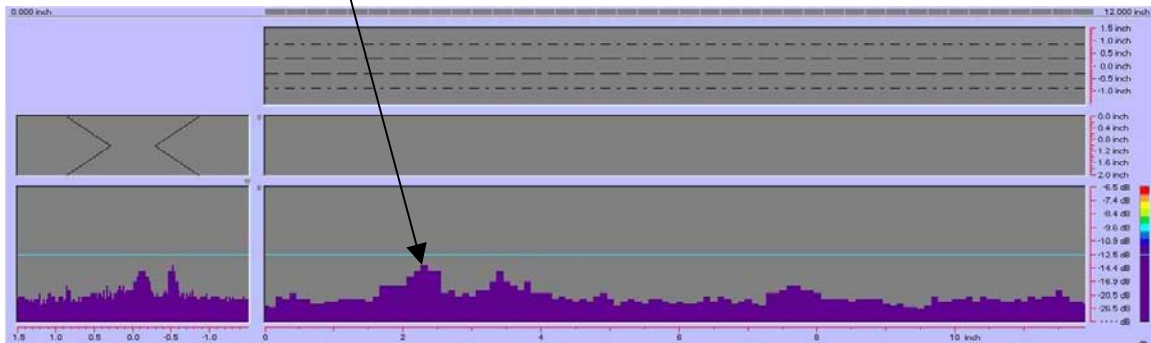
Indications Within Code



1 inch = 25.4 mm

**Figure 105. P-scan images of field specimen FG16D-TF1-BottF-FCM:
From TSC side of centerline using 60-degree probe.**

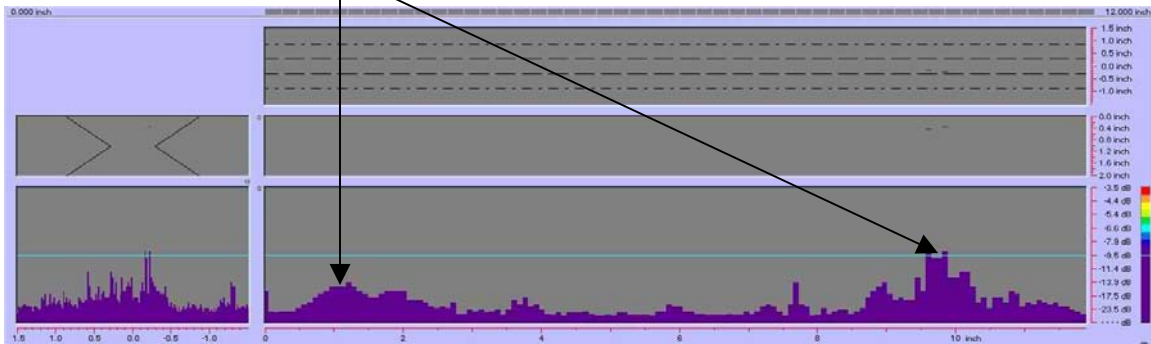
Indication Within Code



1 inch = 25.4 mm

**Figure 106. P-scan images of field specimen FG16D-TF1-BottF-FCM:
From BSC side of centerline using 60-degree probe.**

Indications Within Code



1 inch = 25.4 mm

**Figure 107. P-scan images of field specimen FG16D-TF1-BottF-FCM:
From BSC side of centerline using 70-degree probe.**



**Figure 108. Field specimen FG36K-TF2-TopF-FCM:
Top view of joint.**



**Figure 109. Field specimen FG36K-TF2-TopF-FCM:
Side view of joint.**

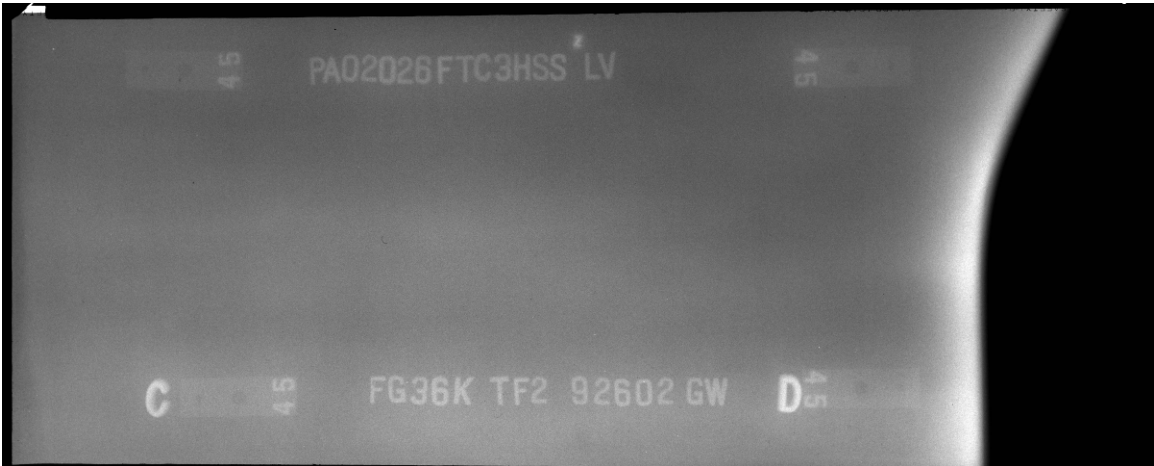


**Figure 110. Radiographic image of field specimen FG36K-TF2-TopF-FCM:
Section C-D.**

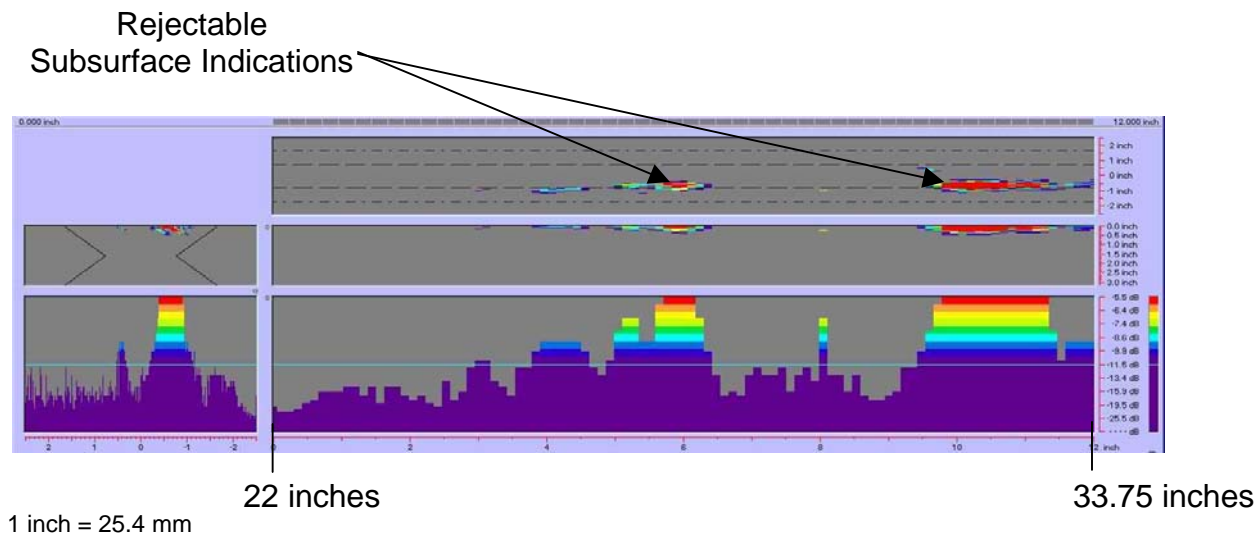


Figure 111. P-scan images of field specimen FG36K-TF2-TopF-FCM using 45-degree probe: From TSC side of centerline.

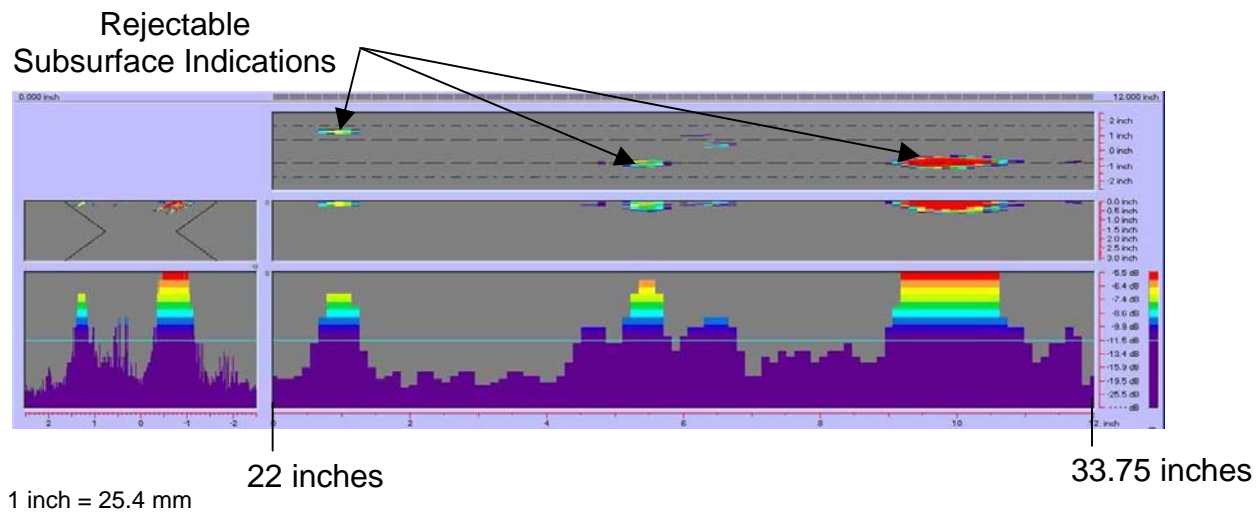


Figure 112. P-scan images of field specimen FG36K-TF2-TopF-FCM using 45-degree probe: From BSC side of centerline.



**Figure 113. Field specimen FG37K-TF3-BottF-FCM:
Top view of joint.**



**Figure 114. Field specimen FG37K-TF3-BottF-FCM:
Side view of joint.**



**Figure 115. Radiographic image of field specimen FG37K-TF3-BottF-FCM:
Section C-D.**

Rejectable Indication

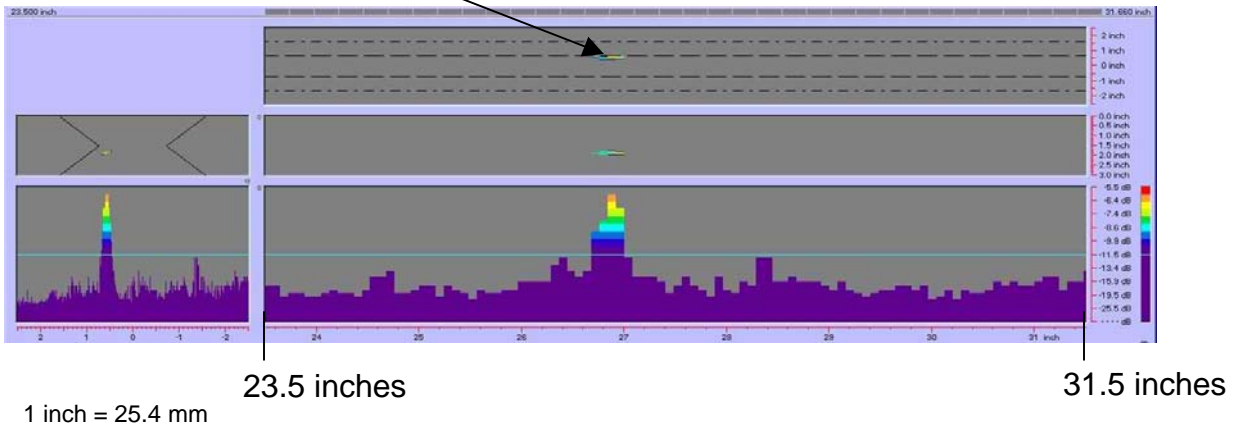


**Figure 116. P-scan images of field specimen FG37K-TF3-BottF-FCM:
Scan using 45-degree probe.**

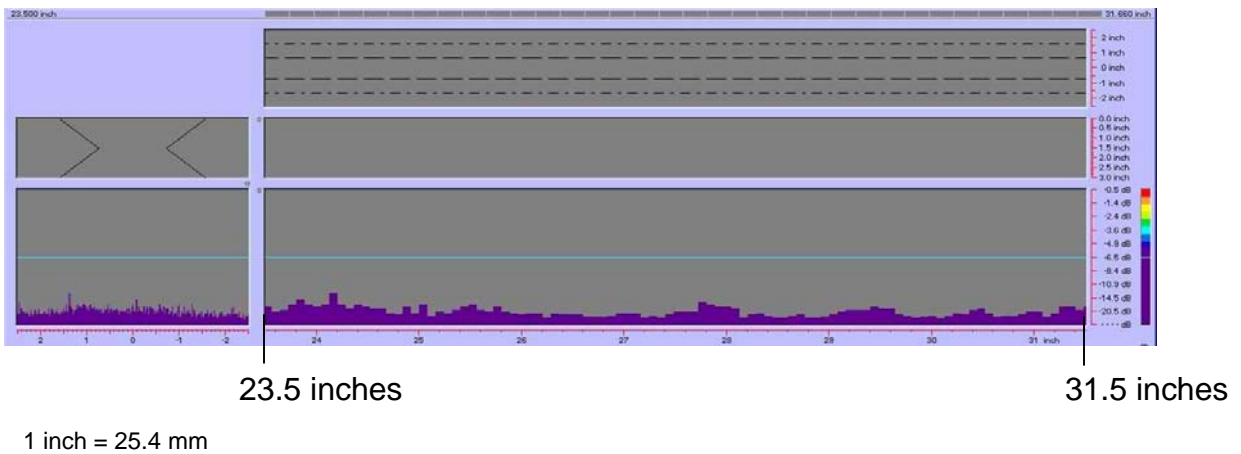


**Figure 117. P-scan images of field specimen FG37K-TF3-BottF-FCM:
Scan using 70-degree probe.**



**Figure 118. HSS procedural test plate TP2:
Top view of joint.**

Rejectable Indications

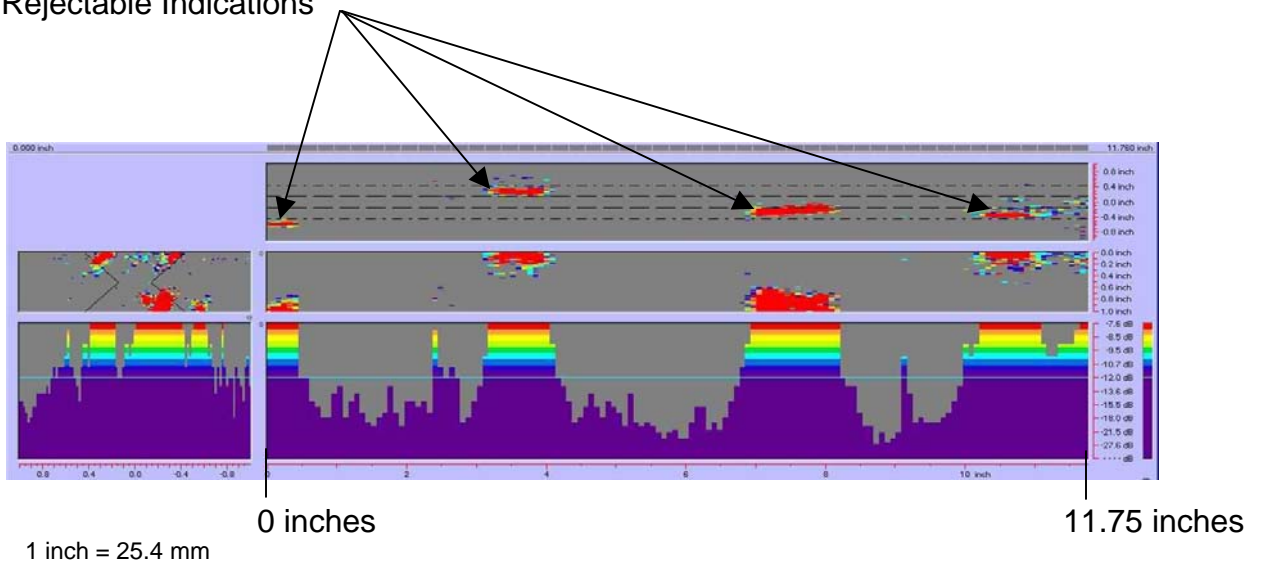


**Figure 119. HSS procedural test plate TP2: P-scan images from BSC side
of centerline.**

The results of the fourth set of field tests at HSS are summarized in table 11. There were 10 field specimens inspected; 5 of the 10 specimens were designated as FCMs. Table 11 indicates that three FCM and three non-FCM specimens were accepted with no rejectable defects by all of the inspection methods. The 76.2-mm- (3-inch-) thick field specimen FG40M-TF1-Curved-FCM (figures 120 and 121) is a plate specially fabricated for a railroad bridge. Unlike conventional plates that are generally fabricated flat, specimen FG40M-TF1-Curved-FCM was fabricated at a right angle. RT accepted the weld with no rejectable defects. Since specimen FG40M-TF1-Curved-FCM is an FCM, it is required to be inspected by UT. Two rejectable indications were detected by manual UT and one rejectable indication was detected by AUT. Figure 122 shows a radiographic image of the weld section where UT detected rejectable indications. Figures 123 through 130 show the P-scan images created by scanning the weld with a 45-degree probe. The rejectable indication is located between $Y = 228.6$ mm and $Y = 457.2$ mm ($Y = 9$ inches and $Y = 18$ inches) (figures 125 and 126). According to table 6.2 in the AASHTO/AWS D1.5M/D1.5: 2002 Bridge Welding Code,⁽¹⁾ a 76.2-mm- (3-inch-) thick plate is required to be scanned by 45-degree and 70-degree probes. However, a P-scan inspection of the weld with a 70-degree probe was not performed because of scheduling constraints. The 50.8-mm- (2-inch-) thick field specimen FG1A-TF2-BottF-FCM (figures 131 and 132) was rejected by all three inspection methods. RT rejected the specimen based on a rejectable slag inclusion in section A-B. According to table 6.2 in the AASHTO/AWS D1.5M/D1.5: 2002 Bridge Welding Code,⁽¹⁾ a 50.8-mm- (2-inch-) thick plate must be scanned by 60-degree and 70-degree probes. Manual UT and AUT rejected the specimen based on an indication detected with the 60-degree and 70-degree probes. The P-scan images of specimen FG1A-TF2-BottF-FCM, scanned with 60-degree and 70-degree probes, are shown in figures 133 through 135. Specimen G3VHW-CF1-BottF (figure 136) was rejected by RT based on a slag inclusion found at location $Y = 250.952$ mm ($Y = 9.88$ inches). The radiographic image of this weld section is shown in figure 137, but the defect is not clearly visible. Manual UT and AUT inspection with a 70-degree probe found an acceptable indication at $Y = 250.952$ mm ($Y = 9.88$ inches). Figure 138 shows the P-scan images from $Y = 0$ mm to $Y = 304.8$ mm ($Y = 0$ inches to $Y = 12$ inches) for specimen G3VHW-CF1-BottF. Field specimen G5VHW-CF1-BottF (figures 139 and 140) was rejected by RT, but was accepted by manual UT and AUT. RT found a 6.35-mm- (0.25-inch-) long slag inclusion at $Y = 639.83$ mm ($Y = 25.29$ inches) (figure 141). The defect is not clearly visible in the radiographic image because of the poor quality of the radiographic film. Specimen G5VHW-CF1-BottF was not required to be tested by manual UT; however, the fabricator used UT to determine the depth of the defect for repair purposes. Manual UT and AUT identified the defect found by RT and this indication was found to be acceptable. The P-scan images from segment 4 in specimen G5VHW-CF1-BottF were produced using 45-degree and 70-degree probes (figures 142 through 144). Figure 142 illustrates that the indication detected by AUT was within code requirements.

The results of the field tests at Stupp are summarized in table 12. There were four field specimens tested, with all three inspection methods accepting all four specimens.



**Figure 120. Field specimen FG40M-TF1-Curved-FCM:
Top view of joint.**



**Figure 121. Field specimen FG40M-TF1-Curved-FCM:
Side view of joint.**

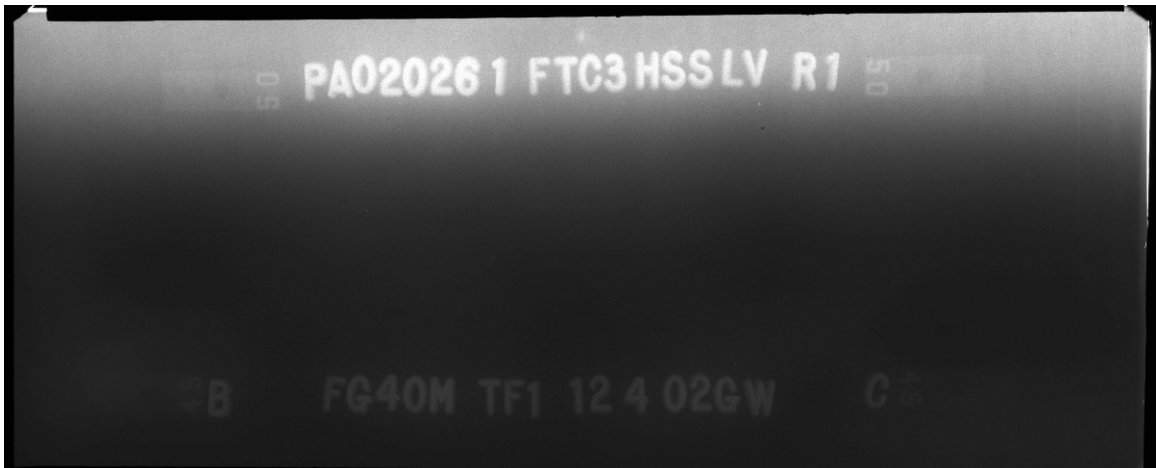


**Figure 122. Radiographic image of field specimen FG40M-TF1-Curved-FCM:
Section B-C.**

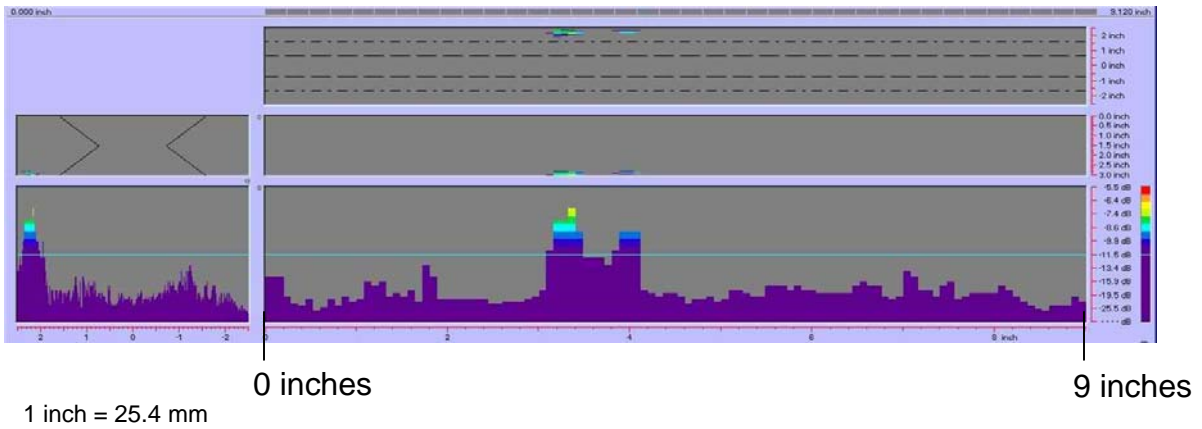


**Figure 123. P-scan images of field specimen FG40M-TF1-Curved-FCM:
From TSC side of centerline between 0 and 228.6 mm (0 and 9 inches).**

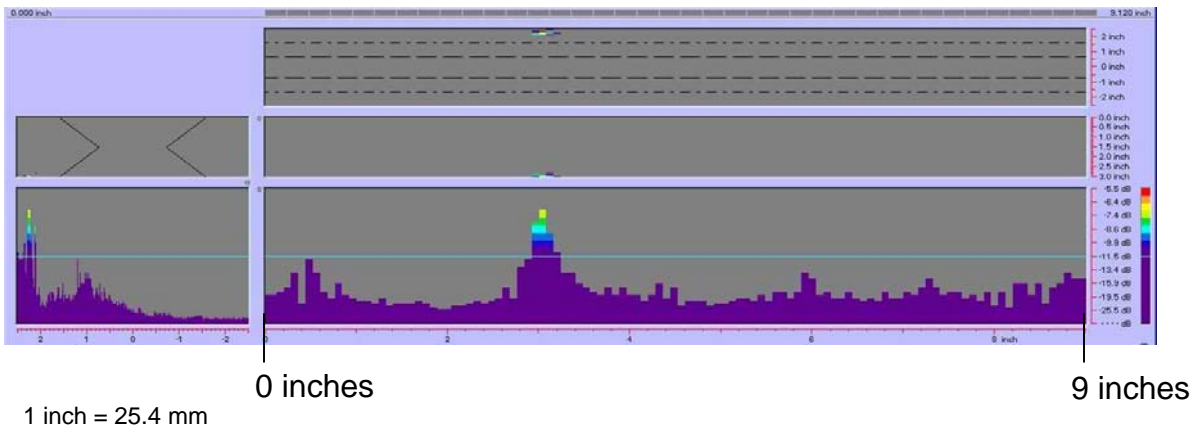
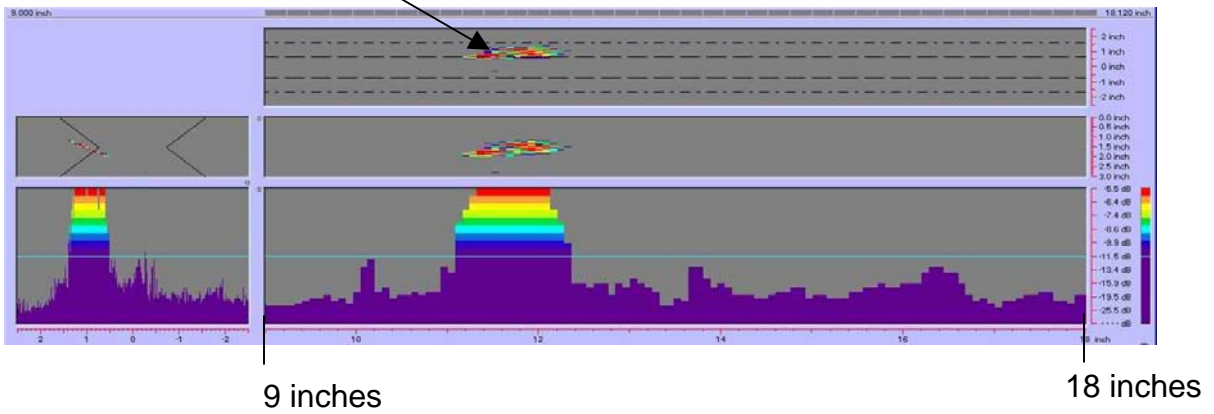


**Figure 124. P-scan images of field specimen FG40M-TF1-Curved-FCM:
From BSC side of centerline between 0 and 228.6 mm (0 and 9 inches).**

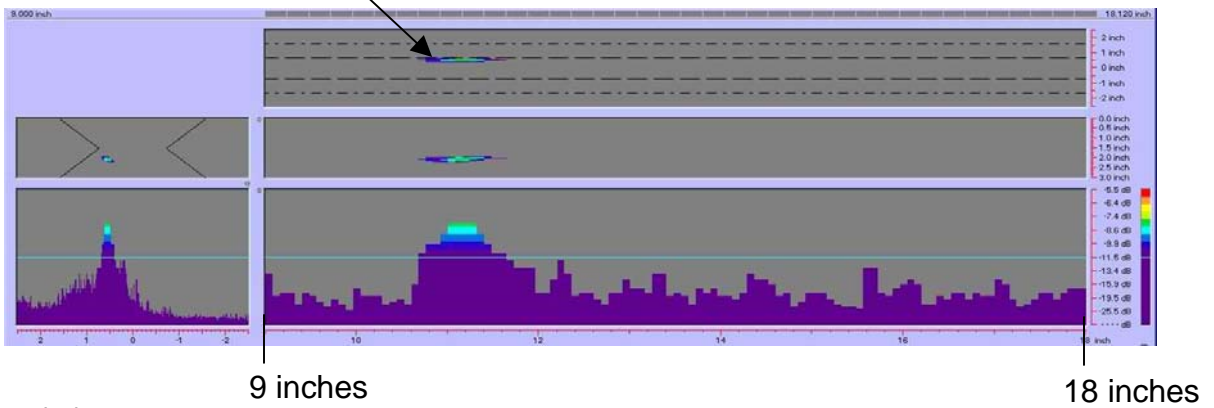
Rejectable Indication



1 inch = 25.4 mm

Figure 125. P-scan images of field specimen FG40M-TF1-Curved-FCM: From TSC side of centerline between 228.6 and 457.2 mm (9 and 18 inches).

Rejectable Indication



1 inch = 25.4 mm

Figure 126. P-scan images of field specimen FG40M-TF1-Curved-FCM: From BSC side of centerline between 228.6 and 457.2 mm (9 and 18 inches).

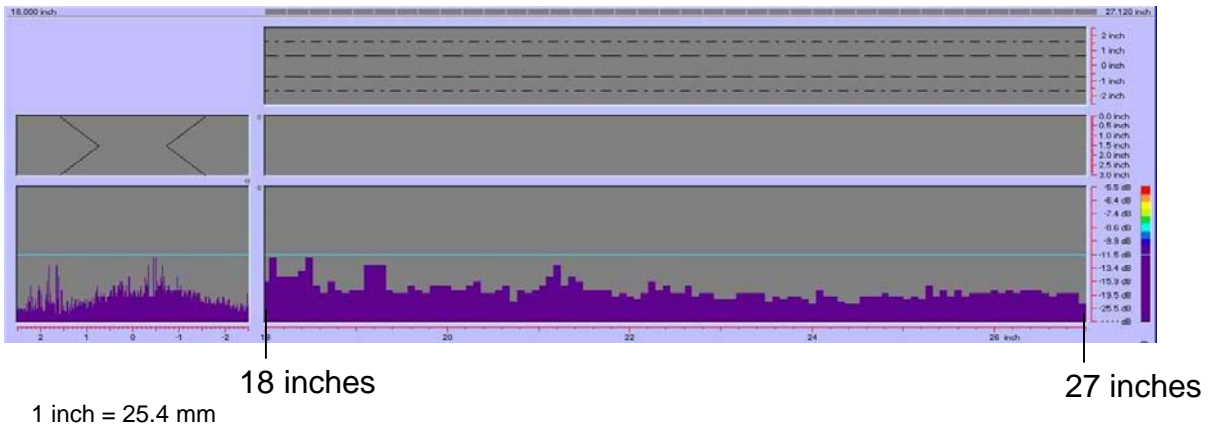


Figure 127. P-scan images of field specimen FG40M-TF1-Curved-FCM: From TSC side of centerline between 457.2 and 685.8 mm (18 and 27 inches).

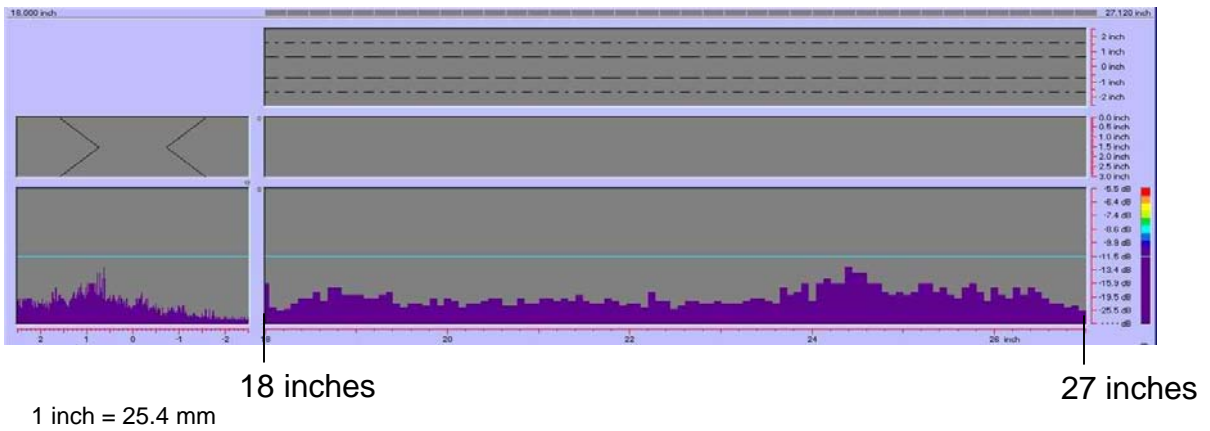


Figure 128. P-scan images of field specimen FG40M-TF1-Curved-FCM: From BSC side of centerline between 457.2 and 685.8 mm (18 and 27 inches).

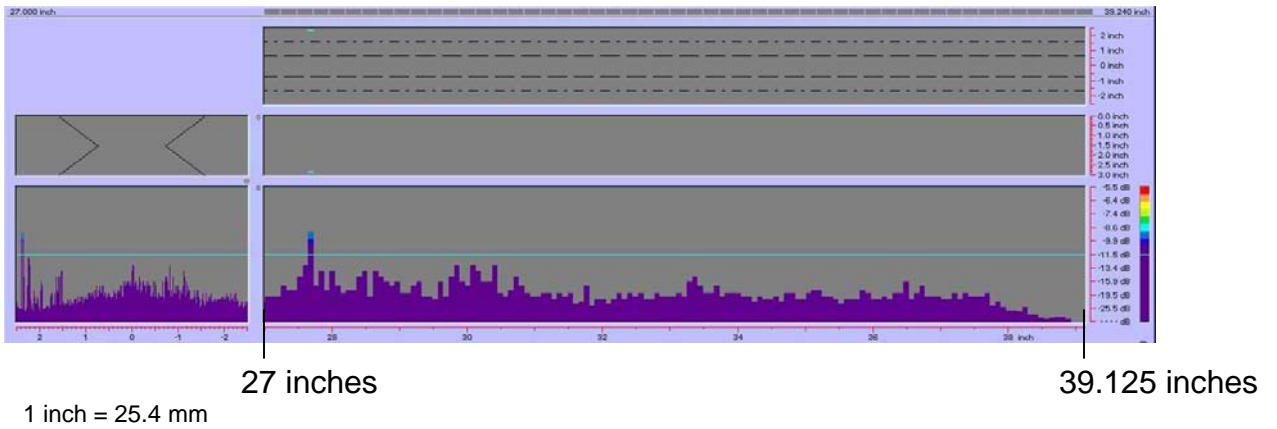


Figure 129. P-scan images of field specimen FG40M-TF1-Curved-FCM: From TSC side of centerline between 685.8 and 993.8 mm (27 and 39.125 inches).

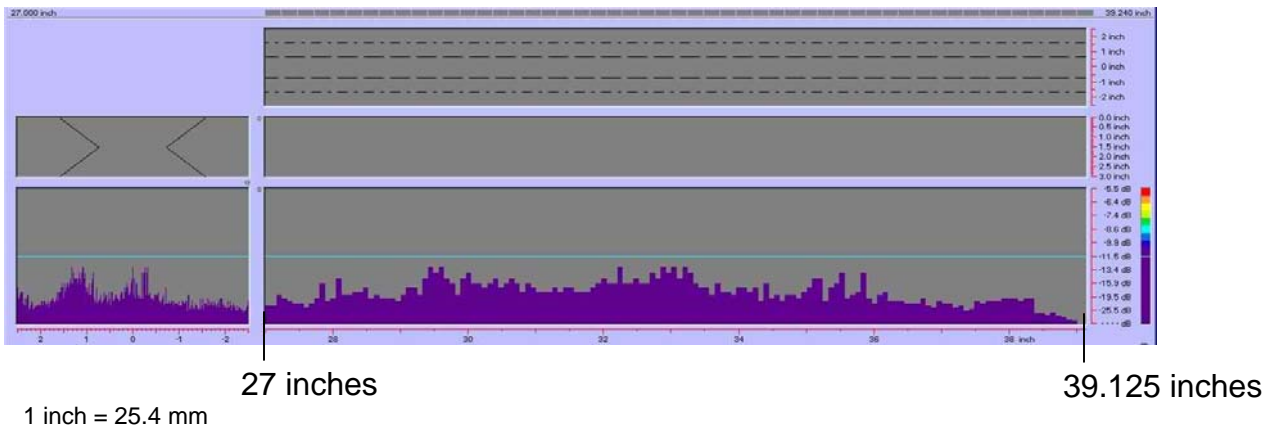


Figure 130. P-scan images of field specimen FG40M-TF1-Curved-FCM: From BSC side of centerline between 685.8 and 993.8 mm (27 and 39.125 inches).



**Figure 131. Field specimen FG1A-TF2-BottF-FCM:
Top view of joint.**



**Figure 132. Field specimen FG1A-TF2-BottF-FCM:
Side view of joint.**

Rejectable Indication

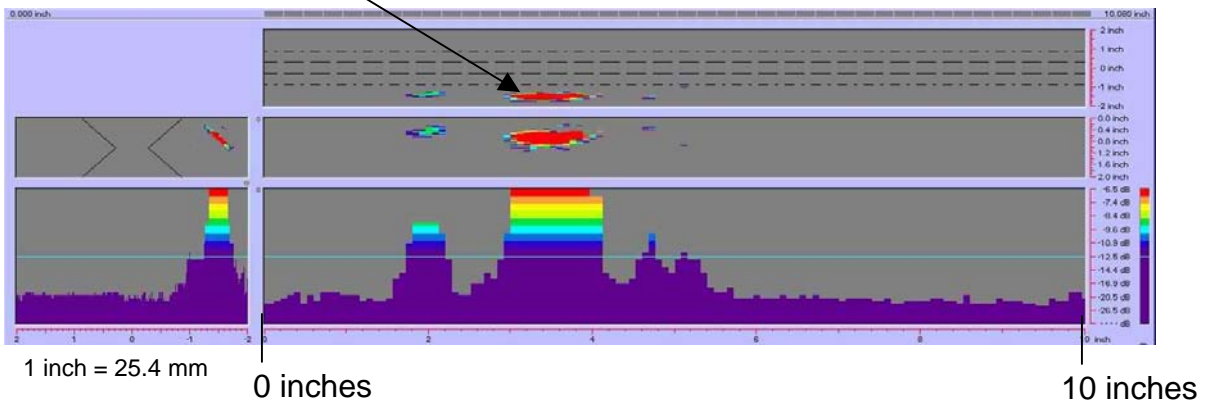


**Figure 133. P-scan images of field specimen FG1A-TF2-BottF-FCM:
From TSC side of centerline using 60-degree probe.**

Rejectable Indication

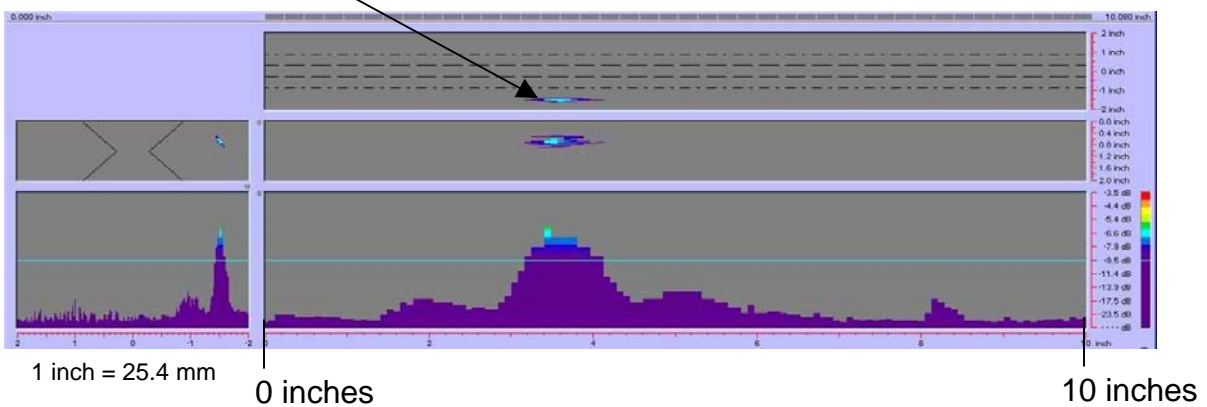


**Figure 134. P-scan images of field specimen FG1A-TF2-BottF-FCM:
From TSC side of centerline using 70-degree probe.**

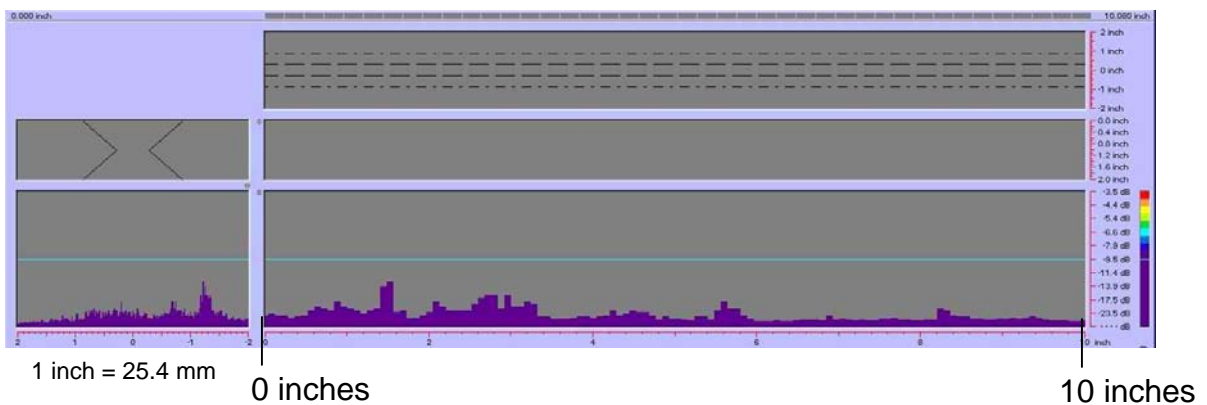


**Figure 135. P-scan images of field specimen FG1A-TF2-BottF-FCM:
From BSC side of centerline using 70-degree probe.**



**Figure 136. Field specimen G3VHW-CF1-BottF:
Top view of joint.**

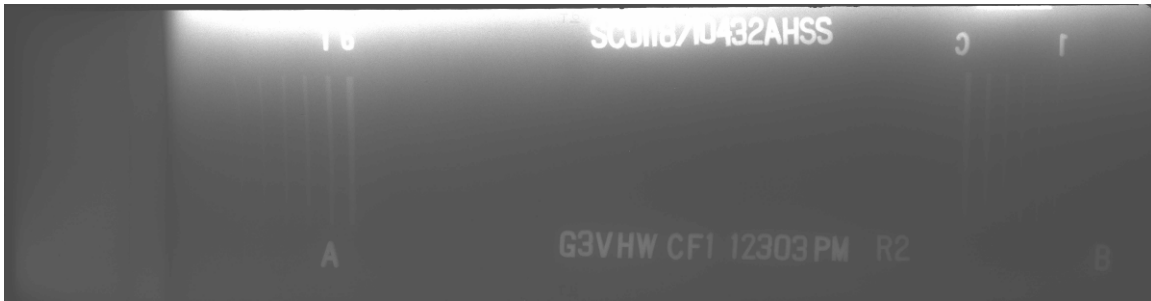


**Figure 137. Field specimen G3VHW-CF1-BottF:
Radiographic image of section A–B.**

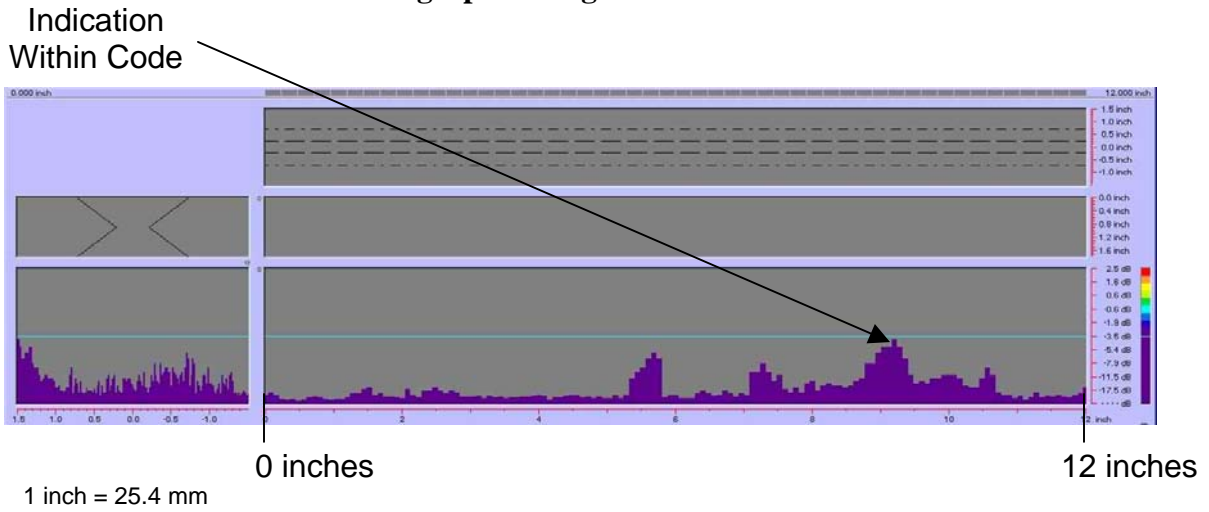


**Figure 138. Field specimen G3VHW-CF1-BottF:
P-scan images from TSC side of centerline using 70-degree probe.**



**Figure 139. Field specimen G5VHW-CF1-BottF:
Top view of joint.**

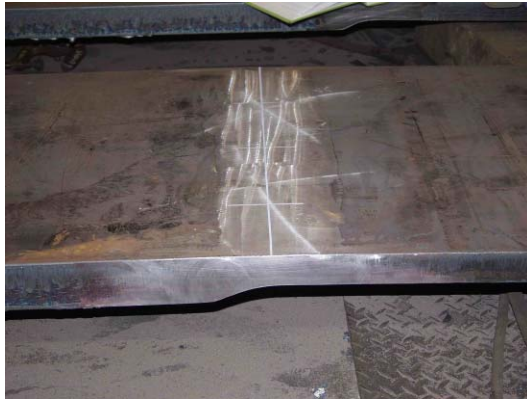


**Figure 140. Field specimen G5VHW-CF1-BottF:
Side view of joint.**

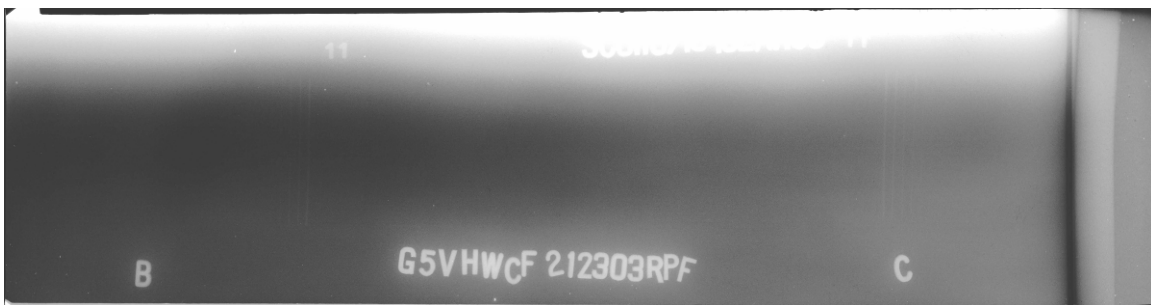


**Figure 141. Field specimen G5VHW-CF1-BottF:
Radiographic image of section B-C.**

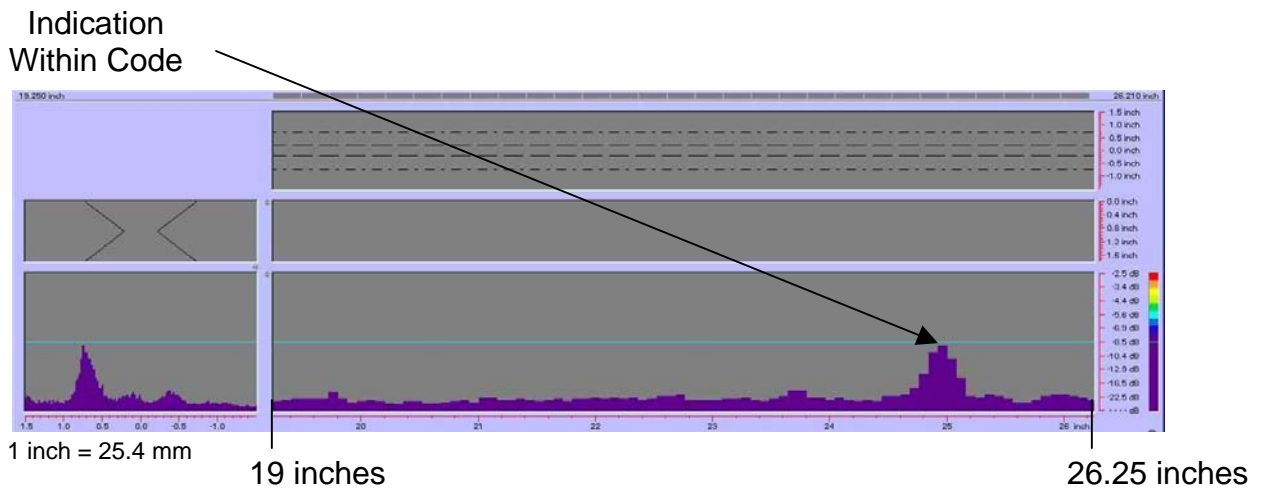


**Figure 142. P-scan images of field specimen G5VHW-CF1-BottF:
From TSC side of centerline using 45-degree probe.**

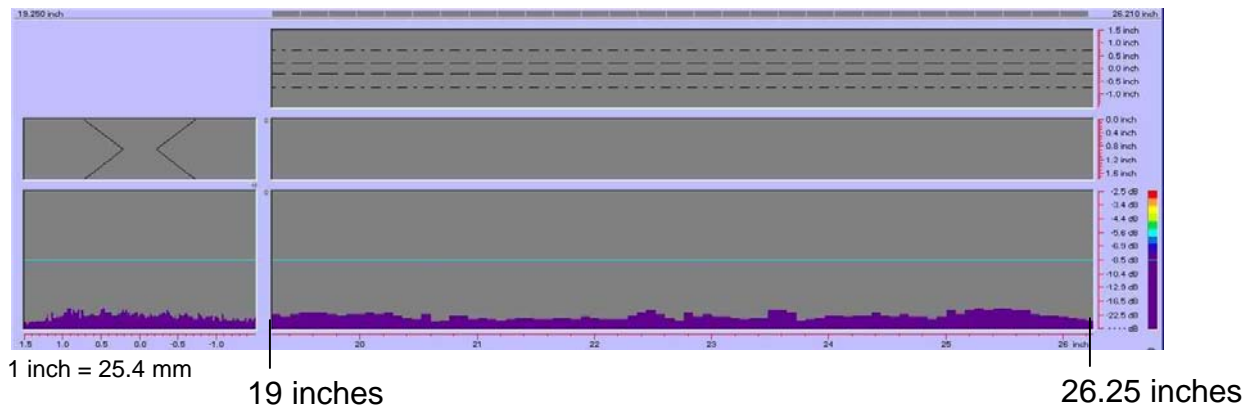


**Figure 143. P-scan images of field specimen G5VHW-CF1-BottF:
From BSC side of centerline using 45-degree probe.**

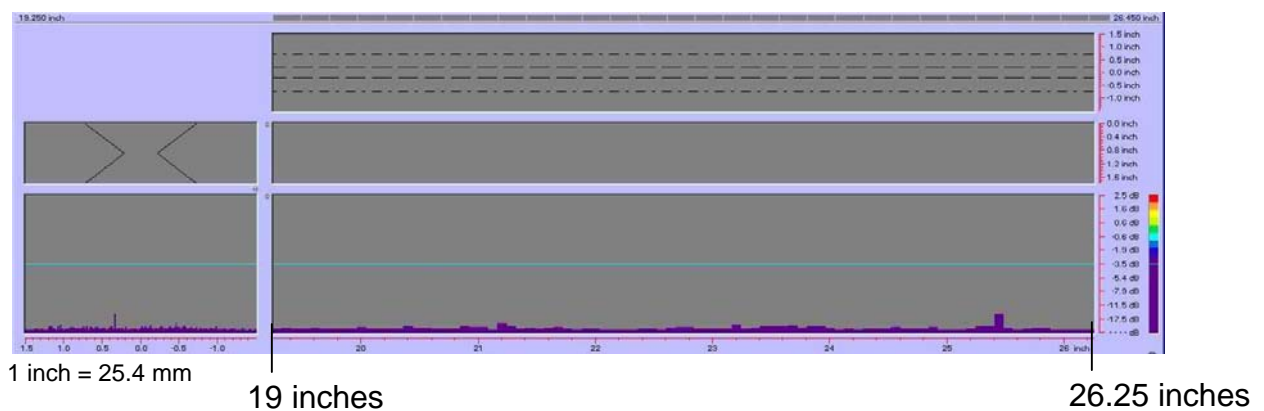


**Figure 144. P-scan images of field specimen G5VHW-CF1-BottF:
From BSC side of centerline using 70-degree probe.**

For comparison, the laboratory and field specimens with rejectable defects were grouped according to plate thickness in 25.4-mm (1-inch) increments (tables 13 and 14). These groupings summarized the results and helped determine the relationship between the effectiveness of each inspection method with respect to the plate thickness. The first column of each table shows the thickness range of the grouped plates. The second column shows the total number of specimens inspected. The third column indicates the number of specimens accepted with no rejectable defects by all three inspection methods. The fourth column shows the number of specimens rejected with rejectable defects by at least one inspection method. The fifth column identifies the rejected specimen. The sixth column shows the number of rejectable defects found. The seventh, eighth, and ninth columns indicate the inspection methods that rejected the particular specimen. The checkmark (√) stands for “Rejected,” indicating that the specimen was rejected by the employed inspection method; X stands for “Accepted,” indicating that the specimen was accepted by the employed inspection method; and DWC stands for “Detected/Within Code,” indicating that the employed inspection method identified an indication that was within code requirements. Table 13 shows that the three inspection methods produced consistent results in the laboratory. In table 14, there are 8 field specimens with thicknesses ranging from 0 to 50.8 mm (0 to 2 inches) that contained 12 rejectable defects. RT rejected all eight specimens, while UT rejected only three specimens. Note that UT identified defects in the five remaining specimens, but found that the defects were acceptable. In addition, 5 specimens with thicknesses ranging from greater than 50.8 to 101.6 mm (2 to 4 inches) containing 8 rejectable defects also were identified. RT rejected only two specimens, while UT rejected all five specimens. Note that FG36K-TF2-TopF-FCM was not rejected by AUT since the defect was located at the curvature region of the width transition and the P-scan system was not configured to inspect this type of region.

Tables 15 and 16 compare the results of the RT and AUT inspections. The tables are arranged to illustrate: (1) the total number of specimens inspected within each 25.4-mm (1-inch) thickness increment, (2) the total number of specimens that were rejected by at least one inspection technique, (3) the number of specimens rejected by each inspection method, and (4) the number of specimens accepted with identifiable indications.

Table 13. Consolidating the results of laboratory testing using laboratory specimens with rejectable defects.

Thickness Range (inch)	Total No. of Laboratory Specimens	No. of Laboratory Specimens Accepted	No. of Laboratory Specimens Rejected by at Least One Technique	Rejected Laboratory Specimen	Ind. No.	Rejected by RT	Rejected by UT	Rejected by AUT
0-1	6	0	6	S033 (0.5" thick)	1	√	√	√
					2	√	√	√
				S034 (0.5" thick)	1	√	√	√
					2	√	√	X [‡]
				S125 (1" thick)	1	√	√	√
					2	√	√	√
					3	√	√	√
				S126 (1" thick)	1	√	√	√
					2	√	√	√
					3	√	√	√
					4	√	DWC	√
				S135 (1" thick)	1	√	√	√
					2	√	√	√
					3	√	√	√
S136 (1" thick)	1	√	√	√				
	2	√	√	√				
>1-2	4	2	2	S132 (1.5" thick)	1	√	√	√
				S133 (1.5" thick)	1	√	√	√

[‡]AUT is not configured to detect transverse crack.

DWC: Detected/Within Code

1 inch = 25.4 mm

Table 14. Consolidating the results of field testing using field specimens with rejectable defects.

Thickness Range (inch)	Total No. of Field Specimens	No. of Field Specimens Accepted	No. of Field Specimens Rejected by at Least One Technique	Rejected Field Specimen	Ind. No.	Rejected by RT	Rejected by UT	Rejected by AUT
0-1	5	3	2	G5G-TF1-TopF (1" thick)	1	√	DWC	DWC
					2	√	DWC	DWC
				TP2 (1" thick)	1	√	√	√
					2	√	√	√
					3	√	√	√
					4	√	√	√
				>1-2	23	17	6	FG26G-TF2-BottF-FCM (1.75" thick)
FG16D-TF1-BottF-FCM (2" thick)	1	√	DWC					DWC
AWS-FCM-02-6A (1.5" thick)	1	√	√					√
FG1A-TF2-BottF-FCM (2" thick)	1	√	√					√
G3VHW-CF1-BottF (1.75" thick)	1	√	DWC					DWC
G5VHW-CF1-BottF (1.75" thick)	1	√	DWC					DWC

1 inch = 25.4 mm

Table 14. Consolidating the results of field testing using field specimens with rejectable defects (continued).

Thickness Range (inch)	Total No. of Field Specimens	No. of Field Specimens Accepted	No. of Field Specimens Rejected by at Least One Technique	Rejected Field Specimen	Ind. No.	Rejected by RT	Rejected by UT	Rejected by AUT
>2-3	13	9	4	FG36K-TF2-TopF-FCM (3" thick)	1	√	√	X [‡]
					2	X	√	√
				FG37K-TF3-BottF-FCM (3" thick)	1	X	√	√
					FG38K-TF2-TopF-FCM (3" thick)	1	√	√
				FG40M-TF1-Curved-FCM (3" thick)		2	X	√
					2	X	√	√
>3-4	3	2	1	G2G-CF1-BottF-FCM (3.15" thick)	1	X	√	√

[‡]AUT is not configured to detect transverse defects or inspect width transition regions.

1 inch = 25.4 mm

Table 15. Assessing the detectability and rejectability of three inspection methods in the laboratory.

Thickness Range (inch)	Total No. of Laboratory Specimens	No. of Laboratory Specimens With Rejectable Defects	No. of Specimens Rejected by RT	No. of Specimens Rejected by AUT	No. of Specimens Accepted by RT Within Code	No. of Specimens Accepted by AUT Within Code
0–1	6	6	6 (100%)	6 (100%)	0	0
>1–2	4	2	2 (100%)	2 (100%)	0	0

1 inch = 25.4 mm

Table 16. Assessing the detectability and rejectability of three inspection methods in the field.

Thickness Range (inch)	Total No. of Field Specimens	No. of Field Specimens With Rejectable Defects	No. of Specimens Rejected by RT	No. of Specimens Rejected by AUT	No. of Specimens Accepted by RT Within Code	No. of Specimens Accepted by AUT Within Code
0–1	5	2	2 (100%)	1 (50%)	0	1
>1–2	23	6	6 (100%)	2 (33%)	0	4
>2–3	13	4	2 (50%)	4 (100%)	0	0
>3–4	3	1	0 (0%)	1 (100%)	0	0

1 inch = 25.4 mm

ARTICULATION ANGLES

To supplement field testing and establish the importance of the code-prescribed transducer articulation, specimen S033 was tested at a series of fixed angles (0 degrees, 2.5 degrees, 5 degrees, 7.5 degrees, and 10 degrees). The angles were measured with respect to a line normal to the weld centerline. The main purpose of articulating the transducer is to obtain the highest possible amplitude echo from a given defect. To accomplish this, the transducer must be articulated so that the direction of the shear wave propagating within the specimen is perpendicular to a plane of the defect. As mentioned earlier, specimen S033 (shown in figures 7 through 10) contained manufactured crack-like defects oriented along the centerline in the weld bevels.

The testing is performed by the P-scan system using a test frame (figure 145) and a series of wedges designed to keep the transducer at a fixed angle during scanning (figure 146). Figure 146 shows an angled wedge attached to a vertical sliding bar which is oriented transverse to the weld axis. The transducer is placed against the angled wedge, holding the articulation angle fixed relative to the weld axis. As the sliding bar is advanced along the length of the weld, the transducer is held at the fixed angle of interest.

The maximum echo amplitudes from the defect were determined from the P-scan images and were plotted against the transducer articulation angles (figure 147). The abscissa in figure 147 represents the transducer articulation angles, and the ordinate represents the indication rating (d). The indication rating of negative dB is indicative of a high-amplitude echo and the indication rating of positive dB is indicative of a low-amplitude echo. It is evident from figure 147 that the amplitude of the echo decreases from a high value of -4 dB to a low value of $+14$ dB as the articulation angle increases from 0 to 10 degrees, respectively. The 0-degree articulation angle, which produces the highest indication rating of -4 dB, reveals that the direction of the incident traveling wave is aligned normal to the plane of the crack thus reflecting the highest amount of ultrasonic energy. For articulation angles other than 0 degrees, the incident traveling wave is no longer perpendicular to the plane of the crack, leading to less ultrasonic energy reflection. The difference in the echo amplitude between the articulation angles of 0 degrees and 2.5 degrees, 2.5 degrees and 5 degrees, 5 degrees and 7.5 degrees, 7.5 degrees and 10 degrees are 5 dB, 6 dB, 5 dB, and 2 dB, respectively. The 2-dB to 6-dB difference in the echo amplitude is significant in rejecting or accepting a weld based on the indication rating criteria set forth in the UT acceptance-rejection criteria in tables 6.3 and 6.4 in the AASHTO/AWS D1.5M/D1.5: 2002 Bridge Welding Code.⁽¹⁾ Therefore, a rejectable defect may be misrepresented as an acceptable indication if articulation of the transducer is eliminated.

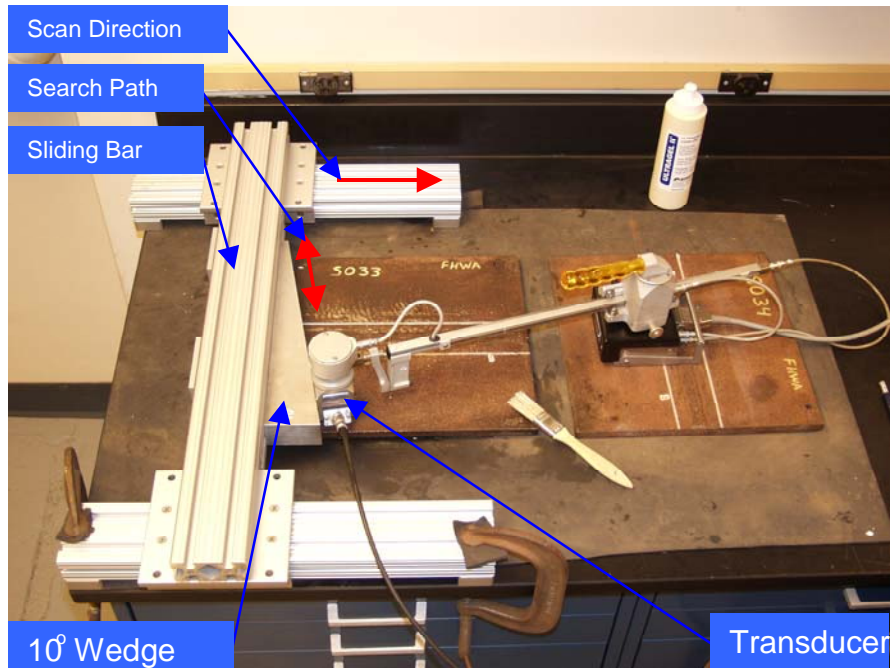


Figure 145. Transducer articulation testing: Test setup.

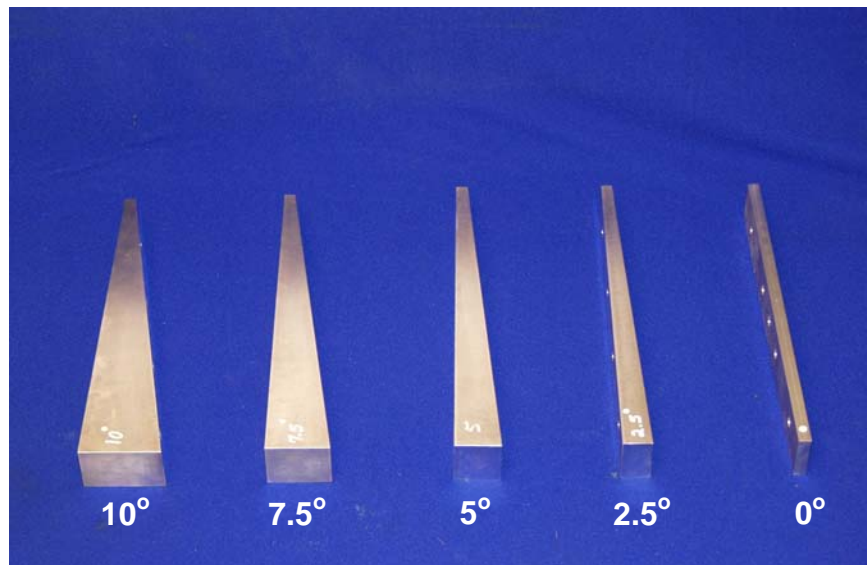


Figure 146. Transducer articulation testing: Various articulation angle wedges.

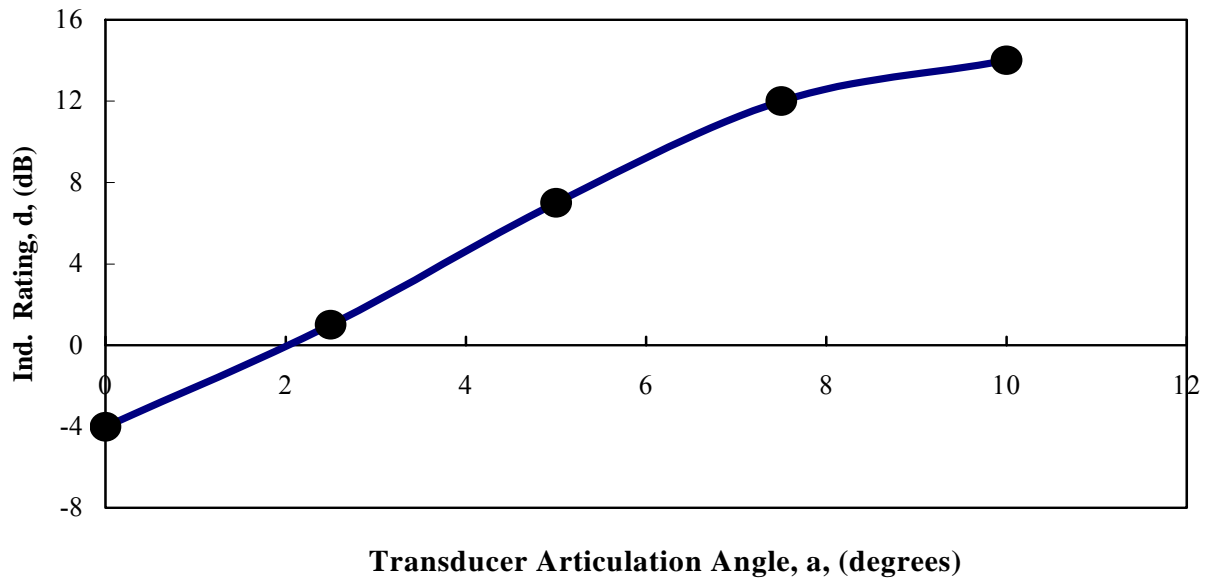


Figure 147. Influence of transducer articulation angle on the maximum amplitude of the reflected signal.

7. CONCLUSIONS

The general goals of this study were to: (1) test and evaluate the AUT method of inspection in parallel with both RT and manual UT to determine possible differences in inspection results, (2) identify possible operational challenges in the fabrication shop environment, and (3) develop the appropriate procedures for implementing AUT as a replacement for RT. The following conclusions are based on the work performed as part of this project:

1. AUT is a viable inspection technique for fabrication inspection of butt welded steel plates.
2. AUT creates projection images of the defects in the weld along three axes. One of the three images (i.e., the C-scan) is analogous to a two-dimensional radiographic film. The other two images provide spatial information about the defect that RT does not provide. AUT images, like RT radiographic films, can be archived permanently as a hard copy or in an electronic format.
3. AUT images provide more complete information than manual UT about the characteristics of the defects in the weld, including defect position, length, depth, and orientation. Note that RT only provides the x-position, y-position, and length of the defect.
4. AUT findings were in full agreement with the RT laboratory results.
5. AUT findings generally agreed with the RT field testing results. The slight lack of agreement is caused, in part, by the basic physics behind each inspection method. AUT operates based on an ultrasonic wave theory, while RT is based on differential absorption of penetrating radiation. The threshold levels prescribed by the code for UT and RT do not yield identical results. Therefore, certain defects that are rejectable by RT may be acceptable under the UT provisions. In this testing, it was found that AUT and UT could detect RT discontinuities; however, some of these discontinuities were acceptable according to the UT and AUT code requirements.
6. AUT provides a relatively objective method of analysis. The decibel ratings yielded by AUT are determined directly from electronic measurements, without human interaction. With manual UT, the inspector must determine the decibel rating while simultaneously applying the transducer to the surface of the test specimen. This process includes maximizing the signals on the instrument screen and identifying the decibel level and transducer orientation when the signal matches the threshold value. For RT, the contrast observed on the radiographic film is subjectively analyzed by the inspector to identify discontinuities.
7. The time required for setting up, calibrating, and performing an AUT inspection was generally greater than the time required by either RT or manual UT. However, AUT took less time than RT and manual UT combined.

8. The P-scan system was not manufactured for use in a bridge fabrication shop environment. The system currently consists of seven separate modules with about eight interface cables. These modules should be interconnected using interface cables prior to performing an inspection at a fabrication shop. Assembling and transporting the P-scan system from one area of the shop to another was time-consuming and cumbersome. Thus, improved packaging by integrating the various modules and interface cables is recommended.
9. Implementation of a fully automated (robotic) scanner instead of a manual scanner is recommended. This will improve the inspection rate and reduce human interaction.
10. Currently, there are defects that can be accepted by RT and rejected by AUT or vice versa. Further research is recommended to explore the defect sensitivity of AUT in comparison to RT. This should provide a clearer understanding of the differences that exist in the acceptance-rejection criteria between AUT/UT and RT.

8. REFERENCES

1. AASHTO/AWS D1.5M/D1.5: 2002 Bridge Welding Code, An American National Standard, American Welding Society.
2. Jessup, T.J.; Mudge, P.J.; and Harrison, J.D., *Ultrasonic Measurement of Weld Flaw Size*, NCHRP Report 242, Transportation Research Board, Washington, DC, December 1981.
3. Jonas, P.G. and Scharosch, D.L., *Ultrasonic Inspection of Butt Welds in Highway Bridges*, Report No. CA-HY-MR-6210-1-72-36, California Department of Transportation, 1972.
4. DeNale, R. and Lebowitz, C.A., "Detection and Disposition Reliability of Ultrasonics and Radiography for Weld Inspection," *Review of Progress in Quantitative Nondestructive Evaluation*, Vol. 9, 1990.
5. Ginzel, E.; Den Boer, P.; and Hoff, M., "Application of Mechanized Ultrasonic Inspection to Manually Welded Pipeline Girth Welds," *NDT.net*, Vol. 2, No. 2, May 1997.
6. Morgan, L., "The Performance of Automated Ultrasonic Testing (AUT) of Mechanized Pipeline Girth Welds," *NDT.net*, Vol. 8, No. 3, March 2003.
7. Shenefelt, G.A., "Ultrasonic Testing: Requirements of the AWS 1969 Building Code and Bridge Specifications," *Welding Journal*, May 1971.
8. AWS D1.1: Structural Welding Code—Steel, American Welding Society.
9. Serabian, S., *Reliability of Ultrasonic Weld Interrogation Methods*, Report No. DOT-RC-92014, U.S. Department of Transportation, 1980.
10. Thavasimuthu, M.; Hemamalini, R.; Subramanian, C.V.; Jayakumar, T.; Kalyanasundaram, P.; and Raj, B., "Detectability of Misoriented Defect by Ultrasonic Examinations—A Few Observations," *Insight*, Vol. 40, No. 11, 1998.
11. Deutsch, W.K., "Automated Ultrasonic Inspection," Fifteenth World Conference on Nondestructive Testing, Rome, Italy, 2000.
12. Dijkstra, B.J.; Farley, J.M.; and Scruton, G., "Babcock Experience of Automated Ultrasonic Nondestructive Testing of PWR Pressure Vessels During Manufacture," *Nuclear Energy*, Vol. 29, No. 3, June 1990.
13. ASTM E1961-98: 1998 Standard Practice for Mechanized Ultrasonic Examination of Girth Welds Using Zonal Discrimination With Focused Search Units, *The ASTM Standard Test Method*, American Society for Testing and Materials, West Conshohocken, PA.

14. Komsky, I.N. and Achenbach, J.D., "A Computerized Imaging System for Ultrasonic Inspection of Steel Bridge Structures," *Structural Materials Technology: An NDT Conference*, eds. Hartbower, P.E. and Stolarski, P.J., San Diego, CA, 1996.
15. Komsky, I.N. and Achenbach, J.D., "A Portable Dual-Line Scanner for Imaging of Steel Bridge Components," *Structural Materials Technology: An NDT Conference*, ed. Alampalli, S., Atlantic City, NJ, 2000.
16. Graybeal, B.A.; Walther, R.A.; and Washer, G.A., "Ultrasonic Inspection of Bridge Hanger Pins," *Transportation Research Record*, No. 1697, Washington, DC, 2000, pp. 19–23.

